

**Multiscale modelling of snow depth over an agricultural field in a small
catchement in southern ontario, canada.**

by

Robert Neilly

A thesis

presented to the University of Waterloo

in fulfillment of the

thesis requirement for the degree of

Master of Science

in

Geography

Waterloo, Ontario, Canada, 2011

© Robert Neilly 2011

I hereby declare that I am the sole author of this thesis. This is a true copy of the thesis, including any required final revisions, as accepted by my examiners.

I understand that my thesis may be made electronically available to the public.

Abstract

Snow is a common overlying surface during winter-time and the redistribution of snow by wind is a very important concept for any hydrological research project located within the cryosphere. Wind redistributes snow by eroding it from areas of high wind speed, such as ridge tops and windward slopes, and deposits it in areas of lower wind speeds, such as the lees of ridge tops, vegetation stands, and topographic depressions. The accurate modelling of blowing snow processes such as erosion, deposition, and sublimation have proven to be rather problematic. The largest issue that many modellers must deal with is the accurate collection of solid precipitation throughout the winter season. Without this, incorrect energy and mass balances can occur. This thesis makes use of a new method of acquiring solid precipitation values through the use of an SR50a ultrasonic snow depth sensor and then incorporates it into a version of the Cold Regions Hydrological Model (CRHM) which includes the Prairie Blowing Snow Model (PBSM) and the Minimal Snowmelt Model (MSM) modules. The model is used to simulate seasonal snow depth over an agricultural field in southern Ontario, Canada and is driven with half-hourly locally acquired meteorological data for 83 days during the 2008-2009 winter season. Semi-automated snow surveys are conducted throughout the winter season and the collected *in situ* snow depth values are compared to the simulated snow depth values at multiple scales. Two modelling approaches are taken to temporally and spatially test model performance. A lumped approach tests the model's ability to simulate snow depth from a small point scale and from a larger field scale. A distributed approach separates the entire field site into three hydrological response units (HRUs) and tests the model's ability to spatially discretize at the field scale. HRUs are differentiated by varying vegetation heights throughout the field site. Temporal analysis compares the simulated results to each day of snow survey and for the entire field season. Model performance is statistically analyzed through the use of a Root Mean Square Difference (RMSD), Nash-Sutcliffe coefficient (NS), and Model Bias (MB). Both the lumped and distributed modelling approaches fail to simulate the early on-set of snow but once the snow-holding capacities are reached within the field site the model does well to simulate the average snow depth during the latter few days of snow survey as well as throughout the entire field season. Several model limitations are present which prevent the model from incorporating the scaling effects of topography, vegetation, and man-made objects as well as the effects from certain energy fluxes. These limitations are discussed further.

Acknowledgements

There are many people that I would like to thank that made it possible to complete this thesis. First and foremost I would like to thank my advisor Dr. Richard Kelly who took a chance on me and allowed me to come back to the University of Waterloo to join his excellent team of snow scientists. His passion for the subject inspired me to want to learn as much as I could during my tenure under his guidance. I especially want to thank him for allowing me the freedom to create my own study. It may have been more time consuming and at times, painful but in the end it was a great learning experience that I will never forget. Most importantly however, I would like to thank him for his enduring patience from start to finish of this little project. First round's on me! I'd also like to thank Dr. Claude Duguay who provided me with the opportunity to gain some valuable and memorable field experiences outside of my own study. I'll never forget our little Alaskan snowmachine excursion in -65°C weather. At Wilfrid Laurier University I would like to thank Dr. Bill Quinton who introduced me to the Cold Regions Hydrological Model and helped peak my interest in its applicability to modelling snow depth. I'd also like to thank Dr. Mike English, whose long-standing local connections at Strawberry Creek helped us establish contact with the Zinger family who granted us permission to set up on Martz farm. At the University of Saskatchewan I would like to thank Mr. Tom Brown and Mr. Matt Macdonald for their help and support when I had a whole host of modelling questions. I feel as if it was a learning experience for us all.

Secondly, but equally as important, I would like to thank my family for their support through this entire process. They saw firsthand the process that I went through in order to complete this thesis and they were there to listen to all the issues even when most of the time they didn't really understand what I was talking about. They were also there for me during all 'the other stuff' that

went on in my life and for that, I am very grateful. It was nice to know that I could always count on them for support and to put a roof over my head or pay the odd bill when I needed it.

Lastly I would like to thank my friends and fellow students who graciously accepted the change in topic whenever they would ask “are you done yet?”

Table of Contents

<i>AUTHOR'S DECLARATION</i>	ii
<i>ABSTRACT</i>	iii
<i>ACKNOWLEDGEMENTS</i>	iv
<i>TABLE OF CONTENTS</i>	vi
<i>LIST OF FIGURES</i>	ix
<i>LIST OF TABLES</i>	x
<i>LIST OF EQUATIONS</i>	xi
<i>LIST OF SYMBOLS</i>	xiii
<i>1. INTRODUCTION</i>	1
1.1 <i>THE NATURE OF SNOW IN THE WATER CYCLE</i>	1
1.2 <i>HYDROLOGICAL MODELLING</i>	3
1.2.1 <i>Small Scale Models</i>	5
1.2.2 <i>Regional Snow Models</i>	5
1.2.3 <i>Global Climate Models</i>	6
1.2.4 <i>Model Challenges</i>	7
1.3 <i>OBJECTIVES</i>	9
1.4 <i>THESIS LAYOUT</i>	10
<i>2. BACKGROUND</i>	11
2.1 <i>PHYSICAL PROCESSES OF SNOW</i>	12
2.1.1 <i>Precipitation</i>	12
2.1.2 <i>Density</i>	13
2.1.3 <i>Snow Depth</i>	15
2.1.4 <i>Snow Water Equivalent</i>	15
2.2 <i>ENERGY AND MASS BALANCE COMPONENT MODELS FOR A SNOWPACK</i>	17
2.2.1 <i>Energy Balance components</i>	17
2.2.2 <i>Shortwave Radiation Input (K)</i>	18
2.2.3 <i>Long-wave Radiation Input (L)</i>	21
2.2.4 <i>Sensible Heat Exchange with the Atmosphere (H)</i>	22
2.2.5 <i>Latent Heat Exchange with the Atmosphere (LE)</i>	23
2.2.6 <i>Heat Input from Rain (R)</i>	23
2.2.7 <i>Heat Input from the Ground</i>	24
2.2.8 <i>A comparison of Four Different Energy Balance Equations</i>	24
2.2.9 <i>Mass Balance Components</i>	26
2.2.10 <i>Sublimation, Evaporation, and Condensation of a Snowpack</i>	27
2.2.11 <i>Canopy Interception</i>	27
2.2.12 <i>Blowing Snow</i>	28
2.3 <i>BLOWING SNOW AND THE WINTER MOISTURE BUDGET</i>	28

2.3.1	<i>The winter moisture budget</i>	30
2.3.1.i	<i>Precipitation</i>	30
2.3.1.ii	<i>Snow depth measurements</i>	31
2.3.1.iii	<i>Sublimation</i>	32
2.4	<i>Summary of Energy Balance + Mass Balance of Snow</i>	33
3.	<i>THE MODELS</i>	35
3.1	<i>THE PRAIRIE BLOWING SNOW MODEL</i>	35
3.1.1	<i>Saltation</i>	35
3.1.2	<i>Suspension</i>	37
3.1.3	<i>Sublimation</i>	39
3.1.4	<i>Erosion and Deposition</i>	41
3.2	<i>THE MINIMAL SNOWMELT MODEL</i>	44
3.3	<i>SUMMARY</i>	45
4.	<i>METHODS</i>	47
4.1	<i>STUDY SITE</i>	47
4.2	<i>DIGITAL IMAGERY AND DATA</i>	51
4.3	<i>METEOROLOGICAL DATA</i>	52
4.3.1	<i>Ultrasonic snow depth sensors vs. traditional snow measurement techniques</i>	53
4.3.2	<i>Meteorological data alteration in order for proper model runs</i>	56
4.4	<i>SNOW SURVEYS</i>	56
4.5	<i>MODEL RUNS</i>	58
4.5.1	<i>Lumped Model – Point Scale</i>	58
4.5.2	<i>Lumped Model – Field Scale</i>	59
4.5.3	<i>Distributed Model – Field Scale</i>	59
4.5.4	<i>Model Parameters</i>	59
4.6	<i>MODEL TESTING AND VERIFICATION</i>	64
4.7	<i>SUMMARY</i>	67
5.	<i>RESULTS</i>	68
5.1	<i>FIELD RESULTS</i>	68
5.2	<i>MODEL RESULTS</i>	70
5.3	<i>COMPARISON OF SIMULATED MODEL RESULTS AND OBSERVED SNOW SURVEY RESULTS AT THE POINT AND FIELD SCALES.</i>	72
5.3.1	<i>Point Scale Results: Lumped</i>	73
5.3.2	<i>Field Scale Results: Lumped</i>	74
5.3.3	<i>Field Scale Results: Distributed</i>	75
5.4	<i>SUMMARY</i>	76
6.	<i>DISCUSSION AND CONCLUSIONS</i>	78
6.1	<i>EVALUATING MODEL PERFORMANCE AND SOURCES OF ERROR</i>	78
6.2	<i>FUTURE CONSIDERATIONS</i>	83

6.3	<i>CONCLUSIONS</i>	84
	<i>REFERENCES</i>	86
	<i>APPENDICES</i>	94
	<i>APPENDIX 1</i>	94
	<i>APPENDIX 2</i>	96

List of Figures

1-1	Classification of hydrological modelling by means of how they deal with the factors of randomness, space, and time	4
1-2	SnowMIP2 analysis from Boulder, CO	7
2-1	A block of snow	17
2-2	Exponential decay of solar radiation with depth for a typical snowpack or glacier	20
2-3	Schematic diagram of the mass balance of a snowpack	26
3-1	Process of saltation and suspension of sediments into the atmosphere	36
3-2	Cross sectional view of a column of blowing snow	42
4-1	Location of Strawberry Creek field site	47
4-2	360° view of field sight from eight cardinal directions	49
4-3	Grand River watershed	50
4-4	<i>In situ</i> view of meteorological tower	53
4-5	Seasonal snow depth measurements from SR50a compared to manual snow depth measurements from the Waterloo-Wellington International Airport	55
4-6	Map of snow depth transects	57
4-7	Distributed map of CRHM hydrological response units	60
4-8	Simplified schematic diagram of the progression of module observations through the CRHM model modules	63
5-1	Corrected meteorological data from Strawberry Creek	69
5-2	Comparison of averaged model and observed snow depth	71
5-3	Comparison of averaged model and observed snow depth for each HRU in the distributed modelling approach	72

List of Tables

1-1	Classification of snow	2
2-1	Classification scheme of SWE	16
4-1	List of selected meteorological instrumentation	52
4-2	CRHM model parameters	61
4-3	Characteristics of HRU parameters for blowing snow	62
5-1	Monthly climatic averages for Strawberry Creek (2008-2009 model season) and Waterloo-Wellington International Airport (1971-2000)	68
5-2	Sample size of snow depth from each day of snow survey used for statistical analysis	73
5-3	RMSD, NS, and MB results for the lumped modelling approach at the point scale	73
5-4	RMSD, NS, and MB results for the lumped modelling approach at the field scale	74
5-5	RMSD, NS, MB results for the distributed modelling approach at the field scale	75

List of Equations

[2.1]	Fresh snow density 1	14
[2.2]	Fresh snow density 2	14
[2.3]	Snow water equivalent (SWE)	15
[2.4]	Simple equation to explain energy balance	17
[2.5]	Net rate of energy exchange	18
[2.6]	Net shortwave radiation	18
[2.7]	Transmission, absorption, and reflectance of shortwave radiation	19
[2.8]	Beer's Law	20
[2.9]	Net longwave radiation	21
[2.10]	Net longwave radiation under full cloud cover	22
[2.11]	Sensible heat exchange with the atmosphere	22
[2.12]	Sensible heat equation adapted for snow	22
[2.13]	Latent heat exchange with the atmosphere	23
[2.14a]	Heat input from the rain for a 'wet' snowpack	23
[2.14b]	Heat input from the rain for a 'cold' snowpack	23
[2.15]	Heat input from the ground	24
[2.16]	Marsh's energy balance equation	24
[2.17]	Male's energy balance equation 1	25
[2.18]	Male's energy balance equation 2	25
[2.19]	Net change in mass storage	26
[2.20]	Snowfall canopy interception	27
[2.21]	Maximum snowload on a canopy	28
[2.22]	The winter moisture budget	30
[3.1]	Saltation transportation	36
[3.2]	Atmospheric friction velocity	36
[3.3]	Roughness height for blowing snow	37

[3.4]	Suspension transportation rate	38
[3.5]	Upper boundary height of a column of blowing snow	38
[3.6]	Lower boundary height of a column of blowing snow	38
[3.7]	Rate of change of mass with respect to time	39
[3.8]	Nusselt and Sherwood Numbers	40
[3.9]	Reynold's Number	40
[3.10]	Ventilation velocity in the suspension layer	40
[3.11]	Ventilation velocity in the saltation layer	40
[3.12]	Undersaturation of water vapour with decreasing relative humidity with increasing height	41
[3.13]	Undersaturation of water vapour with increasing relative humidity with increasing height	41
[3.14]	Rate of sublimation	41
[3.15]	Rate of erosion/deposition	42
[3.16]	Mass balance equation for an HRU	43
[3.17]	Sensible heat flux within the MSM module	44
[3.18]	Latent heat flux within the MSM module	44
[3.19]	Net radiation absorbed by snow surface within the MSM module	45
[3.20]	Energy balance equation within the MSM module	45
[3.21]	Mass balance equation within the MSM module	45
[4.1]	Speed of sound in air	54
[4.2]	Root mean square difference	65
[4.3]	Nash-Sutcliffe coefficient	65
[4.4]	Model bias	65

List of Symbols

Symbol Quantity

SI Units

Roman capital letters

<i>A</i>	<i>surface area</i>	m^3
<i>A_{st}</i>	<i>exposed silhouette area of a single vegetation element</i>	
<i>C_H</i>	<i>surface exchange coefficient</i>	
<i>C_h</i>	<i>boundary layer coefficient</i>	$m^{-0.27} s^{1.27}$
<i>C_{salt}</i>	<i>saltation constant</i>	$m s^{-1}$
<i>C_{st}</i>	<i>coefficient for vegetation</i>	
<i>C_z</i>	<i>coefficient for prairie snowcover</i>	
<i>D</i>	<i>snow water equivalent depth</i>	mm
	<i>diffusivity of water</i>	$m^2 s^{-1}$
<i>D_p</i>	<i>Snow distribution factor</i>	
<i>D_H</i>	<i>diffusivity of sensible heat</i>	$m^2 s^{-1}$
<i>D_M</i>	<i>diffusivity of momentum in turbulent air</i>	$m^2 s^{-1}$
<i>D_{wv}</i>	<i>diffusivity of water vapour in turbulent air</i>	$m^2 s^{-1}$
<i>E</i>	<i>evapotranspiration</i>	$mm; kg m^{-2} s^{-1}$
<i>E_B</i>	<i>blowing snow sublimation rate</i>	$kg m^{-2} s^{-1}$
<i>F</i>	<i>downwind transport rate</i>	$kg m^{-2} s^{-1}$
<i>G</i>	<i>heat input from the ground (substrate)</i>	$W m^{-2}$
<i>H</i>	<i>sensible heat exchange with the atmosphere</i>	$W m^{-2}$
<i>I</i>	<i>canopy interception</i>	$kg m^{-2}$
<i>I*</i>	<i>maximum snow load</i>	$kg m^{-2}$
<i>I₀</i>	<i>snow load</i>	$kg m^{-2}$
<i>K</i>	<i>shortwave radiation input</i>	$W m^{-2}$
<i>K_↓</i>	<i>incoming shortwave radiation</i>	$W m^{-2}$
<i>K_↑</i>	<i>outgoing shortwave radiation</i>	$W m^{-2}$

K_a	<i>Thermal conductivity of air</i>	$W m^{-1} K^{-1}$
L^*	<i>longwave radiation exchange</i>	$W m^{-2}$
L_{\downarrow}	<i>incoming longwave radiation</i>	$W m^{-2}$
L_{\uparrow}	<i>outgoing longwave radiation</i>	$W m^{-2}$
LAI	<i>leaf area index</i>	
LE	<i>latent heat exchange with the atmosphere</i>	$W m^{-2}$
M	<i>molecular weight of water</i>	$kg kmol^{-1}$
	<i>melt rate</i>	$kg m^{-2} s^{-1}$
MB	<i>Model Bias</i>	
N	<i>total number of particles per unit volume</i>	
NS	<i>Nash-Sutcliffe coefficient</i>	
N_{st}	<i>number of vegetation elements per unit area</i>	m^2
Nu	<i>Nusselt number</i>	
P	<i>air pressure;</i>	Pa
	<i>precipitation</i>	
	<i>snowfall rate</i>	$kg m^{-2} s^{-1}$
Q^*	<i>net all-wave energy</i>	$W m^{-2}$
Q_l	<i>specific humidity at the measurement height</i>	
Q_G	<i>heat flux from the ground at the soil-snow interface</i>	$W m^{-2}$
Q_H	<i>sensible heat flux</i>	$W m^{-2}$
Q_i	<i>energy flux due to net radiation, sensible and latent heat fluxes</i>	
	<i>and heat transfers from lower layers of the snowpack</i>	$W m^{-2}$
Q_{LE}	<i>latent heat flux</i>	$W m^{-2}$
Q_M	<i>available energy for melt</i>	$W m^{-2}$
Q_r	<i>radiant energy received by a particle</i>	$W m^{-2}$
Q_{sat}	<i>saturation humidity at the snow surface</i>	
Q_{salt}	<i>saltation transportation rate</i>	$kg m^{-1} s^{-1}$

Q_{subl}	sublimation rate per unit area of snowcover	$kg\ m^{-2}\ s^{-1}$
Q_{susp}	suspension transportation rate	$kg\ m^{-1}\ s^{-1}$
R	heat input from rain	$W\ m^{-2}$
	universal gas constant	$J\ kmol^{-1}\ K^{-1}$
Re	Reynolds number	
RMSD	Root mean square deviation	(same as obs/simulated)
R_s	snowfall rate for a unit of time	$mm\ s^{-1}$
S	net rate of energy exchanges; Sublimation	$W\ m^{-2}$
SD	snow depth	m
Sh	Sherwood number	
S_p	tree species coefficient	
SWE	snow water equivalent	mm
T_a	temperature of air	$K, (^{\circ}C)$
T_{at}	absolute radiative temperature of the atmosphere and canopy	$^{\circ}C$
T_c	cloud base temperature	$^{\circ}C$
T_r	temperature of the rain	$^{\circ}C$
T_s	surface temperature	$^{\circ}C$
T_{ss}	absolute temperature of the snow surface	$^{\circ}C$

Roman small letters

a	extinction coefficient	m^{-1}
c_a	heat capacity of air at a constant temperature	$J\ kg^{-1}\ ^{\circ}C^{-1}$
c_{can}	canopy coverage fraction	
c_{subl}	sublimation loss rate coefficient	
c_{suc}	snow unloading coefficient	
c_w	heat capacity of water	$J\ kg^{-1}\ ^{\circ}C^{-1}$

d_r	particle size increment	m
d_s	snow depth	cm
$dSWE/dt$	surface snow accumulation rate	$kg\ m^{-2}\ s^{-1}$
dT/dz	temperature gradient of the soil	
du/dt	rate of change of internal energy	$KJ\ s^{-1}\ m^{-2}$
e	base of Napierian logarithms	
e_i	saturation vapour pressure over ice	Pa
e_s	vapour pressure at the surface	Pa
g	acceleration due to gravity	$m\ s^{-1}$
h	specific enthalpy	$KJ\ kg^{-1}$
h^*	lower boundary of suspension layer	
h_s	height of snow	m
k	von Karman's constant	m
k_G	thermal conductivity of the soil	$W\ m^{-1}\ ^\circ C^{-1}$
m	measurement height	m
	mass	kg
n	sample size	
$n(z)$	mass concentration of suspended snow	$kg\ m^{-3}$
p	precipitation	mm
	probability of blowing snow occurrence within the HRU	
ph_i	energy transfer due to precipitation	$kg\ m^{-2}\ s^{-1}$
q_v	vertical flux at the top of the controlled volume	$kg\ m^{-2}\ s^{-1}$
r	rate of rainfall	$mm\ d^{-1}$
	radius of snow particle contacting mass	
u	velocity of wind	$m\ s^{-1}$
u^*	atmospheric friction velocity	$m\ s^{-1}$
ν	kinematic viscosity of air	$m^2\ s^{-1}$

v_r	<i>ventilation velocity</i>	$m s^{-1}$
w_s	<i>terminal velocity</i>	$m s^{-1}$
z	<i>vertical distance</i>	m
z_b	<i>upper boundary of suspension layer</i>	
Greek capital letters		
Δt	<i>change in time</i>	s
ΔQ	<i>change in heat energy absorbed by the snowpack</i>	$W m^{-2}$
Δr	<i>net surface and subsurface horizontal exchange</i>	mm
ΔS	<i>net change in mass storage per unit volume (per unit horizontal area)</i>	$kg; kg m^{-3} s^{-1}$ $kg m^{-3} s^{-1}$
Ψ	<i>transmissivity</i>	
Greek small letters		
α	<i>surface albedo</i>	
ε	<i>surface emissivity</i>	
ε_{ss}	<i>emissivity of the snow surface</i>	
ε_{at}	<i>integrated emissivity of the atmosphere and canopy</i>	
ζ	<i>absorptivity</i>	
λ_f	<i>latent heat of fusion</i>	$J kg^{-1}$
λ_s	<i>latent heat of sublimation</i>	$J kg^{-1}$
λ_v	<i>latent heat of vapourization</i>	$J kg^{-1}$
σ	<i>Stefan-Boltzmann constant</i>	$W m^{-2} K^{-4}$
	<i>water vapour deficit with respect to ice</i>	
σ_2	<i>undersaturation of water vapour</i>	
ρ_a	<i>density of air</i>	$kg m^{-3}$
ρ_s	<i>density of snow</i>	$kg m^{-3}$
ρ_{sat}	<i>saturation density of water vapour</i>	$kg m^{-3}$
ρ_w	<i>density of water</i>	$kg m^{-3}$

Subscripts

a *air*

n *sheer stress applied to non-erodible surfaces*

o *surface*

observed values

s *simulated results*

t *sheer stress applied to snow surfaces*

Chapter 1.

Introduction

1.1 The Nature of Snow in the Water Cycle

Snow exerts a major influence on the environment and human activity on the Earth's surface. Through its high albedo, it plays a significant role in the climate system and is a sensitive indicator of climate change and variability. There are many locations in the world that are seasonally covered with snow and people living in these locations have learned to adapt to its many adverse and beneficial effects. Blowing snow on transportation, heavy snow loads on structures and buildings, rapid snowmelt resulting in flooding (especially over frozen ground), and acid-shock entering aquatic systems are just some of the examples of adverse effects of snow (Hiemstra et al., 2002). Snow removal is a prominent feature in municipal budgeting and more often than not, large snow storms can have a significant effect on a population's mobility due to the disruption of power and transportation services. These same storms can also lead to an increased amount of shovelling-related heart attacks, resulting in numerous cases of hospitalization and even fatalities each year. Examples of beneficial effects include the fact that snow acts as an insulator to flora and fauna, providing shelter from the harsh winter climates. Melting snow augments soil water reserves and replenishes ground water supplies and reservoirs. This is very important to agricultural activities in southern Ontario as many farms rely on the melting of the seasonal snow cover to aid in ground water recharge, decreasing the need for increased irrigation. Furthermore, the winter recreation industry relies heavily on seasonal snow cover. In southern Ontario alone there are numerous downhill and cross-country ski centres, as well as thousands of kilometres of groomed snowmobile trails for recreation.

Patterns of snow accumulation are not uniform across the globe. Its physical nature varies from location to location and is highly dependent on latitude, altitude, and meteorological conditions such as temperature, wind, relative humidity, and vapour pressure. Table 1-1 demonstrates a simple classification of snow derived by Sturm *et al.* (1995) from an analysis of snow cover meteorological conditions in Alaska.

Snow Cover Class	Description
Tundra	A thin, cold, windblown snow. Maximum depth, ~75 cm. Usually found above or north of tree line. Consists of a basal layer of depth hoar overlain by multiple wind slabs. Surface zastrugi common. Melt features rare.
Taiga	A thin to moderately deep low-density cold snowcover. Maximum depth 120 cm. Found in cold climates in forests where wind, initial snow density, and average winter air temperatures are all low. By late winter consists of 50-80% depth hoar covered by low-density new snow.
Alpine	An intermediate to cold deep snowcover. Maximum depth, ~250 cm. Often alternate thick and thin layers, common as well as occasional wind crusts. Most new snowfalls are low density. Melt features occur but are generally insignificant.
Maritime	A warm deep snowcover. Maximum depth can be in excess of 300 cm. Melt features (ice layers, percolation columns) very common. Coarse-grained snow due to wetting ubiquitous. Basal melting common.
Ephemeral	A thin, extremely warm snowcover. Ranges from 0 to 50 cm. Shortly after basal melting common. Melt features common. Often consist of a single snowfall, which melts away; then a new snowcover re-forms at the next snowfall.
Prairie	A thin (except in drifts) moderately cold snowcover with substantial wind drifting. Maximum depth, ~100 cm. Wind slabs and drifts common.
Mountain, special cases	A highly variable snowcover, depending on solar radiation effects and local wind patterns. Usually deeper than associated type of snowcover from adjacent lowlands.

Table 1-1. Classification of snow cover (Sturm *et al.*, 1995)

Even though the different classes of snow cover were derived from data acquired in Alaska, they are transferable to many locations. Southern Ontario experiences both ephemeral and prairie-like snow covers depending on the time of year and climatological conditions. In terms of hydrological modelling, the understanding of specific types of snow classes is important because it can lead to appropriate parameterization in the modelled location.

This brief overview of snow highlights some of the environmental, economical, social, and climatological aspects that snow has on our lives. Further information of the physical properties of snow and its importance to energy and mass balance models can be found in Chapter 2.

1.2 Hydrological Modelling

Estimating snow accumulation from point *in situ* measurements and hydrologic models is an important approach to help manage snow resources. To accurately predict or estimate a hydrological process it is important to understand the nature of a system. A system is essentially a set of equations linking the input and the output variables. These variables can be functions of space, time, and whether or not there is an effect of randomness. Hydrological models are “simplified models that are used to represent real-life systems and may be substitutes of the real systems for certain purposes” (Diskin, 1970). To develop a model with time and space varying parameter and variables is challenging. From a practical point of view it becomes necessary to simplify the model by neglecting some of the sources of variation. Chow *et al* (1988) developed a method of classifying hydrological models according to how they deal with these factors of variation. This classification scheme (Figure 1-1) is created by asking three simple questions: Will the model variables be random or not? Will they vary or be uniform in space? Will they vary or be constant in time?

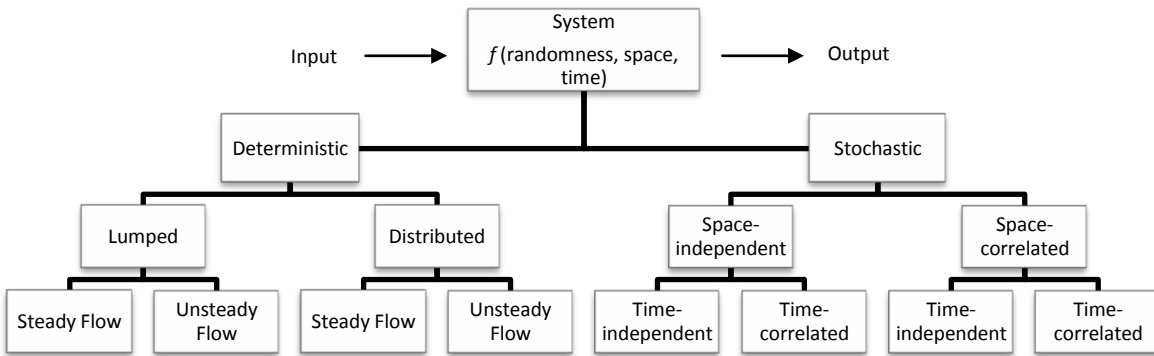


Figure 1-1: Classification of hydrological modelling by the means of how they deal with the factors of randomness, space, and time. Modelled after Chow et al, 1988.

The first line in the classification scheme deals with how the model relates to the factor of randomness. Although all hydrological phenomena often have some form of randomness, the resulting variability in the model output may be quite small when compared to the variability from known factors. When this is the case, a deterministic model is appropriate because this type of model does not consider randomness. In a deterministic model, a given input always produces the same output. Stochastic models on the other hand have outputs that are at least partially random. When the random variation is large, a stochastic model is more appropriate due to the fact that the actual output from such a model could be quite different from the output produced by a deterministic model. This thesis uses a deterministic model, therefore, the following section from this point forward deals solely with deterministic modelling rather than stochastic. For more information concerning stochastic modelling, see Chow et al, (1988). It is important to note that the above statements assume a normal distribution to the observed data. In some cases however, a poor fit to observed data is obtained and a different distribution function should be considered. As a hydrological example, if the probability of a certain number of events occurring

in a specified period of time is needed (e.g. when the temperature exceed a certain amount or certain levels of snowfall are reached), then a Poisson and/or Gamma distribution are frequently used.

The second line in the classification scheme deals with how the model relates to spatial variation. Real life hydrological problems deal with space in all three dimensions but when it comes to developing a model to practically represent such conditions, it can be quite cumbersome. A deterministic lumped model spatially averages the system so that it is represented as a single point in space without dimensions. Contrary to this, a deterministic distributed model defines the model variables as functions of space by considering the hydrological process to be occurring at various points in space.

The third line in the classification scheme deals with how the model relates to the variability of time. Deterministic models can be broken down into either steady-flow models, where the flow rate varies with time, and unsteady-flow.

Many hydrological models can provide the user with an accurate simulation over the required domain. These models are generally quite simple and may in fact only be able to simulate a few processes and tend to be rather small in scale. When attempting to increase the scale and/or the number of processes being modelled, many hydrological models are coupled with land surface models as well as atmospheric circulation models. These models range from being simple to complex.

1.2.1 Small Scale Models

Most of the smaller scale snow models are one-dimensional energy balance models that deal with a snow pack over a very small area. Some of the more complicated models venture into two

or three dimensions but are more susceptible to error due to an increase in the amount of variables involved. Some examples of such models include: SNTHERM (Jordan, 1991), SNOWPACK (Bartelt and Lehning, 2002), CROCUS (Brun et al., 1989), SnowTran-3D (Liston and Strum, 1996) and the Prairie Blowing Snow Model (Pomeroy et al., 1993). These models are straightforward although not always simple to use and require computing power. Input variables for these models are primarily gathered from local meteorological stations.

1.2.2 Regional Snow Models

Larger scale models are designed to cover a larger area and can become more complicated as they deal with regional scale processes. These types of models range from spatial models of catchment run-off processes with strong snow showing (UEB (Tarboton et al., 1995)) to large-scale land surface models (CLASS (Verseghy, 2000), MESH(Pietroniro, et al., 2006)). These larger models will typically incorporate other small models within them which allow them to simulate a number of processes, often simultaneously. In order to run these models successfully, a larger number of forcing variables are necessary, due to the larger number of processes being simulated, as well as a larger amount of computing power. Input variables for these models are usually gathered from (but are not limited to) a network of local meteorological stations and depending on the size of the study area, can also be remotely sensed from satellites and aircrafts.

1.2.3 Global Climate Models

The largest scalar models are lumped into the grouping of global climate models (GCM). These models cover very large areas, require a large amount of input variables, and take time and computing power to run. Examples of these models include the CGCM1 (Flato et al., 2000), the ECHAM models (Roeckner, 1992, 1996, 2003, Roesch and Roeckner, 2006) and the HadCM3 (Gordon et al., 2000) to name a few. Due to the scale of these models, input variables are gathered remotely through satellite sensors.

1.2.4 Model Challenges

The concept of scale is also very important as it determines the input requirements and the output restrictions. Singh (1995) provides a brief outline into 25 different hydrological models. Of those 25 models, only 11 include snow processes (Singh, 1995). This demonstrates the problems that many modellers face when attempting to design a model that can simulate the natural processes that occur in the cryosphere during the snow accumulation and ablation season. In many cases, the models do not consider every snow process and instead, focus on just a few. There is a common belief that parameterization with accurate data and representative forcing data will increase the model's accuracy. However, recent studies comparing many models clearly demonstrate the inability of some models to accurately simulate the *in situ* conditions of snow processes (Essery, et al., 2008, Rutter, et al., 2009). The SnowMIP (Model Inter-comparison Project) was a comparison of atmospheric general circulation models, hydrologic snowmelt

models, numerical weather prediction models, and detailed avalanche and snow physics models (Essery and Yang 2001).

Figure 1-2 demonstrates the simulated results for snow water equivalent (SWE) from the 24 models in the SnowMIP project.

The black lines are the model runs from each model and the green dots are the *in situ* measurements.

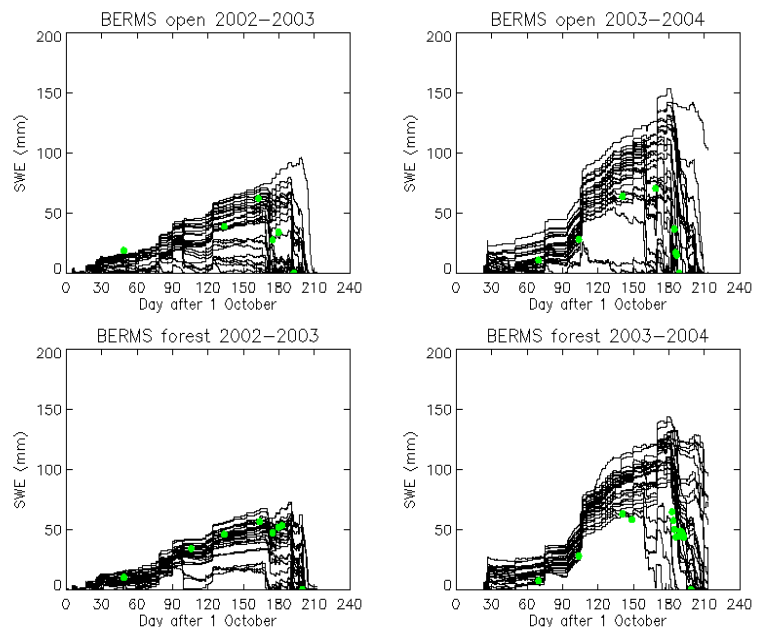


Figure 1-2: SnowMIP2 analysis from Boulder, CO. The solid black lines are the model runs. The green dots are the *in situ* values. (from Rutter et al., 2009)

This project is a clear example of how difficult it can be to simulate *in situ* observations and how site-specific models can be. One of the main problems with snow modelling is the fact that each model has been designed to simulate a specific type of landscape and may not (or on the rare occasion, may) be transferable from one location to another without serious error.

This thesis is concerned with the application of the Prairie Blowing Snow Model (PBSM) (Pomeroy et al., 1993). The model is a physically-based collection of algorithms that work in a deterministic lumped fashion. Distributed models need to be altered and usually coupled with other models in order to work properly. It was first developed in 1987 as a single column mass and energy balance that calculates blowing snow transport and sublimation rates (Pomeroy, 1988, 1989) and later extended to include a snow cover mass balance for the case of two dimensions (Pomeroy et al., 1993). The model has been updated several times to deal with issues including varying fetch and land use (Pomeroy et al., 1993) and varying terrain (Pomeroy et al., 1997; Essery et al., 1999). The current version that is used in this thesis is based on the 1997 version and is a modified, single column calculation with updated methods to calculate the inputs and scales of the fluxes from a point to a landscape in an areal snow mass balance calculation. It is located as a module within the 6.0 platform of the Cold Regions Hydrological Model (CRHM) (Pomeroy, 2007). CRHM is a modular modelling environment with a library of hydrological modules which can be selected and linked together to simulate the hydrological cycle in the natural environment. In this thesis, CRHM is used as a diagnostic tool to examine the blowing snow processes and seasonal changes in the accumulated snowpack. CRHM separates the landscape into individual units termed 'hydrological response units' (HRUs). HRUs are the largest landscape units having definable hydrological characteristics, meaning they can be described by unique sets of parameters, variables, and fluxes (Pomeroy *et al.*, 2007b). In order

for PBSM to work correctly it must be coupled to a snowmelt module. In this thesis it will be coupled to the MSM (Minimal snowmelt model) model. Further details about PBSM and MSM are found in the section devoted to the model descriptions.

1.3 Aims and Objectives

The aim of this thesis is to characterize snowpack changes throughout the 2008-2009 winter season at Strawberry Creek, Ontario, and to consider the scaling effects of the model as it is applied to various scales and in different formats with similar forcing data. To achieve this aim three objectives are identified. The first of these objectives is to implement the PBSM and MSM modules as a single model within the CRHM platform at the point scale. The second objective is to implement the model over the entire agricultural field in a lumped format. The third objective is to implement the model in a distributed format over the entire field.

a) Implementing PBSM and MSM at the point scale

The first objective is to implement the modules as a single model within the CRHM model platform at the point scale and then assess the model performance at this scale. This scale is defined as the area immediately surrounding the meteorological station (0.025km^2).

b) Implementing the model over an agricultural field in a lumped format

The second objective is to scale up from the point scale and apply the model over the entire agricultural field in a lumped format followed by assessing the model performance. This scale is defined as the area contained within the property borders (0.406km^2).

c) Implementing the model over an agricultural field in a distributed format

The third objective in this thesis is to implement the model at the same field scale as objective 2 but in a distributed format. The field is subdivided into three HRUs which have been determined based on vegetation height. The model performance is then assessed to determine the effects of vegetation height across the entire field at that scale.

1.4 Thesis Layout

This thesis is a modelling study of snow distribution in a blowing snow model by taking both a lumped and distributed approach. Chapter 1 covers the basics of hydrological modelling, problems associated with modelling snow, as well as a quick overview of snow properties. Chapter 2 provides a more in depth look at the physical properties of snow as well as energy and mass balance systems. Chapter 3 covers the background information about the models and modules used in this thesis. Chapter 4 outlines the study site and methodology of the project at Strawberry Creek. Chapter 5 displays the field results, both meteorological and snow survey, as well as the model results. Model performance and statistical analysis are also covered in this chapter. Chapter 6 further discusses the model performance as well as some of the sources of error that affect the model performance. Future considerations and concluding remarks round out this chapter.

Chapter 2.

Background – Snow accumulation and energy and mass exchanges through water

Seasonal snow falls and remains on the ground until later on in the season when it ablates. This seasonal cycle of snowfall can be broken down into two phases; the accumulation phase and the melting phase. The melt phase can be further broken down into phases of warming, ripening, and output (Dingman, 2002).

The accumulation phase occurs when there is a general increase in water equivalent and a decrease in temperature and net input of energy (Dingman, 2002). As snow falls through the atmosphere it is subject to a variety of physical processes until it either becomes intercepted by the vegetation canopy or is allowed to fall straight to the ground surface where it is further subjected to physical and metamorphic processes over time. Once on the ground, these effecting physical and metamorphic processes are dependent upon whether or not the snowpack is wet or dry. A snowpack is considered ‘wet’ when its temperature is at or above 0°C and a snowpack is considered ‘cold’ when its temperature is below 0°C. The accumulation phase is often dominated by dry snow conditions. Under these conditions, the metamorphic processes depend on whether the snowpack is isothermal or exhibits a temperature gradient (Male, 1980).

When the net energy within the snowpack is positive, the melt phase begins. The main processes of melt are dependent upon climate and location. In temperate regions, radiation is the main source of melt energy, followed by sensible and latent heat fluxes. Heat energy added by rain and the ground can also play important roles during the melt phase in both temperate and arctic environments.

The water which is generated from surface snow melt, or input from rainfall, results in a wet snowpack. Wet snow causes different metamorphic processes than dry snow because it causes smaller snow particles to disappear and allows larger particles to grow and fuse together with other particles. This results in a snowpack with less structural strength between the particles and a higher density. Colbeck (1978) states that the following loss in surface area causes a drop in capillary potential and may be the reason that a pack can be observed to release a lot of water very quickly in the early stages of melt.

Within the melt phase, the warming phase is the period in which the snow temperature increases to 0°C, the ripening phase is the period at which the melting snowpack can no longer hold any more water, and the output phase is the period when the snowpack releases the water (Dingman, 2002). The differentiation between all three of these melt phases is not always straightforward. A snowpack can undergo several stages before reaching a stage of isothermal energy due to the fact that there are large energy gradients between the atmosphere, snow, and ground which can cause the snow within the pack to melt and refreeze several times throughout the season. In many cases, snow will accumulate and melt several times in one season, often re-accumulating upon partially melted snowpacks. This can complicate the prediction of net snow water equivalent.

The following section will discuss some of the physical properties of snow as well as the energy and mass balances of a snowpack.

2.1 Physical Processes of Snow

2.1.1 Precipitation

Snow forms in the atmosphere where cloud temperatures are below 0°C. The large diversity of initial snow shapes is a result of the variety of temperature and humidity conditions possible

during crystal formation. As the snow falls through the atmosphere, the changes in temperature and humidity that the crystals encounter alters their form, compounded by collisions that further modify their structure (Male 1980). Many factors affect the characteristics of snow from formation to deposition. In the simplest of terms, precipitation can come in the form of rain or snow, or as a mixture of rain and snow, depending on the meteorological conditions as precipitation falls through the air. Further information on the various forms of precipitation, specifically snow, can be found within *The International Classification of Seasonal Snow on the Ground* (UNESCO/IHP, 2009).

2.1.2 Density

The density of snow is the mass per volume, usually specified in kilograms per cubic metre (kg/m^3). It is usually referred to as a ratio to the density of water (1000kg/m^3) and can vary dramatically depending on temperature. The growth of individual snowflakes depends on temperature and both the horizontal and vertical wind gradients. Predominately however, it is the temperature that derives the overall size and shape of the snowflake (DeWalle and Rango, 2008). Higher density snow usually results from warmer temperatures and/or higher winds whereas lower density snow results from cooler temperatures and less wind. Warmer temperatures allow snowflakes to rapidly decompose and coagulate with other snowflakes in the air or on the ground surface. This increase in mass as well as the fact that the snowflake temperature is closer to the melting point results in it having a higher density. Colder temperatures allow the snowflakes to remain angular and faceted for a longer period of time in the air and on the ground surface. This extended period of time results in a delayed coagulation of the snowflake with other flakes, leading to lower density values. Higher wind speed can compact snow on the ground surface into slab-like conditions, raising the density to a higher point than snow that has been left to settle at

lower wind speeds. New snow will have a much smaller density value than older snow due to snow settling. This is because older snow within a snowpack has been exposed to periods of melting, re-freezing, and wind fluctuations. As soon as a snowflake comes in contact with the ground surface it begins to change shape, losing its angular, faceted structure and developing into a small cluster of grains. Due to melting and re-freezing, these small grain clusters can coagulate with other grain clusters within the snowpack, developing a hard packed surface with a high density value. Fresh snow density has been found to vary from 70 to 100 kg/m³ by Goodison *et al.* (1981). Male (1980,) reported that fresh snow density can vary from 10 to 500 kg/m³. La Chapelle (1961) related snow density to air temperature from data collected at the Alta Avalanche Study Center and derived an equation for calculating the density of fresh snow which can be seen in equation 2.1. By examining the works of Diamond and Lowry (1953) and Schmidt and Gluns (1991), Hedstrom and Pomeroy (1998) developed another equation for calculating the density of fresh snow, which can be seen in equation 2.2 below.

$$\rho_s(\text{fresh}) = 50 + 1.7(T_a + 15)^{1.5} \quad [2.1]$$

$$\rho_s(\text{fresh}) = 67.92 + 51.25e^{\left(\frac{T_a}{2.59}\right)} \quad [2.2]$$

In both equations, $\rho_s(\text{fresh})$ is the fresh snow density (kg/m³), and T_a is the air temperature (°C). Snow density increases exponentially with time, as wind, sublimation, gravity, and warm periods change the internal structure of the snowpack. The maximum density of a snowpack ultimately depends on its location, landcover, and other factors (Fassnacht, 2000).

The snow density can also be measured using both *in situ* measurements as well as ground-based remotely sensed measurements. *In situ* measurements are gathered through the use of snow pit and gravimetric samples. Remotely sensed measurements include microwave radar (Frequency-

Modulated Continuous Waves and Ground Penetrating Radar) (Marshall et al., 2004), and gamma ray attenuation.

2.1.3 Snow Depth

Snow depth is the accumulation of snow over a given period of time. The depth of snow at a given area is a factor of the climatological conditions (temperature + precipitation), the topography (slope + aspect), wind conditions (direction + velocity), as well as the land-use cover and vegetation characteristics. Changes in snow depth can be the result of an increase in accumulated precipitation after a snow storm, and can decrease due to melting. Furthermore, snow depth varies in response to changes in snow density (e.g. decrease in volume without a change to mass). For energy and mass balance purposes, it is more pertinent to measure a net change in mass storage rather than just the depth of the snowpack. The snow cover depth can be measured *in situ* or remotely sensed using an automated measuring device (e.g. MagnaProbe), a snow ruler, graduated rod, aerial markers, and ultrasonic snow depth sensors (sonar).

2.1.4 Snow Water Equivalent

Snow water equivalent (SWE) is the equivalent depth of water of a snow covered area. Since a uniform depth of 1mm of water spread over an area of 1m² weighs 1kg, SWE is calculated from the snow depth, d_s , and the snow density, ρ_s , by the expression:

$$SWE = 0.01d_s\rho_s \quad [2.3]$$

in which SWE is in mm when d_s is in cm and ρ_s is in kg/m³ (Dingman, 2002). As the density of the snowpack changes, so too will the SWE. An average density of 100kg/m³ is often assumed for freshly fallen snow. This gives 1 unit of water equivalent for 10 units of snow depth. It is

however, not appropriate to use a common conversion for all environments (Pomeroy and Gray, 1995). Once the amount of water equivalent is established, it becomes simple to determine how much energy is needed to either melt or freeze this depth of water given the appropriate latent heat values.

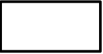

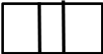


Term	Remarks	Approximate Range of θ	Graphic Symbol
Dry	Usually T is below 0°C, but dry snow can occur at any temperature up to 0°C. Dissaggregated snow grains have little tendency to adhere to each other when pressed together, as in making a snowball	0%	
Moist	T = 0°C. The water is not visible even at 10 x magnification. When lightly crushed, the snow has a distinct tendency to stick together.	<3%	
Wet	T = 0°C. The water can be recognized at 10 x magnification by its meniscus between adjacent snow grains, but water cannot be pressed out by moderately squeezing the snow in the hands. (Pendular regime)	3-8%	
Very Wet	T = 0°C. The water can be pressed out by moderately squeezing the snow in the hands, but there is an appreciable amount of air confined within the pores. (Funicular regime)	8-15%	
Slush	T = 0°C. The snow is flooded with water and contains a relatively small amount of air.	>15%	

Table 2-1. Classification scheme of SWE (Colbeck et al, 1990)

Table 2-1 shows that there are many different classification terminologies that can be assigned to a certain percentage of liquid water content (θ). Much like the depth and density, the SWE can be measured both *in situ* as well as by using a variety of remote sensors. *In situ* measurements include gravimetric sampling and snow pillows. Remotely sensed measurements (satellites, aircraft, etc) make use of algorithms and values of snow depth and density.

2.2 Energy and Mass Balance Component Models for a Snowpack

The following section provides a basic theoretical background for many different mathematical components that pertain to snow processes. It is important to have this background knowledge in order to fully understand how the model arrives at its results as well as to better understand what is naturally occurring in the environment.

2.2.1 Energy Balance components:

There are many different energy balance models that exist for snow but the differences between these models are quite subtle. In order to completely understand the mathematical models pertaining to snow it is necessary to view the snow in a finite condition. Figure 2-1 demonstrates a typical block of snow and describes the energy balance associated with that element of snow of surface area A and height h_s .

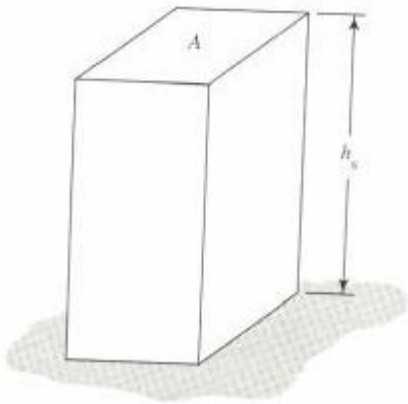


Figure 2-1: A Block of Snow (Dingman, 2002)

Dingman (2002) provides a simple equation to explain this energy balance and can be seen below:

$$(\Delta t)S = \Delta Q \quad [2.4]$$

Where S ($\text{E L}^{-2}\text{T}^{-1}$) is the net rate of energy exchanges into the element by all processes over a time period Δt (T), and ΔQ (E L^{-2}) is the change in heat energy absorbed by the snowpack during Δt . Dingman expresses the measurable quantities of S , Δt , and ΔQ in terms of fundamental physical dimensions of energy [E], length [L], and time [T]. The net rate of energy exchange, S (W m^{-2}) can be expanded, as seen in Equation 2.5:

$$S = K + L + H + LE + R + G \quad [2.5]$$

Where K (W m^{-2}) is the shortwave radiation input, L (W m^{-2}) is the long-wave radiation input, H (W m^{-2}) is the sensible heat exchange with the atmosphere, LE (W m^{-2}) is the latent heat exchange with the atmosphere, R (W m^{-2}) is the heat input from rain, and G (W m^{-2}) is the heat input from the ground. Determining a complete energy balance for a given snowpack is complicated. As will be discussed below, each term in Equation 2.5 can in turn be difficult to acquire due to the constant fluctuation of shortwave radiation penetration depths and diurnal and seasonal thermal variations within the snowpack.

2.2.2 Shortwave Radiation Input (K):

The net shortwave radiation input is described in Equation 2.6.

$$K = K \downarrow - K \uparrow = K \downarrow (1 - \alpha) \quad [2.6]$$

$K \downarrow$ is the incoming shortwave radiation, $K \uparrow$ is the outgoing shortwave radiation, and α is the albedo. Albedo is the representation of the fraction of radiation reflected from the snow surface and can vary from 0.04- 0.95, with new snow having the highest values and lesser values as the snow ages (Oke, 1987). Since snow is highly reflective, even the shallowest of snow covers alters the land surface albedo. Furthermore, the albedo of snow can vary diurnally with higher

values occurring in the early morning and later in the evening when solar incidence angles are low. At these lower angles, specular reflection dominates over diffuse reflection. Meteorological conditions such as cloud cover, seasonality, and the physical state of the snowpack can all have an influence on the albedo as well, allowing even more diurnal variation. The albedo for snow also varies with wavelength where higher albedo is found with shorter wavelengths and lower albedo with longer wavelengths.

Snow differs from other surfaces because it allows some transmission of shortwave radiation throughout the snowpack. This means that at any depth, the shortwave radiation can be transmitted (Ψ), reflected (α), or absorbed (ζ) according to the following equation (Oke, 1987):

$$\Psi + \alpha + \zeta = 1 \quad [2.7]$$

It is interesting to note however, that this transmittance, absorption, or reflectance of shortwave radiation is not universal throughout the vertical profile of the snowpack. The shortwave radiation at the surface ($K\downarrow_0$) is much stronger than that found at any depth below. As the shortwave radiation passes through the upper layers of the snow profile it begins to lose intensity at an exponential rate.

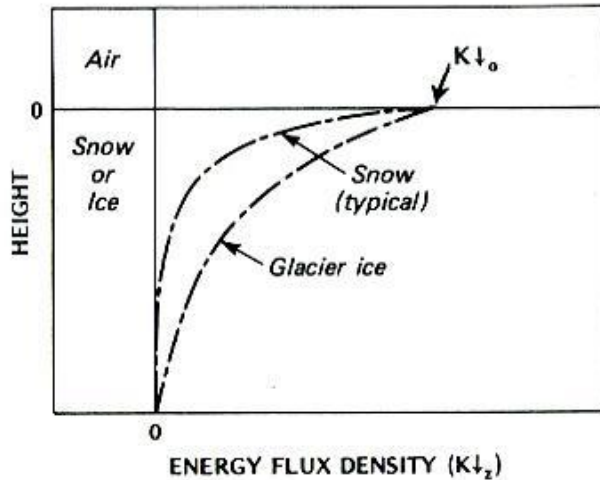


Figure 2-2: Exponential decay of solar radiation with depth for a typical snowpack and glacier. (Oke, 1987 after Geiger, 1965)

According to *Beer's Law*:

$$K \downarrow_z = K \downarrow_0 e^{-az} \quad [2.8]$$

the shortwave radiation reaching any depth z , is dependent on the shortwave radiation $K \downarrow_z$ at depth z , the base of natural logarithms e , and an extinction coefficient a (m^{-1}). The extinction coefficient is dependent on the nature of the medium that is being transmitted through and the wavelength of the radiation. As can be seen in the above diagram (Figure 2-2), snow has a larger coefficient than ice, therefore snow has a much shallower penetration depth. This penetration depth can be as great as 1m for snow and as much as 10m for ice (Oke, 1987).

The transmission of solar radiation within a snowpack can create problems when trying to monitor or observe the radiation for energy balance purposes. Instruments mounted above the snow surface may not only be measuring the reflectance from the surface but also some of the reflectance from some of the subsurface layers. The resulting albedo calculation would therefore be a volume and not a surface value.

2.2.3 Long-wave Radiation Exchange (L^*):

The net long-wave radiation exchange is described in Equation 2.9.

$$L^* = L \downarrow - L \uparrow = \varepsilon_{ss}\varepsilon_{at}\sigma T_{at}^4 - \varepsilon_{ss}\sigma T_{ss}^4 \quad [2.9]$$

$L \downarrow$ is the incoming long-wave radiation, $L \uparrow$ is the outgoing long-wave radiation, ε_{ss} is emissivity of the snow surface, ε_{at} is the integrated effective emissivity of the atmosphere and canopy, and σ is the Stefan-Boltzman constant ($5.67 \times 10^{-8} \text{ W m}^{-2}\text{K}^{-4}$). T_{at} is the absolute radiative temperature of the atmosphere and canopy and T_{ss} is the absolute temperature of the snow surface. Snow (especially fresh snow) is almost a perfect radiator. The emissivity of snow is usually assumed to be 1.0 but much like albedo, it too can vary with the age of the snow from 0.85 – 0.99 (Oke, 1987) as well as due to metamorphological processes (Grody, 1996). Even though the emissivity can be relatively high, the surface temperature T_{ss} is low, leading to $L \uparrow$ being overall, quite small. One of the major issues with implementing Equation 2.9 can be found in properly estimating absolute values for ε_{at} and T_{at} , or equivalently, to estimate a value for $L \downarrow$ under various conditions of cloudiness and forest cover. Methods for estimating $L \downarrow$ can be found in Dingman (2002).

Oke (1987) presents a very interesting scenario for estimating $L \uparrow$ when the snow surface is melting ($T_0 = 0^\circ\text{C}$ [273.2 K]). If we assume ε for snow to be a value of 1, and the surface temperature to be at the freezing point, then the value of $L \uparrow$ is constant at 316 W m^{-2} (substituting into equation 2.9). If this melting occurs under complete cloud cover, then the net long-wave exchange (L^*) between a fresh snowpack and the overcast sky becomes a function of their respective temperatures due to the fact that clouds are also close to being full radiators. This process can be seen in the following equation:

$$L^* = L \downarrow - L \uparrow \cong \sigma T_c^4 - T_0^4 \quad [2.10]$$

where T_c^4 is the cloud base temperature. If the cloud base temperature is warmer than the snow surface temperature then L^* will be positive. Under clear skies however, L^* is almost always negative.

2.2.4 Sensible Heat Exchange with the Atmosphere (H):

When vertical temperature gradients and turbulent eddies exist above the surface, sensible heat is transferred to the atmosphere. Equation 2.11 expresses the sensible heat exchange with the atmosphere.

$$H = \frac{D_H}{D_M} c_a \rho_a \frac{k^2 u_m}{\left\{ \ln \left[\frac{z_m - z_d}{z_0} \right] \right\}^2} (T_s - T_m) \quad [2.11]$$

D_H is the diffusivity of sensible heat, D_M is the diffusivity of momentum in turbulent air, c_a is the heat capacity of air at a constant temperature ($\text{J kg}^{-1} \text{ }^\circ\text{C}^{-1}$), ρ_a is the density of air (kg m^{-3}), k is a dimensionless constant (0.4), u_m is the velocity of wind (m s^{-1}) at height z_m (m), z_d is the zero-plane displacement, z_0 is the roughness height (m), T_s is the surface temperature ($^\circ\text{C}$), and T_m is the temperature of the measurement height ($^\circ\text{C}$). This equation can further be adapted for snow if we assume that both the wind speed, v_m , and air temperature, T_a , are measured at the same height, z_m (typically 2m above the ground surface), that the diffusivity of sensible heat and momentum are the same ($D_H = D_M$), and finally, that the zero-plane displacement, z_d , is negligibly small. With these assumptions Equation 2.11 becomes

$$H = c_a \rho_a \frac{u_m}{6.25 \left\{ \ln \left[\frac{z_m}{z_0} \right] \right\}^2} (T_s - T_m) \quad [2.12]$$

2.2.5 Latent Heat Exchange with the Atmosphere (LE):

When turbulent eddies and a vertical pressure gradient are both present, latent heat (water vapour) is transferred to the atmosphere. Equation 2.13 expresses the latent heat exchange with the atmosphere.

$$LE = \frac{D_{WV}}{D_M} \lambda_v \frac{0.622 \rho_a}{P} \frac{k^2 v_m}{\left\{ \ln \left[\frac{z_m - z_d}{z_0} \right] \right\}^2} (e_s - e_m) \quad [2.13]$$

In addition to the terms that have already been defined above, D_{WV} is the diffusivity of water vapour in turbulent air, λ_v is the latent heat of vaporization (J kg^{-1}), P is the air pressure (mb), e_s is the vapour pressure (Pa) at the surface and e_m is the vapour pressure (Pa) at height z_m .

2.2.6 Heat Input from Rain (R):

There are two equations that apply to the heat input from rain. These two equations are dependent on whether or not the snowpack is a ‘wet’ snowpack at or above the freezing point (Equation 2.14a) or if the snowpack is a ‘cold’ snowpack below freezing (Equation 2.14b).

$$R = \rho_w c_w r (T_r - T_m) \quad [2.14a]$$

$$R = \rho_w c_w r (T_r - T_m) + \rho_w \lambda_f r \quad [2.14b]$$

ρ_w is the density of water (kg m^{-3}), c_w is the heat capacity of water ($\text{J kg}^{-1} \text{ }^\circ\text{C}^{-1}$), r is the rate of rainfall (m s^{-1}), and T_r is the temperature of the rain ($^\circ\text{C}$). The only additional term for the heat input from rain in a snowpack below freezing is λ_f , which is the latent heat of fusion. If rain percolates through the snowpack it becomes an additional heat source which can then melt the surrounding snow and/or result in a possible addition to meltwater run-off.

2.2.7 Heat Input from the Ground (G)

Summer storage of thermal energy results in temperatures in the soil profile to increase downwards from the snowpack. The rate of heat that is conducted to the base of this snowpack is described in Equation 2.15.

$$G = k_G \frac{dT}{dz} \quad [2.15]$$

k_G is the thermal conductivity of the soil ($\text{W m}^{-1} \text{ }^\circ\text{C}^{-1}$) and dT/dz is the vertical temperature gradient in the soil. G becomes significant when the snowcover over top of the ground surface is thin and there a heat exchange across the base of the snowpack (Oke, 1987). When the snowpack is larger, it acts as a thermal insulator and the effect of G becomes rather unimportant (Oke and Hannell, 1966). Dingman (2002) states that G is usually negligible during a snowmelt season, but can be significant during the accumulation season.

2.2.8 A comparison of Four Different Energy Balance Equations:

The following section will examine several energy balance equations as they pertain to varying types of snowpack and how they deal with the different types of energy. For a more in depth comparison of snowmelt energy balances see Kuusisto (1986). The first of the four equations was put forth by Dingman (2002) and described above as Equation 2.5. The second equation comes from Marsh (1990) and is described below as Equation 2.16.

$$Q_M = Q^* + Q_H + Q_E + Q_R + Q_G - \frac{dU}{dt} \quad [2.16]$$

Q_M (W m^{-2}) is the available energy for melt (latent heat storage due to melting or freezing), Q^* (W m^{-2}) is the net all-wave radiation ($K + L$), Q_H (W m^{-2}) is the sensible heat flux, Q_E is the latent

heat flux, Q_R (W m^{-2}) is the heat flux from rain, Q_G (W m^{-2}) is the heat flux from the ground at the soil-snow interface, and dU/dt ($\text{KJ s}^{-1} \text{m}^{-2}$) is the rate of change of internal energy. The third and fourth equations both come from Male (1980) and can be seen as Equations 2.17 and 2.18 respectively below.

$$\sum Q_i + \sum (ph)_i = 0 \quad [2.17]$$

$$\frac{dU}{dt} = \sum Q_i + \sum (ph)_i \quad [2.18]$$

In Equation 2.17, Q_i (W m^{-2}) is the energy flux due to net radiation, sensible and latent heat fluxes, and heat transfer from the lower layers of the snowpack. $(ph)_i$ is the energy transfer due to precipitation, p ($\text{kg m}^{-2} \text{s}^{-1}$) with an associated specific enthalpy, h (KJ kg^{-1}). The second of Male's equations, Equation 2.18, dU/dt ($\text{KJ s}^{-1} \text{m}^{-2}$) is the change in internal energy of the pack. Male (1980, p.349) states that Equation 2.17 only requires measurements taken at or near the upper surface and is therefore suitable for deeper snowpacks. Equation 2.18 describes the entire thermal regime of the snowpack and can be practically used for shallow snowpacks of less than 40cm. When horizontal advection is substantial (i.e. not near open water, or patchy snow cover), neither equation is considered valid.

Of all the equations presented above, Equation 2.17 is the simplest. Equations from Dingman (Equation 2.5), Marsh (Equation 2.16), and Male (Equation 2.18) all consider the internal energy of the snowpack but the latter two equations also include the melt energy. In Equation 2.16 the melt energy remains in the form of energy but in Equation 2.18, the melt energy is actually the melt-water from the bottom of the snowpack. Both of Male's equations focus primarily on the melt phase but, as was previously mentioned, could be used for the accumulation phase so long as the conditions of negligible horizontal advection are met. Dingman and Marsh's equations

include both the accumulation and melt phases and are assumed to work for a snowpack of any depth. For the sake of this thesis the above statements shall remain strictly theoretical but a quick application of a common data set would help to better understand the differences among and uses between each equation.

2.2.9 Mass Balance Components

Acquiring a proper mass balance for a given snowpack can be rather difficult due to the constant phase changes occurring within the snowpack throughout the season. As was discussed in the above sections, a snowpack can be influenced by a variety of different factors that can result in diurnal and seasonal fluctuations in both the energy and mass balances.

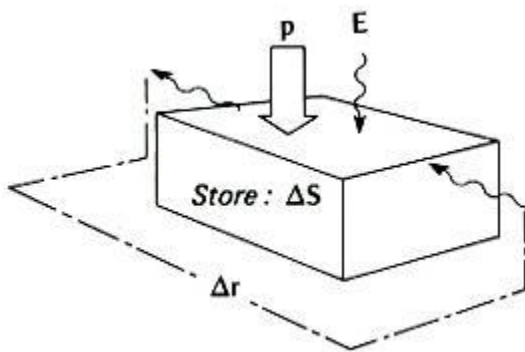


Figure 2-3: Schematic diagram of the mass balance of a snowpack (after Oke, 1987)

A simple mass balance can be determined if we assume a snowpack where the top section is exposed to the air interface and its lower section is either at the ground interface or is at a depth of negligible water percolation (Figure 2-3), we can assume that the net change in mass storage ΔS , is given by:

$$\Delta S = p - E + \Delta r \quad [2.19]$$

Where p is the precipitation input from either snow or rain, E is the net turbulent exchange with the atmosphere and can be in the form of condensation, sublimation (inputs) or evaporation and sublimation (outputs), and Δr the net surface and subsurface horizontal exchange (surface snow drifting and meltwater flow or subsurface meltwater throughflow) (Oke, 1987).

2.2.10 Sublimation, Evaporation, and Condensation of a Snowpack

As was mentioned above, water within a snowpack is susceptible to the physical processes of sublimation, evaporation, and condensation. These processes are driven by the vapour pressure gradient between the surface of the snowpack and the atmosphere. When the vapour pressure above the snowpack is greater than the vapour pressure at the surface, condensation occurs. When the vapour pressure above the surface is lower than the vapour pressure at the surface, sublimation or evaporation occurs.

2.2.11 Canopy Interception

When a vegetated canopy is present, snow can become trapped by the branches and foliage of the canopy, potentially inhibiting the trapped snow from reaching the snowpack on the ground surface. While suspended in the canopy, snow is susceptible to the same physical processes as snow on the ground surface and is not only significant to the overall energy and mass balance equations but is also subject to its own energy and mass balances. Falling snow is not the only method for which snow can become trapped within a canopy. Horizontally blown snow can also become a significant source of trapped snow. Hedstrom and Pomeroy (1998) estimated the snowfall canopy interception, I , as can be seen in Equation 2.20:

$$I = c_{suc}(I^* - I_0) \left(1 - e^{-\frac{c_{can}R_s}{I^*}}\right) \quad [2.20]$$

where c_{suc} is a dimensionless snow unloading coefficient found to be 0.697, I^* is the maximum snow load (kg m^{-2}), I_0 is the snow load (kg m^{-2}), R_s is the snowfall for a unit of time, and C_{can} is the canopy coverage fraction.

The maximum snow load can be determined using Equation 2.21; where S_p is a tree species coefficient, LAI is the leaf area index, and $\rho_s(fresh)$ is the fresh snow density (kg m^{-3}).

$$I^* = S_p LAI \left(0.27 + \frac{46}{\rho_s(fresh)} \right) \quad [2.21]$$

For the purpose of this thesis, canopy interception is considered negligible. Even though the field site is bordered by a small forest on one side and a thin treeline on another, the model has difficulty simulating the effects from these canopies due to the exclusion of canopy interception algorithms in the modules being used.

2.2.12 Blowing Snow

Blowing snow is a very important process as it is the main form of snow redistribution on the ground and within the atmospheric boundary layer. This redistribution of snow can and will have an effect on other processes such as the sensible and latent heat fluxes. It can be divided into two parts: saltation and suspension. Sublimation also plays an integral role in blowing snow transport and further information will be covered in the next few sections devoted to blowing snow and the Prairie Blowing Snow Model.

2.3 Blowing Snow and the Winter Moisture Budget

The redistribution of snow by wind is a very important concept for any hydrological research project located within the cryosphere. Wind redistributes snow by eroding it from areas of high wind speed, such as ridge tops and windward slopes, and deposits it in areas of lower wind

speed, such as the lees of ridge tops, vegetation stands, and topographic depressions (Benson and Sturm, 1993; Pomeroy et al., 1993; Liston and Sturm, 1998; Sturm et al., 2001a; Liston et al., 2002). When the prevailing winds constantly come from the same direction, a pattern of heterogeneous snow drifts occur in the same location year after year. This redistribution can lead to patterns of environmental conditions and ecosystem properties. Affected properties include net solar radiation, chemical inputs, meltwater distribution, rock weathering, pedogenesis, decomposition and mineralization, animal habitat, and vegetation (Hiemstra et al., 2002).

Snow is a loose surface, allowing saltation and suspension to act as the primary mechanisms for distributing it by wind (Kobayashi, 1972; Male, 1980; Takeuchi, 1980; Schmidt, 1982, 1986; Pomeroy, 1988; Pomeroy and Gray, 1990). Empirical and analytical relationship between wind speed and blowing snow transport rate developed by these researchers can be found within their snow-transport models and those developed by others (Tabler and others, 1990; Liston and others, 1993a; Bintanja, 1998a,b; Sundsbø, 1997; Purves and others, 1998). Others have shown that sublimation can be important, reducing the snowcover water balance by a significant fraction under certain conditions (Goodison, 1981; Benson, 1982; Benson and Sturm, 1993; Pomeroy and others, 1993, 1997). Modelling provides an alternative method for representing winter wind-transported processes over various landscapes. It offers an opportunity to evaluate the relative importance of driving variables, and producing scenarios based on alterations in these variables. Model outputs can in turn be distributed across realistic terrain and vegetation representations to produce landscape models that integrate key blowing snow processes (Pomeroy et al., 1997, Liston and Sturm, 1998). The following section explains the winter moisture budget and some of the associated problems that occur when attempting to acquire information that can be used in a blowing-snow transportation model.

2.3.1 The winter moisture budget

When the temperature falls consistently below freezing, the simplest way to describe the winter moisture budget (in the absence of any net horizontal transport) is: snow-water-equivalent depth (D) equals precipitation (P) minus sublimation (S) (Liston and Sturm, 2004, equation 2.22):

$$D = P - S \quad [2.22]$$

The use of this equation is based on a few assumptions including the fact that spatial variation in erosion and deposition are negligible and that sublimation is easily modelled or measured.

2.3.1.1 Precipitation

Precipitation accumulates on the ground, building a snow cover that affects atmospheric and soil temperatures by moderating conductive, sensible, and latent heat energy transfers between the atmosphere, snowcover, and ground (Hinzman et al., 1998; Nelson et al., 1998; Liston, 1999).

Precipitation on the other hand has proven to be quite challenging to measure accurately. Solid precipitation generally falls when it is windy and windy environments can pose significant underestimation in solid precipitation amounts (Larson and Peck, 1974; Goodison et al., 1981; Benson, 1982; Yang et al., 1998, 2000), however, in some extremely windy conditions, blowing snow can be caught by precipitation gauges, causing an overestimation (Yang and Ohata, 2001).

Yang *et al.* (1998) stated that;

“Even the most complex and advanced shielded gauges, such as the WMO Solid Precipitation Measurement Intercomparison Project’s ‘octagonal vertical Double Fence Intercomparison Reference’ (DFIR), are unable to measure the true precipitation (liquid or solid) and require corrections for wind speed.”

These corrections are not that large but are necessary. The standard unshielded 8-inch precipitation gauge used by the National Weather Service (NWS) has an undercatch of nearly

75% when exposed to windy environments (Goodison et al., 1981; Benson, 1982; Yang et al., 1998, 2000). Others have shown that another form of gauge, the shielded Wyoming gauge, has an undercatch of 6% for snowfall in non-windy conditions and 55% for blowing snow (Rechard and Larson, 1971; Benson, 1982; Goodison et al., 1998; Yang et al., 2000). This is not only important at the local scale but also at the regional and global scale. Precipitation gauge networks are a crucial component to larger scale projects but there are very few networks that contain a large amount of gauges. This means that one gauge is responsible for covering a very large area which would induce a significant amount of potential error. There is some advocacy to increase the number of monitoring stations that record precipitation across the Arctic but the reality of is that this number is actually decreasing rather than increasing (Shiklomanov et al., 2002).

2.3.1.2 Snow depth measurements

In addition to the problems associated with precipitation gauges, there are also issues that arise when attempting to record snow depth. The most accurate method of acquiring snow depth measurements is to measure the amount of snow on the ground. Direct measurement using snow courses (Pomeroy and Gray, 1995) and watershed surveys (Elder et al., 1991) can be effective but time consuming, not to mention costly. It can even be very dangerous in certain terrain (e.g. in avalanche zones). Liston and Sturm have found that due to the occurrence of blowing snow and drifting snow, the snow depth and SWE distribution can be highly heterogeneous (Liston and Sturm, 2002; Sturm and Liston, 2003). Both topography and vegetation play an important role in this distribution and in many cases; require the use of models to help finalize the snow depth amounts. Snow distribution is easier to estimate in flat terrain where there are no drift traps present. It is assumed that the amount of snow being removed from one location due to blowing snow and drifting will be countered by the same amount being brought in by the same

mechanisms. Under these conditions, Equation 1 is valid. Otherwise, the use of blowing snow models are important in acquiring values for snow depth in any area, large or small.

2.3.1.3 Sublimation

If snow is not caught in drift traps, and if the blowing snow event lasts long enough and the air remains unsaturated, then particles can sublimate away. Tabler (1975) introduced the concept of a particle transport distance – the distance an average-sized snow/ice grain can travel before it completely sublimates away. Tabler (1975) found that for Wyoming, the average transport distance was 3km. Following Tabler's methods, Benson (1982) found that this distance decreases to 2-3km for the Arctic. There appears to be two separate schools of thought when it comes to snow sublimation. One school of thought states that the highest rates of sublimation occur when the snow particles are moving. Schmidt (1982) states that when the particles are in the wind stream, their high surface-area to mass ratios and high ventilation velocities are responsible for the high rates of sublimation. This research also demonstrated that these rates are as much as two orders of magnitude higher than those for static snow under similar conditions (Schmidt, 1982). The dependence of blowing snow sublimation rates on air temperature, humidity deficit, wind speed, and particle size distribution, can be seen in the works of Tabler (1975), Lee (1975), Schmidt (1982), and Pomeroy and Gray (1995). Schmidt's work has led to the creation of blowing snow models such as the Prairie Blowing Snow Model (Pomeroy et al., 1993) and SnowTran-3D (Liston and Sturm, 1998) to name a few. These models base their estimation of sublimation as a direct result of wind transportation and do not include static snow sublimation rates.

Contrary to this school of thought, other studies have shown that blowing-snow sublimation is not as important as sublimation from a static snow surface (Mann et al., 2000; Déry and Yau, 2001, 2002; King et al., 2001). In these studies, it is suggested that the atmospheric boundary layer (ABL) quickly becomes saturated under blowing snow events and is therefore unable to promote further ABL sublimation. Déry and Yau (2002) have found that static snow sublimation rates were 5-10 times higher than those found in blowing snow conditions.

Liston and Sturm (2004) suggest that perhaps there may indeed be two different sublimation regimes, with the interaction between the ABL and the overlying air mass determining which regime dominates. They suggest both a “humid” regime and a “dry” regime. A “humid” regime exists when the ABL is unable to mix with the overlying air mass and that the air is already saturated. In this case static-snow sublimation is the dominate regime. Contrary to this, a “dry” regime exists when the ABL is able to continuously mix with an overlying dry air mass, wicking away any moisture from the near surface layer of air and from snow particles. In this case, blowing-snow sublimation is the dominant regime (Liston and Sturm, 2004).

2.4 Summary

This chapter is focussed on providing background information about the physical properties of snow and energy and mass exchanges through water. Information, importance, and data collection of the physical processes of snow including precipitation, density, snow depth, and snow water equivalent are all discussed. Energy and mass balance component models are also discussed. Within the energy balance components there is a focus on the radiation budget as it pertains to snow as well as a comparison of several different energy balance equations from multiple sources. Mass balance components include changes to the snowpack through

sublimation, evaporation, and condensation, canopy interception, and blowing snow. Blowing snow is a very important component to this thesis and is further discussed as it pertains to the winter moisture budget. Multiple trains of thought exist as to what is actually occurring in the atmospheric boundary layer and these trains of thought are discussed.

Chapter 3

The Models

3.1 The Prairie Blowing Snow Model

The prairie blowing snow model (PBSM) is an ensemble of physically based blowing snow transport and sublimation algorithms which calculates the distribution of seasonal snowfall in agricultural areas of the Canadian prairies. Snow transport is divided into two parts: saltation – the movement of particles in a ‘skipping’ action just above the snow surface, and suspension – the movement of particles suspended by turbulence in the atmospheric layer extending to the surface boundary-layer. Sublimation rates are calculated for a column of saltating and suspended blowing snow extending to the top of the boundary layer (Pomeroy *et al.*, 1993). The model was designed to be able to predict: 1) mean vertical profiles of snow transport flux; 2) the effect of grain stubble height on blowing snow transport and sublimation losses from snow cover; 3) the effect of land use and unobstructed fetch distance on blowing snow transport and sublimation losses from snowcovers. The process algorithms used that make up the model make use of readily available meteorological information such as wind speed, temperature, humidity measured at a single height, occurrence of blowing snow and land use information.

3.1.1 Saltation

The occurrence of high winds over a loose surface can allow particles to become induced into several types of aeolian movement: saltation, suspension and, in some instances, surface ‘creep’ (Kind, 1990). Saltation is the process by which particles are transported horizontally by bouncing along the surface and is usually initiated by the collision of one particle into another (Bagnold, 1941) (Fig. 3-1). The distance travelled by a saltating particle is determined in part by the mean flow of the fluid, the particle size and surface conditions (Pomeroy and Gray, 1995).

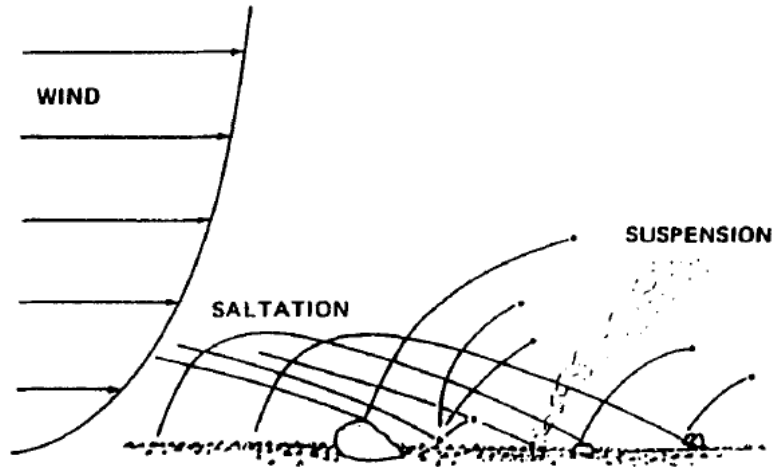


Figure 3-1: Diagram showing the processes of saltation and suspension of sediments into the atmosphere (adapted from Greeley and Iversen, 1985)

Pomeroy and Gray (1990) found that the expression for the vertically integrated saltation transport rate, Q_{salt} ($\text{kg m}^{-1} \text{s}^{-1}$), used in the PBSM is as follows

$$Q_{salt} = \frac{C_{salt}\rho u_t^*}{u^*g} (u^{*2} - u_n^{*2} - u_t^{*2}) \quad [3.1]$$

where C_{salt} is an empirically derived constant found to equal to 0.68 ms^{-1} , ρ is the air density (kg m^{-3}), g is the acceleration due to gravity (m s^{-2}), u^* is the atmospheric friction velocity (m s^{-1}) and the subscripts n and t refer to the friction velocity (shear stress) applied to the non-erodible surface elements (e.g. rocks and bushes that are protruding through the snow) and to the snow surface, respectively, at the transportation threshold. This friction velocity is dependent on the wind speed and the surface roughness and can be expressed as follows

$$u^* = \frac{u(z)k}{\ln\left(\frac{z}{z_0}\right)} \quad [3.2]$$

where k is von K arm an's constant (0.4), $u(z)$ is the wind speed at height z and z_0 is the aerodynamic roughness height. Further explanations and examples of the threshold velocities of non-erodible and snow surfaces can be found in Pomeroy *et al.* (1993). McEwen (1993) found

that, close to the surface, the wind profile is modified because some of the sheer stress is carried by the saltating or suspended particles. As well, the apparent roughness length is also modified. Pomeroy (1988) found that the roughness height for blowing snow over complete snowcovers can be expressed as follows

$$z_0 = \frac{C_z u^{*2}}{2g} + C_{st} N_{st} A_{st} \quad [3.3]$$

in which C_z is a dimensionless coefficient found equal to 0.1203 for prairie snowcovers, C_{st} is a coefficient equal to 0.5m, N_{st} is the number of vegetation elements per unit area and A_{st} is the exposed silhouette area of a single typical vegetation element which can be expressed as the product of the stalk diameter and the exposed stalk height (total stalk height minus snow depth). As an example, a typical value of N_{st} for a wheat field in Saskatchewan is 320 stalks m^{-2} (Pomeroy *et al.*, 1993). Under high threshold conditions an efficient, particle-surface interaction enhances saltation transport at high wind speeds but inhibits transport at low wind speeds. This leads to an approximately linear relationship between wind speed and the saltating transport rate.

3.1.2 Suspension

Suspension of snow can only occur once particles that are already saltating have reached a terminal velocity that is balanced by the upward-moving winds of the atmospheric boundary layer due to turbulence. Calculating the rate of transportation for suspended snow can be found by integrating the mass flux over the depth of flow, which can be classified as the area between the top of the saltation layer to the top of the surface-boundary layer. Schmidt (1982) defined the mass flux as the mass concentration multiplied by the mean downwind particle velocity. On average this velocity is equal to the velocity of the parcel of air. From the equation for u^* , the transportation rate of suspension, Q_{susp} ($kg\ m^{-1}s^{-1}$), is

$$Q_{susp} = \frac{u^*}{k} \int_{h^*}^{z_b} n(z) \ln\left(\frac{z}{z_0}\right) dz \quad [3.4]$$

where h^* and z_b are the lower and upper boundaries of the suspension layer, respectively, $n(z)$ is the mass concentration of suspended snow (kg m^{-3}) at height z (m). Further information and calculations of $n(z)$ can be found in Pomeroy and Male (1992) and Pomeroy and Gray (1990). The upper boundary height, z_b , is assumed to be dependent on the fetch over uniform, mobile snow, however in the PBSM code there is a 5m upper limit that is often imposed for snow transport calculations. Pomeroy (1998) suggested that snow particles that have been lifted to heights above 5m are unlikely to settle back to the surface before sublimation removes much of their mass. Therefore, for ‘surface hydrological purposes’, only the mass flux below 5m heights are considered when calculating the snow transport rates. In order for flow to fully develop, a minimum fetch distance of 300m is required. Knowing this, the modelled equation for z_b can be written as

$$z_b = 0.3 + k^2(x - 300) \left\{ \ln\left(\frac{0.3}{z_0}\right) \ln\left(\frac{z_b}{z_0}\right) \right\}^{-0.5} \quad [3.5]$$

where x is the downwind distance from the beginning of the fetch over which the surface roughness and the aerodynamic roughness, z_0 , can be considered uniform. This equation is a modified version that now incorporates the value of 0.3, which was taken from Takeuchi (1980) as the value for the top of a plume of diffusing particles at an elapsed time, $z_p(t)$. Following Pomeroy and Male (1992), the estimations for the value of h^* can be expressed as

$$h^* = c_h u^{*1.27} \quad [3.6]$$

where c_h is a coefficient found equal to $0.08436 \text{ m}^{-0.27} \text{ s}^{1.27}$.

Suspension transport increases as a power function of wind speed (Pomeroy, 1988). While the presence of exposed crop stubble increases the wind speed required to attain particle suspension,

an increase in turbulence due to this exposed stubble also increases the suspended transport rate for a given wind speed above this limit.

3.1.3 Sublimation

Sublimation also plays a key role in blowing snow transportation rates. It can act as a significant source of water vapour and as a sink for sensible heat in the air. It may also lead to a decrease in size (radius) and mass of snow and ice particles, resulting in a reduction in their drag coefficients. This means that in real terms, the problem of blowing snow can incorporate a multitude of particle sizes and therefore should be dealt with in such a manner. The model however, treats the problem with a mean particle size from a certain distribution of particles in a steady-state atmosphere. Pomeroy and Gray (1994, 1995) have argued that, in the Canadian Prairies, up to 75% of the annual snowfall over a one-kilometre fallow field is eroded by wind, and that, typically, up to half of this amount is sublimated before deposition occurs. According to Schmidt (1972, 1991), the rate of sublimation of a snow particle may be modelled by a balance between radiative energy exchange, convective heat transfer to the snow particle, turbulent transfer of water vapour from the snow particle and the consumption of heat by sublimation. If we assume thermodynamic equilibrium, the rate of change of mass with respect to time can be expressed as follows

$$\frac{dm}{dt} = \frac{2\pi r \sigma \frac{Q_r}{K_a T_a \text{Nu}} \left(\frac{\lambda_s M}{RT_a} - 1 \right)}{\frac{\lambda_s}{K_a T_a \text{Nu}} \left(\frac{\lambda_s M}{RT_a} - 1 \right) + \frac{1}{D \rho_{sat} \text{Sh}}} \quad [3.7]$$

(for more information on the derivation of this equation, see Schmidt 1991) where r is the radius of a snow particle containing mass, m ; σ (dimensionless and negative) is the water vapour deficit with respect to ice $(e - e_i)/e_i$, where e_i is the saturation vapour pressure (svp) over ice, and approximately equal to relative humidity minus one (RH-1); Q_r is the radiant energy received by

the particle; λ_s is the latent heat of sublimation ($2.838 \times 10^6 \text{ J kg}^{-1}$); M is the molecular weight of water ($18.01 \text{ kg kmol}^{-1}$); R is the universal gas constant ($8313 \text{ J kmol}^{-1}\text{K}^{-1}$); D is the diffusivity of water (m^2s^{-1}); T_a is the ambient air temperature; ρ_{sat} is the saturation density of water vapour (kg m^{-3}); K_a is the thermal conductivity of air ($\text{W m}^{-1} \text{K}^{-1}$); and Nu and Sh are the Nusselt and Sherwood numbers, respectively. The Nusselt number is a dimensionless number that represents the ratio of convective to conductive heat transfer. The Sherwood number is also a dimensionless number (also referred to as the mass transfer Nusselt number) which represents the ratio of convective to diffusive mass transport. Lee (1975) found that adjacent to a blowing snow particle in a turbulent atmosphere Nu is identical to Sh ($\text{Nu} \equiv \text{Sh}$). Both terms are dependent on Reynolds number, $Re(r,z)$ as

$$\text{Nu} = \text{Sh} = 1.79 + 0.606 Re^{0.5} \quad [3.8]$$

in which,

$$Re = \frac{2rV_r}{\nu} \quad [3.9]$$

where V_r is the ventilation velocity and ν is the kinematic viscosity of air ($1.88 \times 10^{-5} \text{ s}^{-1}$). In the suspension layer, one could ignore the effects of turbulence on V_r (Schmidt, 1982b; Pomeroy and Male, 1986) resulting in V_r being equal to the terminal velocities (w_s) of the particles expressed as

$$V_r = w_s(r) = 1.1 \times 10^7 r^{1.8} \quad [3.10]$$

In the saltation layer, the ventilation velocity is divided into vertical ($C_{salt} u^*$) and horizontal components ($2.3u_t^*$) (Pomeroy and Gray, 1990). We already know the value of C_{salt} from Equation 2 as 0.68, thus V_r can be written as

$$V_r = 0.68u^* + 2.3u_t^* \quad [3.11]$$

In terms of order of magnitude, Pomeroy (1988) argues that “the speed of the saltating particles relative to the wind speed is equal to the speed of the saltating particles relative to the surface”

The rate of change in mass of a particle requires the specification of the undersaturation of water vapour, $\sigma(=RH-1)$ given by

$$\sigma(z) = \sigma_2(1.02 - 0.027 \ln z) \quad [3.12]$$

where σ_2 is the undersaturation at $z = 2\text{m}$ when there is a decrease in relative humidity with increasing height during blowing snow. When the opposite occurs, Déry and Taylor (1996) have shown that the undersaturation can be given by

$$\sigma(z) = \sigma_2(0.98 + 0.027 \ln z) \quad [3.13]$$

Taken from Déry and Taylor (2006), the sublimation rate (negative) per unit area of snowcover, q_{subl} ($\text{kg m}^{-2}\text{s}^{-1}$), can be determined by integrating the sublimation loss rate coefficient [$c_{subl}(z)$] for the entire column of blowing snow extending from the snow surface to the top of the suspension layer, multiplied by the frequency of a certain particle size and its mass, over the particle spectrum and over height. Giving us

$$Q_{subl} = \iint N(z)c_{subl}(z)f(r, z)m(r)dr dz \quad [3.14]$$

where dr is the particle size increment (m) and N is the total number of particles per unit volume.

Further information on the sublimation loss coefficient, frequency distribution, and particle radius can be found in Pomeroy *et al.* (1993) and Déry and Taylor (1996).

3.1.4 Erosion and Deposition

The PBSM is also able to calculate the rate of surface erosion and deposition at distance x , downwind of the leading edge of a fetch $q_v(x,0)$. This rate is established by the net mass of snow entering or leaving a controlled volume of atmosphere, which extends from the snow surface to

the top of the surface boundary-layer for blowing snow, in x and z directions and through sublimation occurring within this volume as well (Fig 3-2).

This erosion/deposition rate can be expressed as follows

$$q_v(x, 0) = \frac{dQ_{salt}}{dx}(x) + \frac{dQ_{susp}}{dx}(x) + q_{subl}(x) + q_v(x, z_b) \quad [3.15]$$

in which the vertical flux at the top of the controlled volume, $q_v(x, z_b)$, is equal to the negative of the snowfall rate. In order for flow to fully develop, the surface erosion rate must equal the sublimation rate minus the snowfall rate and will develop under invariant atmospheric and surface conditions so long as there is an adequate fetch of mobile snow. The amount of fetch will vary depending on land use and land cover. Pomeroy (1988) suggests a distance of 500m for full development of flow to a height of 5m. Deposition on the other hand, occurs when the surface roughness is great enough to, or there are topographic depressions that, decrease the wind speed and the saltation and the suspension rates of transport, or when the snowfall is greater than the surface erosion rate.

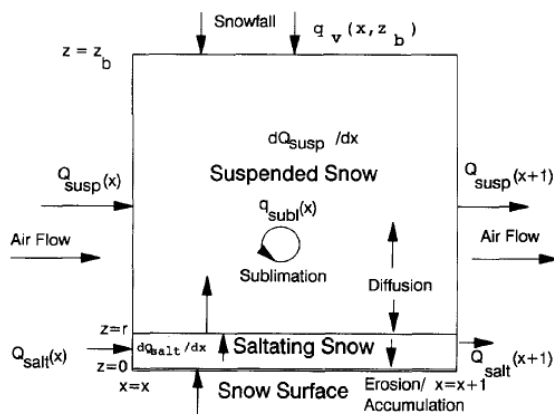


Figure 3-2. Cross sectional view of controlled volume of atmosphere extending from the snow surface to the top of the boundary-layer for blowing snow (Pomeroy et al., 1993)

Within CRHM, the snow mass balance is dealt with slightly differently than the original model.

The snow mass balance for an HRU is due to the distribution and divergence of blowing snow

fluxes in and around said HRU. With a fetch, x (m), the following expression for mass balance can be drawn over an HRU,

$$\frac{dSWE}{dt}(x) = P - p \left[\nabla F(x) + \frac{\int E_B(x) dx}{x} \right] - E - M \quad [3.16]$$

where $dSWE/dt$ is the surface snow accumulation rate ($\text{kg m}^{-2}\text{s}^{-1}$), P is the snowfall rate ($\text{kg m}^{-2}\text{s}^{-1}$), p is the probability of blowing snow occurrence within the HRU, F is the downwind transport rate ($\text{kg m}^{-2}\text{s}^{-1}$), E is the snow surface sublimation rate ($\text{kg m}^{-2}\text{s}^{-1}$), E_B is the blowing snow sublimation rate ($\text{kg m}^{-2}\text{s}^{-1}$), and M is the melt rate ($\text{kg m}^{-2}\text{s}^{-1}$). Proper application of the blowing snow algorithm requires every term to be solved for. This is why PBSM is coupled with MSM in this thesis. Nipher snowfall gauge undercatch is corrected for in the PBSM module and SWE accumulation is calculated as a residual of snow transport, snowfall, and sublimation rates. The other terms are found when linked to a snowmelt module. Interval data for temperature, relative humidity, and wind speed are used to calculate the transport and sublimation of blowing snow.

Using a unique parameterization scheme of employing cascading HRUs, PBSM, as implemented within CRHM, enables the parameterization of the flow of snow transport from HRU to HRU. Snow is redistributed amongst HRUs by basing it upon snow transport calculations, HRU size, vegetation characteristics, and a distribution factor, D_p . By implying the distribution factor, PBSM allocates blowing snow transport from areas that are aerodynamically smoother (windier) to areas that are aerodynamically rougher (calmer) within a basin. The distribution factor value ranges from 0 to 10, 10 being the roughest (Fang and Pomeroy, 2009).

3.2 Minimal Snowmelt Model

In order for PBSM to work properly it needs to be coupled with a snow melt model. CRHM has a few different melt modules to choose from but the minimal snowmelt model (MSM) was chosen for this thesis based on its simplicity and its ease of use using the available collected meteorological data.

The MSM module is based from Essery and Etchevers, 2004. It is a simple snow model with only three adjustable parameters (fresh snow albedo, albedo decay rate for melting snow, and surface roughness length). It performs the energy and mass balances with a focus on the surface of the snowpack. Changes in the internal snowpack energy, energy from precipitation, and energy from the ground are all neglected. It is driven by average inputs of incoming shortwave ($K\downarrow$) and longwave ($L\downarrow$) radiation respectively, air temperature, specific humidity (Q_1), wind speed (u), and snowfall rate (R_s). Surface pressure (P_s) and the measurement height (z_1) both must be specified as well.

MSM follows common procedures used in snow models and land surface schemes to calculate radiant and turbulent exchanges. Surface fluxes of sensible heat (H) and latent heat (LE) exchanges and can be seen as follows,

$$H = \rho C_p C_H u (T_s - T_a) \quad [3.17]$$

and

$$LE = \rho C_H u [Q_{sat}(T_s, P_s) - Q_1] \quad [3.18]$$

where ρ and C_p are the density and heat capacity of air respectively, $Q_{sat}(T_s, P_s)$ is the saturation humidity at the snow surface temperature (T_s) and pressure (P_s), C_H is a surface exchange coefficient. Net radiation (R) absorbed by the snow surface is calculated by

$$R = (1 - \alpha)K \downarrow + L \downarrow - \sigma T_s^4 \quad [3.19]$$

where α is the snow albedo and σ is the Stefan-Boltzmann constant.

MSM also deals with albedo decay and atmospheric stability. Further information about the above as well as the derivation for C_H can be seen in Essery and Etchevers, 2004.

Due to the neglecting of heat fluxes within the snowpack, heat advection from precipitation, and the substrate, the energy balance becomes

$$R = H + \lambda_s LE + \lambda_f M \quad [3.20]$$

where λ_s and λ_f are the latent heats of sublimation and fusion respectively. M is the melt energy (W m^{-2}). The mass balance is then calculated following

$$\Delta S = (R_s - LE - M)\Delta t \quad [3.21]$$

3.3 Summary

This chapter provides a brief synopsis of the Prairie Blowing Snow Model and the Minimal Snowmelt Model. It highlights the key equations and derivations from the models as they help lead to a better understanding of the experiments of this thesis. PBSM is a collection of physically based blowing snow transport and sublimation algorithms and is used to calculate transportation rates in the forms of saltation and suspension as well as sublimation rates. The model also calculates erosional and depositional rates with the aid of the snowmelt model MSM.

MSM is a simplified snowmelt model that ignores internal energy exchanges within the snowpack, energy from precipitation, and energy from the ground. This simplified model is easily coupled with PBSM using the collected met data and provides the missing variables to complete a mass balance equation that includes blowing snow fluxes. Both PBSM and MSM are modules found within the 6.0 platform of CRHM which is the main modelling platform used in this thesis.

Chapter 4.

Methods

4.1 Study Site

The study site for this thesis project is located on a small agricultural farm within the Strawberry Creek watershed (0.4054 km²) which is about 15km northeast of Waterloo, Ontario, Canada

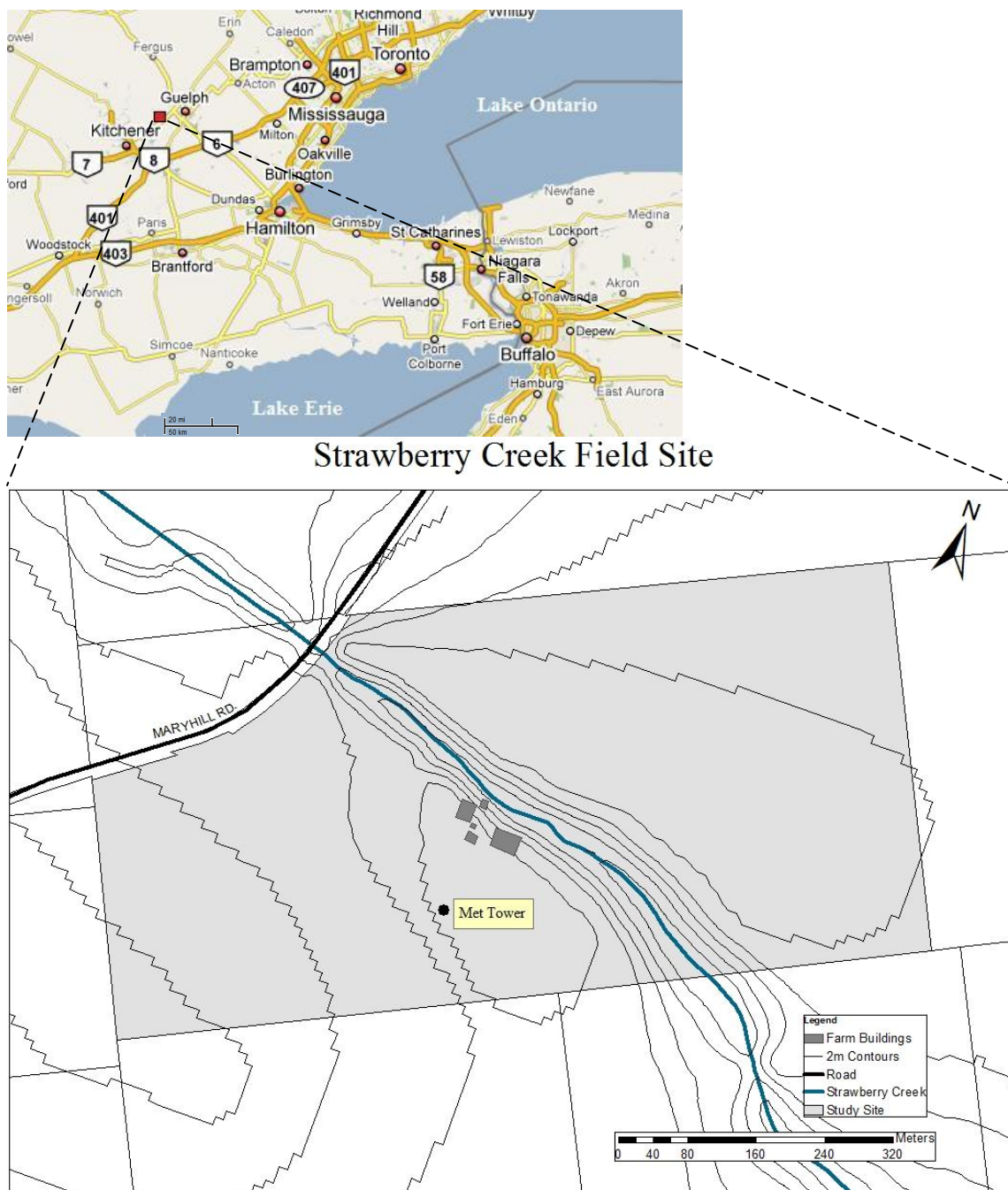


Figure 4-1: Location of Strawberry Creek field site

(43° 33' 1"N, 80° 23' 24"W). This domain can be seen Fig 4-1 and Fig 4-2. Strawberry Creek is a first order stream that flows into Hopewell Creek and eventually flows into Lake Erie through the Grand River. The Grand River is the largest catchment basin in southwestern Ontario with a total flow collection of approximately 6800km² (Chapman and Putnam, 1984). Figure 4-3 illustrates the Grand River catchment.

The physiography of Strawberry Creek was shaped by late Quaternary processes and is located in an area referred to as the Guelph Drumlin field (Chapman and Putnam, 1984). Glacial till is the predominant sub-surface physiology in this area and is assumed to be comprised of approximately 50% sand, 35% silt, and 15% clay (Chapman and Putnam, 1984). The landscape is predominantly gently rolling till plains which primarily consist of agricultural fields and very little pasture. The dominant field crops in the area consist of hay, corn (for grain), soybeans, corn (for silage), and winter wheat. Several eskers and moraines are located in this region as well (Karow, 1968). Further information about the physiography, soil structure, vegetation, and human development of this area can be seen in Chapman and Putnam (1984), Harris (1999), and Karow (1974, 1993). The purpose of this subsection is to provide a simple overview of the study site as it pertains to the over-land flow of wind-transported snow.

The farm (0.4km²) is located just outside the small town of Maryhill. It consists of three separate vegetated fields (N, NE, SW), the creek running SE through the centre of the farm, and a farm house and barn located in the centre of the land plot. The N and SW fields are separated from the NE field by the creek and the N and SW fields are separated by the farmhouse and its driveway. The N and NE fields were tilled in the late fall, and are therefore unvegetated in the winter and have small rows of raised earth ridges (~5cm) as a result from the tiller. The SW field has a winter grass crop with an average height of 10cm.

a)



b)



c)



d)



e)



f)



g)



h)



Fig 4-2: A 360° view of the field site from eight cardinal directions. a) Northwest, b) North, c) Northeast, d) East, e) Southeast, f) South, g) Southwest, h) West.

The topography is gently sloping towards the creek with roughly a 9m difference in elevation between the SW and NE corners to the creek bed (336-345m). There is also a gentle hill located in the centre of the SW field. The creek is narrow, roughly 1.5m deep and 2m wide under bank-full conditions and has a general U shape. Dredging of the creek in the past has increased the

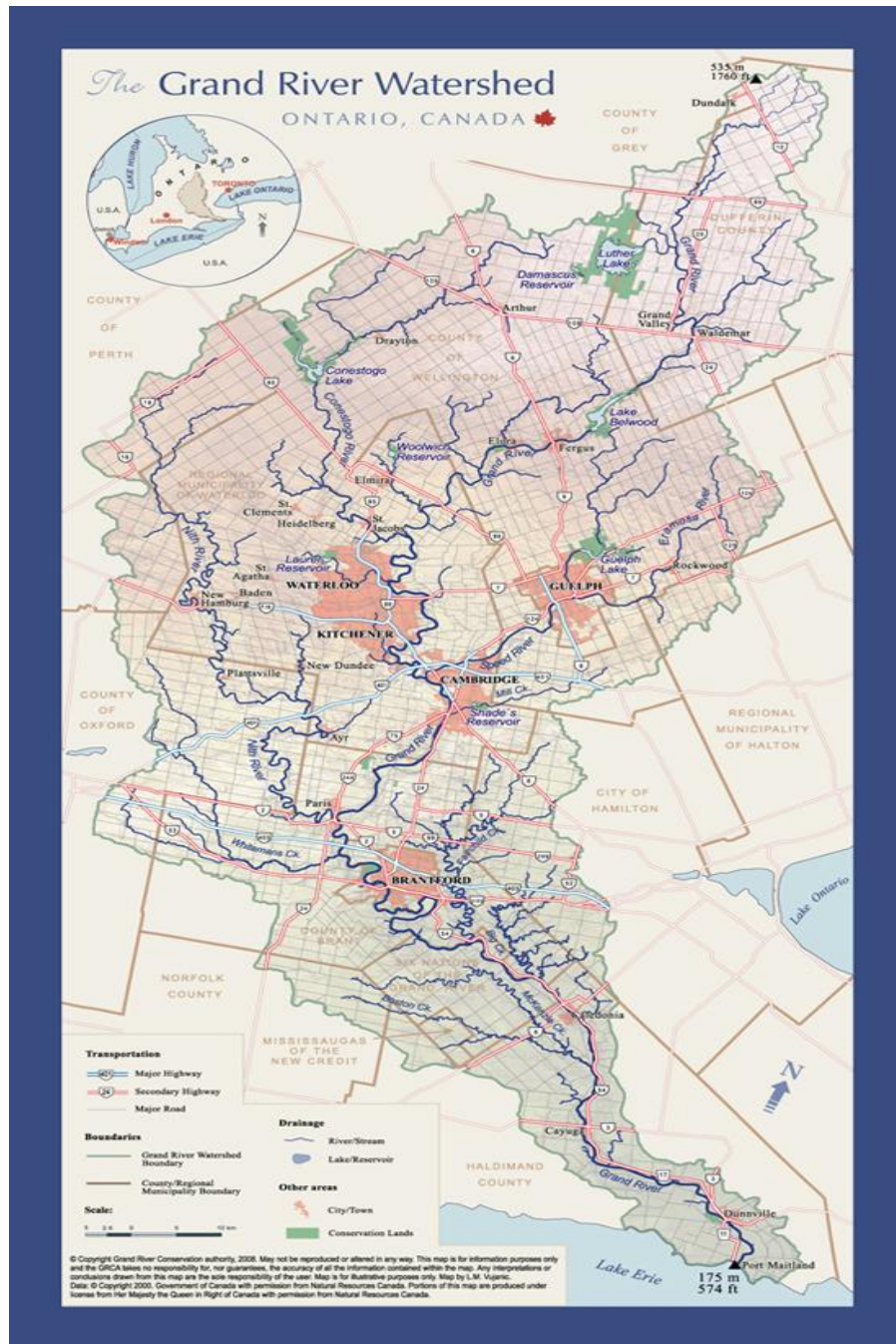


Figure 4-3: Grand River watershed (GRCA, 2008)

height and steepness of the banks and has also altered the riparian zone on either side.

This study site was chosen for several reasons:

1) It is a good representation of prairie-like conditions in southern Ontario. This is important as the focus of this thesis is to test the model, which largely consists of the Prairie Blowing Snow module, in a small, local catchment under different climatic conditions.

2) It is located in an area that is in closer proximity to the University of Waterloo so that it is easy to get to for the purpose of performing multiple snow courses and data collection over the entire snow season.

3) A good working relationship between the land owners, farmers and the Universities of Waterloo and Wilfrid Laurier is already present, making accessibility straightforward.

4.2 Digital Imagery and Data

Digital data coverage for Strawberry Creek included orthoimagery, contour mapping (2m resolution), road and water networks, and township field boundary maps. All of the data were collected from the Grand River Conservation Authority's Grand River Information Network (GRIN) (GRCA, 2008), and was used in ArcGIS 9/ArcView version 9.3 Geographical Information System (GIS) (Environmental Systems Research Institute, Inc. [ESRI], Redlands, CA). The orthoimagery was collected as a series of digital aerial photography in the spring of 2006 as a larger project named the South West Ontario Orthophotography Project (SWOOP). Tiles 548_4822 and 548_4820 were used in this project and have a ground pixel size of 30cm with an estimated positional accuracy of +/-1 metre.

4.3 Meteorological data

Half-hourly measurements of windspeed and direction, temperature, relative humidity, precipitation (rain), snow depth, solar radiation, and air pressure, were taken from a 3m meteorological tower which was located in the centre of the SW field (as seen in Fig. 1-1). Data was stored on a Campbell Scientific CR1000 data logger and was uploaded using Campbell Scientific's LoggerNet software package. Error free solid precipitation (snow) is difficult to obtain (see section on winter moisture budget). Therefore, in order to achieve a value of this precipitation, snow depth was recorded by the sonic snow depth sensor for time series analysis. If any significant increase in depth occurred, it was recorded as an increase in precipitation. Snowfall amounts were generated by examining the difference between precipitation values on a daily basis and them added together to create a daily snowfall amount. All of the collected meteorological data was assumed to be consistent across the entire study domain. Table 4-1 demonstrates all of the sensors used on the met tower and their purposes. The meteorological observations were used to drive the model for the period of 21 November 2008 to 12 February 2009.

Meteorological Condition	Instrument
Wind Speed and Direction	05103-10 RM Young wind monitor CSC Spec
Temperature and Relative Humidity	HC-S3-XT relative humidity and Air temp probe
Solar Radiation	CNR1 KIPP and ZONEN net radiometer sensor
Precipitation (rain)	TE525M Texas Instrument tipping bucket
Barometric Pressure	61205V RM Young Barometric pressure sensor
Snow Depth	SR50A Sonic ranger 50 KHz module

Table 4-1: List of selected meteorological instrumentation



Figure 4-4: View of meteorological tower looking south towards the town of Maryhill, Ont.

Over the entire winter season there were two significant melt periods where the snow cover completely melted away except in areas of significant drifting. The first occurred in late December, the second occurred in early February. Both melt periods were the result of a combination of warmer temperatures and rain events. Due to instrument malfunction of the SR50a sonic sensor, data from after the second severe thaw period (Feb. 12/09) was discarded. This truncated the entire data set to only 83 days.

4.3.1 Ultrasonic snow depth sensors vs. traditional snow measurement techniques

Ultrasonic snow depth sensors (USDS) have been around since the early 1980s (Goodison et al., 1984). They send out a sound pulse (50 kHz) and measure the time it takes the pulse to reach the ground and return to the sensor. The pulse is projected downwards over a cone of 30° and for accurate measurement it is imperative that there are no interferences between the sensor and the ground surface. The time for the pulse to return to the transducer in the sensor is adjusted for the

speed of sound in air based on measured air temperature, and the timing is converted to a distance via internal algorithms. To adjust the speed of sound in air (V_{sound}) in meters per second for the ambient air temperature (T_a) in kelvins, the following equation is applied:

$$V_{sound} = 331.4 \sqrt{\frac{T_a}{273.15}} \quad [4.1]$$

The distance the sound pulse travels decreases as snow accumulates on the ground, thus reducing the time for the pulse to return to the sensor.

Traditional snow measurements consist of gauge precipitation, snowfall, and snow depth. Gauge precipitation is defined as the liquid equivalent obtained by a nonrecording/recording, standard precipitation gauge. As is mentioned in the winter moisture budget section of this thesis, gauge precipitation is greatly affected by wind speed and direction and can lead to erroneous values obtained for evaluation. Snowfall is defined as the maximum accumulation of new snow since the last observation and is customarily measured manually with a ruler. Snow depth is defined as the total depth of snow on the ground at the time of observation and indicates both old and new snow on undisturbed surfaces. The measurement of snow depth may be the average of several total depth measurement to obtain a representative sample (NWS, 1996).

USDS measurements are done with respect to manual measurements which are assumed to be ‘ground truth’. Uniformity and consistency in manual measurements are difficult to attain with any data collector. There is an inherent uncertainty in manual measurements due to the fact that snow melts, settles, blows, and drifts and does not accumulate uniformly on the ground.

Depending on time of day, the frequency, the measurement surface, the extent of nonuniformity in snow accumulation, and overall care and detail of the individual observers, some variation in

manual observation is to be expected. According to Ryan et al. (2008), there are no known studies that have attempted to quantify this uncertainty in terms of measurement error, but they estimate it to be in the magnitude of $\pm 25\%$.

The choice to use a Campbell Scientific SR50a sonic sensor to derive solid precipitation values over traditional measurement techniques was made in part for the ease of obtaining an automated daily snow depth measurement based on hourly readings which can be personally monitored. Obtaining a manual snow depth measurement on a daily basis at the field site for the entire season was feasibly impossible. A daily measurement of snow on the ground was manually recorded every morning at the Waterloo-Wellington International Airport located in Breslau, 10 km to the southwest but due to any number of potential issues mentioned above, this data was not used as an input in any model runs for this thesis. A comparison between the SR50a data from Strawberry Creek and the manual snow depth data from the airport is seen in Fig. 4-5 below. The average seasonal difference between the two data sets was approximately 8.0 cm.

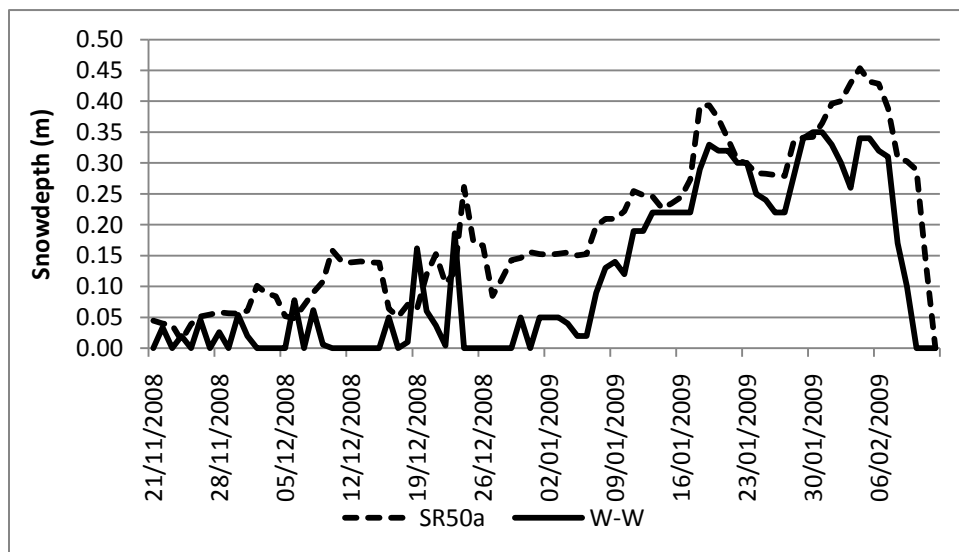


Figure 4-5: Comparison of seasonal snow depth measurements from the automated SR50a sensor at Strawberry Creek (dashed line) and the manual measurements from the Waterloo-Wellington International Airport (solid line).

4.3.2 Meteorological data pre-processing in order for proper model runs

As with many models, the CRHM platform requires specific formats of input data. Therefore, in order to correctly run the model some of the meteorological data format had to be pre-processed. Time and date stamps were combined into a decimal value, solar radiation was split up into incoming and outgoing short and longwave radiation, the windspeed was adjusted from a 2 m reference height to a 10 m reference height, solid precipitation was averaged on a daily basis, and the vapour pressure was derived within the model using an observation filter from values of temperature and relative humidity. Data from the SR50a sonic ranger was only used if it had a signal quality between the range of 152 to 210. Signal quality of 151 and below resulted in the sensor's inability to read distance. Signal qualities between 211 and 300 and 300+ had reduced echo signal strength and high measurement uncertainties respectively, and were therefore discarded. Any missing data was replaced with the preceding data of good quality.

4.4 Snow Surveys

A systematic linear transect sampling strategy was adopted to sample the mean, variance, and distribution of snow throughout the entire field site. Snow depth surveys were conducted over the winter of 2008-2009 using a GPS-magnaprobe from *Snowhydro*[®]. Surveys were conducted on a winter storm basis or a bi-weekly basis if no new accumulation of snow had fallen since the previous storm. Surveys were completed on the days of Dec. 08, in 2008 and Jan. 15, 21, 29, Feb. 04, in 2009. Gaps in the surveying structure were due to the fact that several melt periods occurred where there was no longer any snow on the ground surface to be measured. This occurred twice over the entire season, once in the middle of December and once again in the middle of February.

Initially, only two transects were chosen to cover the entire field site; a NW-SE transect and a NE-SW transect creating an 'X' pattern across the site. After much review, it was decided to include a perimeter transect as well as two more parallel transects (N-S) in order to better represent snow depth through spatial interpolation. Perimeter transects were labelled in order of geographical location (ie. Northern, Eastern, Southern, Western, Northwestern) and the interior transects were labelled numerically (ie. 1, 2, 3, 4). The following diagram (Fig. 4-6) demonstrates the pattern of snow depth transects used. Snow depths were measured at 5-m intervals along these transects.

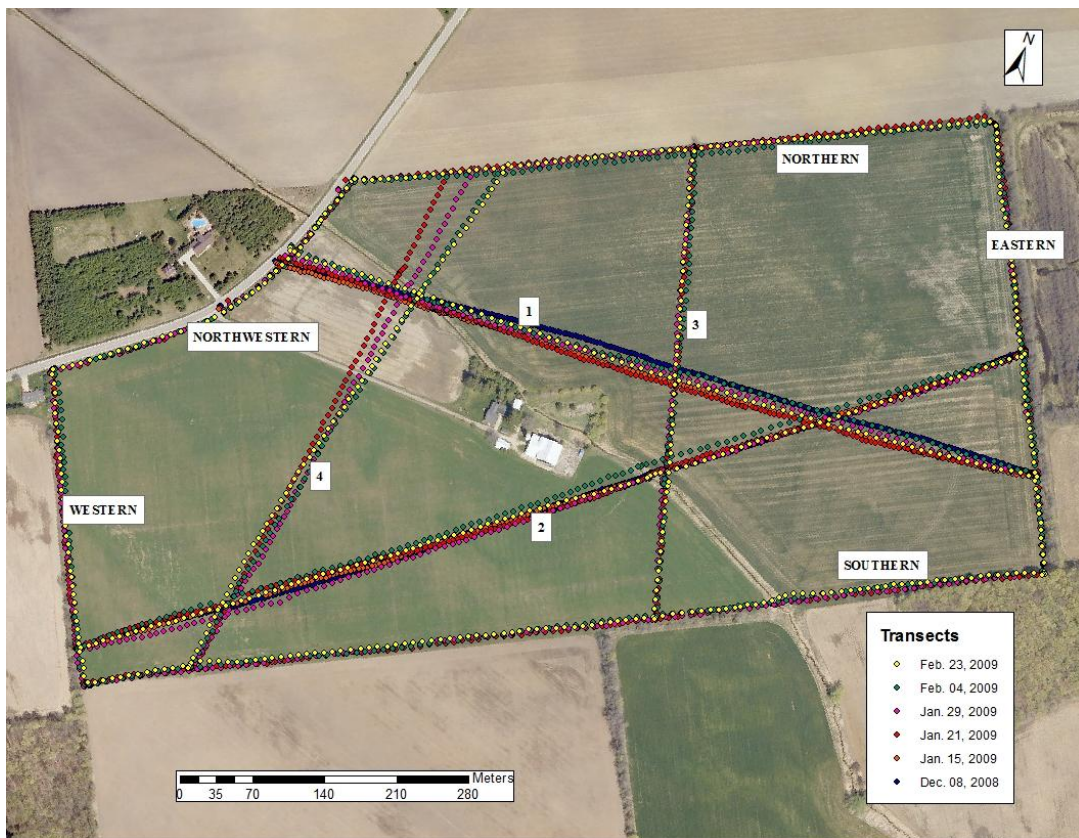


Figure 4-6: Map showing field site and snow depth transects

When using the Magnaprobe, the depth accuracy is $\pm 3\text{mm}$ if accurately calibrated but this is conditional on snow conditions, underlying vegetation, and battery power. On several occasions

when there were only trace amounts of snow on the ground, no surveys were conducted because the Magnaprobe was unable to detect these small amounts. The accuracy may be $\pm 3\text{mm}$ but that is only when there is enough snow at the right density threshold to allow the depth sensor to move along the rod and record a value. The GPS accuracy (both absolute and relative) has been shown to be $\pm 5\text{m}$ but is dependent on atmospheric conditions and satellites availability. This did not prove to be an issue at this field site. Data from the MagnaProbe is stored on a Campbell Scientific CR800 datalogger and is downloaded for analysis using Campbell Scientific's LoggerNet software package.

4.5 Model Experiments

In addition to field sampling, PBSM and MSM modules were used within the CRHM model to estimate the snow accumulation and distribution over the entire field site. The model was driven with half-hourly averaged air temperature, wind speed, humidity, incoming and outgoing short and longwave radiation, and daily averaged solid precipitation data during the snow accumulation period, 21 November 2008 to 12 February 2009, (as was derived from the SR50a data). It is assumed that all forcing data were uniform across the entire field site. The model runs were divided into two different methods, lumped and distributed, respectively. Furthermore, the lumped method experiments were sequentially run at two different scales; point scale and field scale. The distributed method was run solely at the field scale.

4.5.1 Lumped Model – Point Scale

Initially, the model was run in the lumped format at the point scale using the forcing data from the meteorological station and then compared to an average of 10 observed snow depth points

from the same location and timestamp. Model runs at this scale assume a single HRU (approximately 0.025 km²).

4.5.2 Lumped Model – Field Scale

Secondly, the model was scaled up in lumped format to the field scale using the same forcing data and then compared to observed snow depth points from the entire field site for each date of survey. Model runs at this scale also assume a single HRU (approximately 0.406 km²).

4.5.3 Distributed Model – Field Scale

In order to test the model's ability to spatially discretize, the model was then run at the field scale but in a distributed format. In order to do so, the field site was subdivided into three separate HRUs named Field 1 (0.183km²), Stream (0.011km²), and Field 2 (0.212km²) as seen in Figure 4-7 and Table 4-2, and modelled results are compared to observed snow depth points gathered from each HRU.

4.5.4 Model Parameters

In order to adapt the model for the Strawberry Creek field site, modifications were made to the model parameters. Control case parameters include the basin area being set to 0.4054 km², the basin and observation elevation being set to 343 m asl, latitude set for 43.5°N, observation reference height (Z_{ref}) set to 2.47m above the ground surface, and the vegetation height set to 0.05m. Due to the rolling terrain of the field site, the blowing snow fetch distance was assumed to be the PBSM minimum of 300 m. All other parameters were set to default (Table 4-2, Appendix 1). Based on the literature (Pomeroy et al, 1993) and knowledge of the terrain, the model snow density was assumed to be 250 kg m⁻³. Distributed method parameters include

adjusting the HRU areas to those specified above and vegetation heights of 0.1m, 1.5m, and 0.05m respectively for Field 1, Stream, and Field 2. These values were determined based on *in situ* observations. The value of 1.5m of vegetation height for the stream was determined to best represent the combination of the vegetation height in the riparian zone as well as the topographic depression of the stream itself.

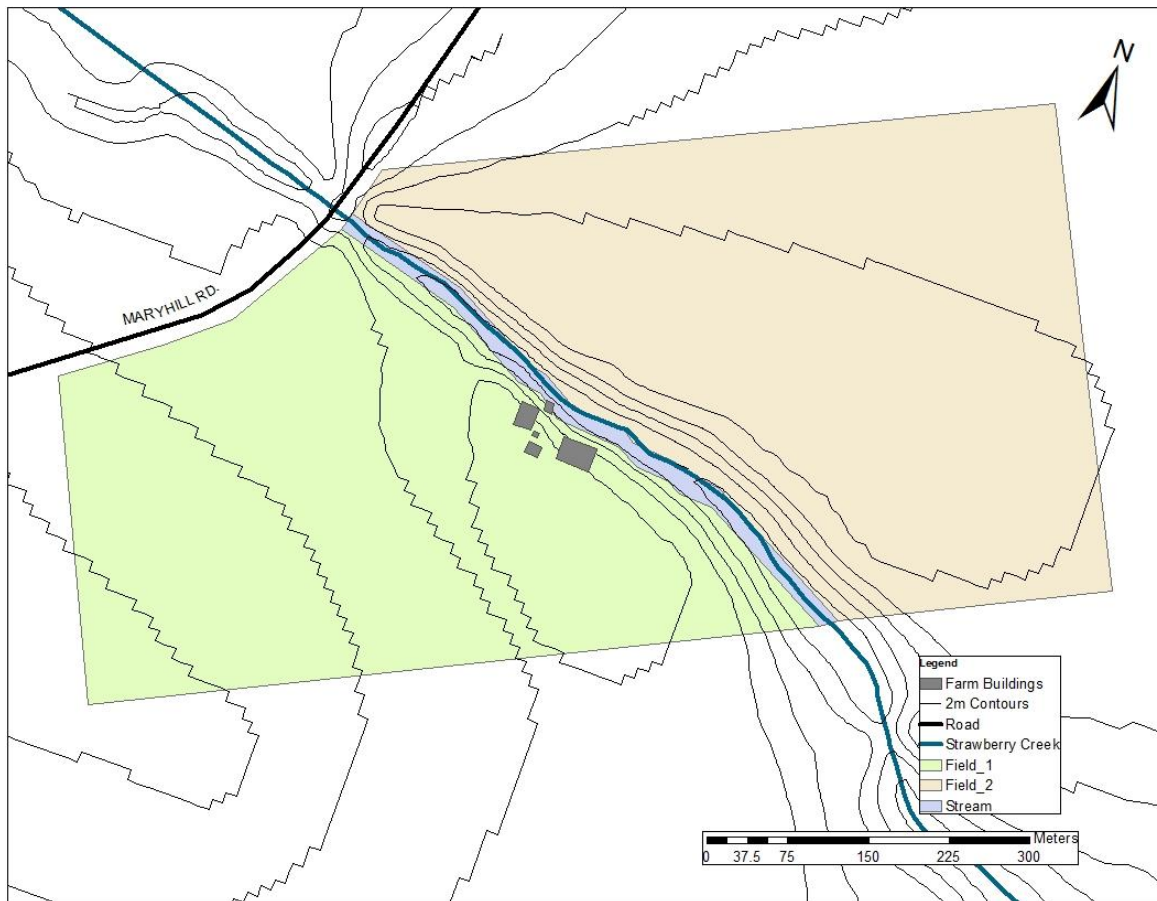


Figure 4-7: Distributed map of CRHM hydrological response units Field 1 (green), Stream (blue), and Field 2 (pink)

Table 4-2 demonstrates all of the model parameters and their values. A definition of each of these parameters can be found in Appendix 1. Sheltering effects of the farm buildings, driveway, and garden vegetation were not considered in any of the model runs.

CRHM Module	Parameter	Lumped	Distributed		
			HRU1	HRU2	HRU3
Basin	basin_area	0.4054			
	basin_name	SC			
	hru_area	0.4054	0.1827	0.01062	0.2121
	hru_AS_L	0	0	0	0
	hru_elev	343	343	343	343
	hru_GSL	0	0	0	0
	hru_lat	43.5	43.5	43.5	43.5
	hru_names	HRU	Field 1	Stream	Field 2
	Run_ID	1			
OBS	catchadjust	0	0	0	0
	HRU_OBS	1	1	1	1
	lapse_rate	0.75	0.75	0.75	0.75
	Obs_elev	343	343	343	343
	ppt_daily_distrib	1	1	1	1
	tmax_allrain	0	0	0	0
	tmax_allsnow	0	0	0	0
MSM_Org	a1	1.08E+07	1.08E+07	1.08E+07	1.08E+07
	a2	7.20E+05	7.20E+05	7.20E+05	7.20E+05
	amax	0.84	0.84	0.84	0.84
	amin	0.5	0.5	0.5	0.5
	smin	10	10	10	10
	Z0 snow	0.01	0.01	0.01	0.01
	Zref	2.47	2.47	2.47	2.47
PBSM	A_S	0.001	0.001	0.001	0.001
	distrib	0	0	1	1
	fetch	300	300	300	300
	Ht	0.05	0.1	1.5	0.05
	inhibit_bs	0	0	0	0
	inhibit_evap	0	0	0	0
	N_S	320	320	320	320

Table 4-2: CRHM model parameters

Values for the blowing snow distribution factor, D_p , were determined by trial-and-error runs with the knowledge of geographical proximity and aerodynamic roughness for each HRU.

HRU name	Area (km ²)	Vegetation Height (m)	Blowing snow fetch distance (m)	Blowing snow distribution factor D_p
Field 1	0.183	0.1	300	2
Stream	0.011	1.5	300	10
Field 2	0.212	0.05	300	1
Total field site	0.405	0.05	300	1

Table 4-3: Characteristics of HRU parameters for blowing snow experiments at Strawberry Creek

In Table 4-3, a D_p value of 1 and 2 was assigned to Field 2 and Field 1 HRUs respectively because they both have low aerodynamic roughness and are typically blowing snow ‘sources’. A D_p value of 10 was assigned to the Stream HRU due to it being a topographic depression with a high aerodynamic roughness and therefore acting as a blowing snow ‘sink’. For the lumped model experiment, a D_p value of 1 was given for the entire field site.

A schematic diagram depicting the flow of inputs and outputs between the modules within CRHM can be seen in Fig. 4-8. In addition to the MSM and PBSM modules, basin (BASIN), observation (OBS) and interception (INTCP) modules were added as they were required for complete model construction. The BASIN module allows the model user to set the parameters as required for each HRU being used. Meteorological forcing data is put into the OBS and MSM modules where it is filtered into specific HRU observations and used for the generation of snowmelt energy values respectively. The INTCP module is required by PBSM to deal with any incoming precipitation being held within a canopy. In the case of this thesis, there is no canopy to deal with therefore, INTCP is negligible and merely acts to change the name of incoming

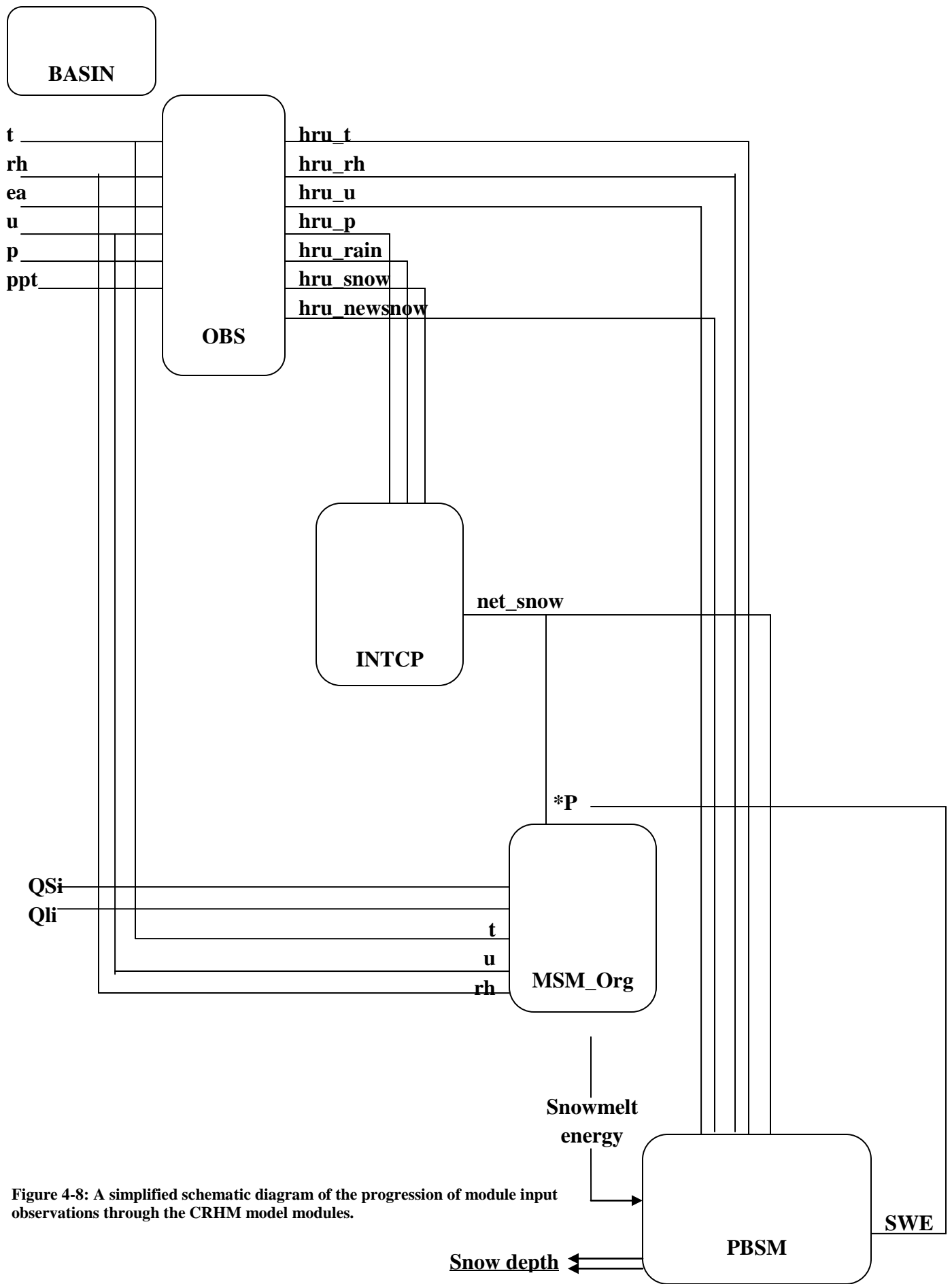


Figure 4-8: A simplified schematic diagram of the progression of module input observations through the CRHM model modules.

precipitation between OBS and MSM/PBSM. This is a necessary step in order for the MSM/PBSM modules to recognize the precipitation. The *P denotes a backwards *PUT* variable which is an input variable that is derived from another module. In this case, the MSM_Org module requires both SWE and net_snow from PBSM and INTCP before any snowmelt energy values are generated. Once snowmelt energy values are generated, they are input into PBSM and a final value for snow depth is achieved.

4.6 Model testing and verification

Initially, model results of snow depth are compared to measured snow depth for each day of snow surveying and then compared throughout the entire season. This creates a temporal analysis that enables testing of the model performance on a daily and seasonal basis. Spatial analysis is accomplished by analyzing the model results between the various scales of modelling. According to Rykiel (1996), “validation is a demonstration that a model within its domain of applicability possesses a satisfactory range of accuracy consistent with the intended application of the model.” In order to uphold this criterion, the purpose, performance criteria and context of the model are all well defined. The purpose of the model is to simulate the seasonal snow accumulation occurring at Strawberry Creek during the winter of 2008-2009. The performance criteria include the production of a quantitative agreement between observed and simulated snow depths. The model context was limited to the Strawberry Creek field site and the winter of 2008-2009 for three specific reasons: 1) the vegetation and topography represent a prairie-like condition on a small scale in as much as the field was not sheltered significantly by trees or relief, 2) the snow accumulation and melt periods are well defined and easily determined, and 3) the forcing meteorological data is year specific. Qualitative comparisons were made by visual inspection of

modelled and observed results of snow depth in graphical formats. The evaluation of the model performance is done by three statistical approaches, Root Mean Square Difference (RMSD), Nash-Sutcliffe coefficient (NS) (Nash and Sutcliffe, 1970) and Model Bias (MB), which are calculated as:

$$RMSD = \frac{1}{n} \sqrt{\sum (SD_s - SD_o)^2} \quad [4.2]$$

$$NS = 1 - \frac{\sum (SD_o - SD_s)^2}{(\sum SD_o - \overline{SD_o})^2} \quad [4.3]$$

$$MB = \frac{\sum SD_s}{\sum SD_o} - 1 \quad [4.4]$$

Where n is the number of samples, SD_o , SD_s , and $\overline{SD_o}$ are the observed, simulated, and mean of the observed snow depths, respectively. The RMSD is a weighted measure of the difference between simulated and observed snow depths and has the same units of measurement. The NS coefficient measures the model efficiency and MB supports NS by quantifying the model's under and overprediction.

As the number of environmental models have increased over the past few decades, so too has the need for the development of more precise and accurate estimates of the desired variable(s) from the model results. This in turn led to an increase in the use of a variety of different statistical methods assessing accuracy or goodness of fit and error (as seen in recent papers: Fekete et al., 2004; Cavazos and Hewiston, 2005; Willmott and Matsuura, 2005). Some of the more popular and widely reported error measures found in the literature include coefficients of correlation (also known as Pearson's product moment correlation; r) and determination (r^2) as well as the root mean square deviation (RMSD). There is much debate over which statistical method provides the best evaluation of model accuracy and selecting a method can be difficult seeing as

how it is based not only on the researcher's personal preference but also on the type of model being used, the method in which the model was calibrated, and the amount of estimated data points being compared against observed data. W.R. Black (1991) argues that the coefficients of correlation and determination are measures of relationship or association between estimated and observed data but they are not the best measure of accuracy or goodness of fit when comparing model estimates with observed data. Instead, RMSD should be used (Black, 1991). Previous model experiments using PBSM have included RMSD as one of the main methods of assessing model accuracy/error and it seemed only fitting to use the same method in this thesis. Even though RMSD is one of the most widely reported error measures in the literature, it is not without its own inherent error (see Willmott and Matsuura, 2005). RMSD is not standardized, making it difficult to look at on its own as a sole measure of model performance. Even though it demonstrates an amount of average error in the same units as the variables being estimated, this error value is only a relative term. It is for this reason that other statistical methods were selected (Nash-Sutcliffe coefficient (NS) and the Model Bias (MB)) in addition to RMSD to demonstrate the model's performance in this paper. NS is widely used and reliable statistic for assessing goodness of fit of hydrological models. It is very similar to the Pearson product in that the values of the coefficient give a measure of correlation and can be anywhere between $-\infty$ and $+1$. However, unlike the Pearson product, which is theoretically only applicable to linear models that include an intercept and is greatly affected by model bias, NS can be applied to a variety of models regardless of model bias (Nash and Sutcliffe, 1970; McCuen et al., 1990, 2006). With NS, a value of 1 implies that the model perfectly predicts the simulated results compared to the observed. A value equal to zero indicates that the simulated results are no better than the average of the observed values. A value less than zero indicates that the observed mean is a better

predictor then the simulated results. Therefore, any positive value of this coefficient indicates that the model has some predictive power and the higher the value, the better the model performs. Model Bias (MB) is added to support the predictive power of the model as seen in the Nash-Sutcliffe coefficient. A positive value and negative value of MB indicate overprediction and underprediction of the model, respectively. Following similar research from Fang and Pomeroy (2009), an acceptable range of model performance was chosen to be $<30\%$ ($MB < 0.30$).

4.7 Summary

This chapter provides a description of the methodology and modelling approach used in this thesis. It provides a detailed description and geological history of the study site as well as all of the data used to map out the study site and snow surveys. All methods of acquiring meteorological data and the required alterations to this data used in the model experiments are discussed in length. Snow surveys play a key role in validating the model experiments and this section describes in full the steps taken to acquire snow depth values across the entire field site using a GPS-magnaprobe throughout the winter season of 2008-2009. Model experiments as well as model validation and testing processes are also outlined. The final section justifies the statistical methods used to assess the accuracy or goodness of fit of the model compared to the observed data.

Chapter 5.

Results

5.1 Field Results

The precipitation pattern at Strawberry Creek during the winter season of 2008-2009 featured a dry fall and early winter with snow accumulating on the ground in late November. Most of the snow accumulation in this area occurs between the months of December and March. In some anomalous years snow accumulation can begin as early as October and remain as late as April. Most of the snow accumulation occurs due to several large precipitation events throughout the entire winter season which was the case for this particular winter season. Table 5-1 demonstrates monthly averages from Strawberry Creek compared to the monthly climatic average from the Waterloo-Wellington International Airport located in Breslau, 10km to the southwest.

Variable	Strawberry Creek				Waterloo-Wellington Airport			
	Nov.	Dec.	Jan.	Feb.	Nov.	Dec.	Jan.	Feb.
Temp (°C)	-2.96	-4.92	-10.39	-5.17	2.30	-3.80	-7.10	-6.40
Rel. Humidity (%)	97.27	98.93	97.86	96.41	87.50	87.00	86.40	83.60
Wind Speed (m/s)	2.62	4.02	2.96	3.23	3.94	4.06	4.28	3.89
Wind Direction (deg)	195.91	212.04	216.85	210.15	225.00	225.00	225.00	270.00
Snow depth (m)	0.05	0.12	0.26	0.36	0.01	0.05	0.12	0.14

Table 5-1: Calculated monthly climatic averages for Strawberry Creek during the 2008-2009 winter season compared to 1971-2000 climatic averages from the Waterloo-Wellington Airport (Environment Canada, 2010)

Climatic averages for temperature, relative humidity, and snow depth were all above the long term average for the area. Wind speed was not as strong and the wind direction came from a more southerly direction than the long term average. Collected meteorological data from Strawberry Creek can be seen in Fig 5-1.

Field observations demonstrate that the Strawberry Creek field site has a characteristic and predictable snow distribution pattern associated with wind direction, wind speed, topography,

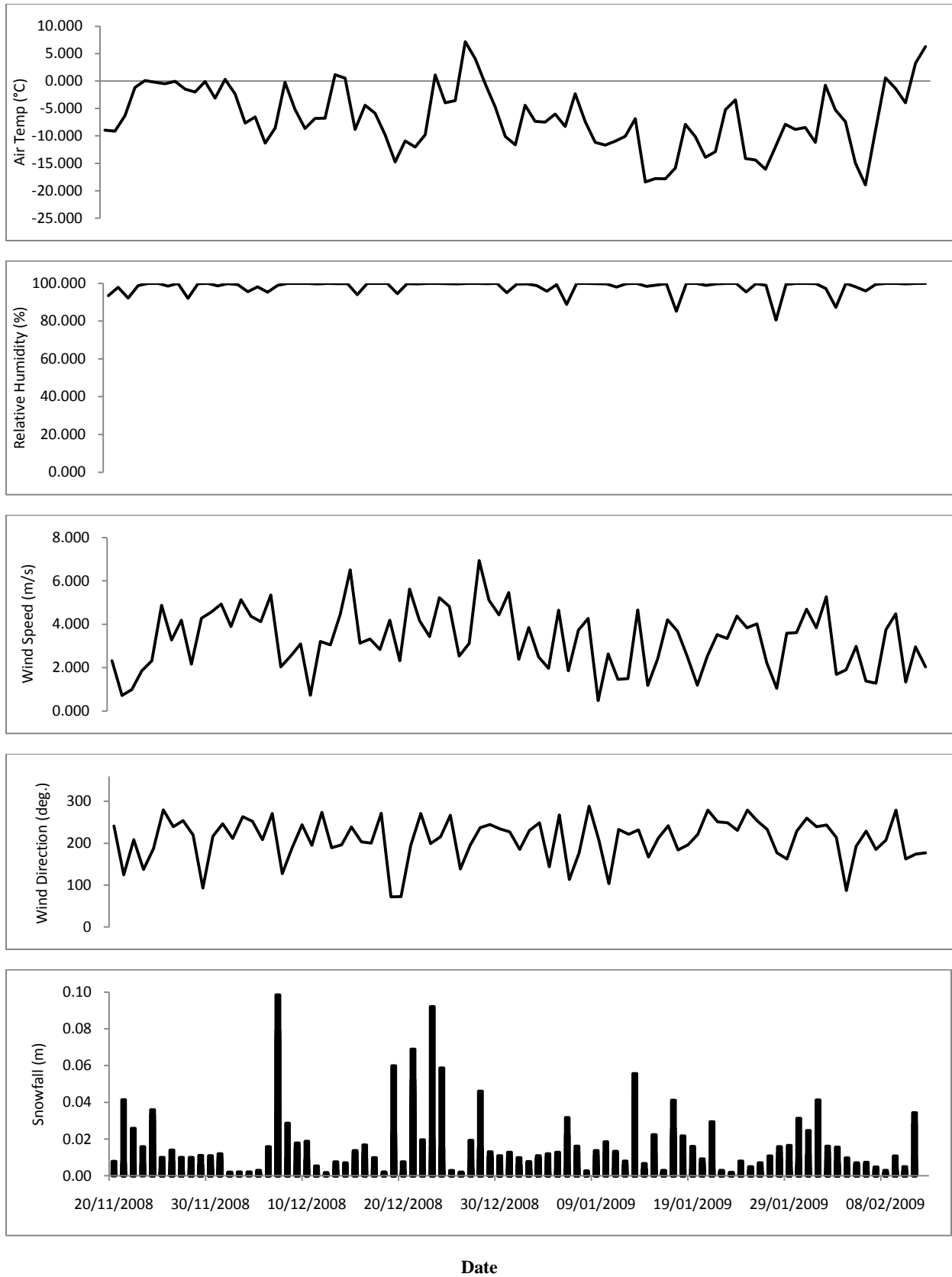


Figure 5-1: Corrected meteorological data for Strawberry Creek from November 21, 2008 to February 12, 2009

and vegetation. During the 2008-2009 winter season, the wind direction typically came from the south southwest (196° to 217°) with an average speed of 3 m s⁻¹ (Table 5-1, Fig. 5-1).

Definitive snow accumulation patterns appeared across the entire field site with drifts occurring around the edges of vegetation stands and within the creek banks. Scouring occurred in the open tilled farmlands (N and NE fields) which have a low snow-holding capacity. The SW field had a slightly higher snow-holding capacity due to the presence of the winter grass crop and therefore had an increase in snow depth compared to the other two farm fields. The forested borders along the eastern and western edges of the field site reduced the wind speed substantially, effectively acting as snow fences, facilitating the accumulation of large quantities of snow (40 to 90 cm deep). Within the creek banks the snow drifts would completely fill the banks (100 cm) in some areas and at times, even pile higher, pushing the magnaprobe to its depth limit of 120 cm.

Transect profiles demonstrating snow depth and elevation can be seen in Appendix 2. Fig. 5-2 is a graphical representation of both the observed snow depth averages on the days of snow surveying and the modelled snow depth results. It shows the gradual increase in mean field-scale snow depth from transect data throughout the winter season.

The extreme values in the data are due to snow depth readings from within the creek banks and drifts along the field site borders. The black circles represent the mean snow depth and the upper and lower box limits represent the 1st and 3rd quartiles respectively.

5.2 Model Results

Two modelling approaches were taken in this study: Lumped and distributed. The result of these approaches can be seen in Fig 5-2 and 5-3 respectively. In both approaches, the model failed to simulate the early onset of snow until the middle of December and then steadily simulated the

seasonal snow accumulation throughout the rest of the test season, which as was previously mentioned, fell between November 21, 2008 and February 12, 2009. The lumped approach reached a maximum snow depth of 33.0 cm on two different occasions in the month of January. In the distributed approach the maximum snow depth from the HRUs Field 1, Field 2, and Stream were 29.0cm, 28.0cm, and 41.0 cm respectively and occurred at the middle and end of January.

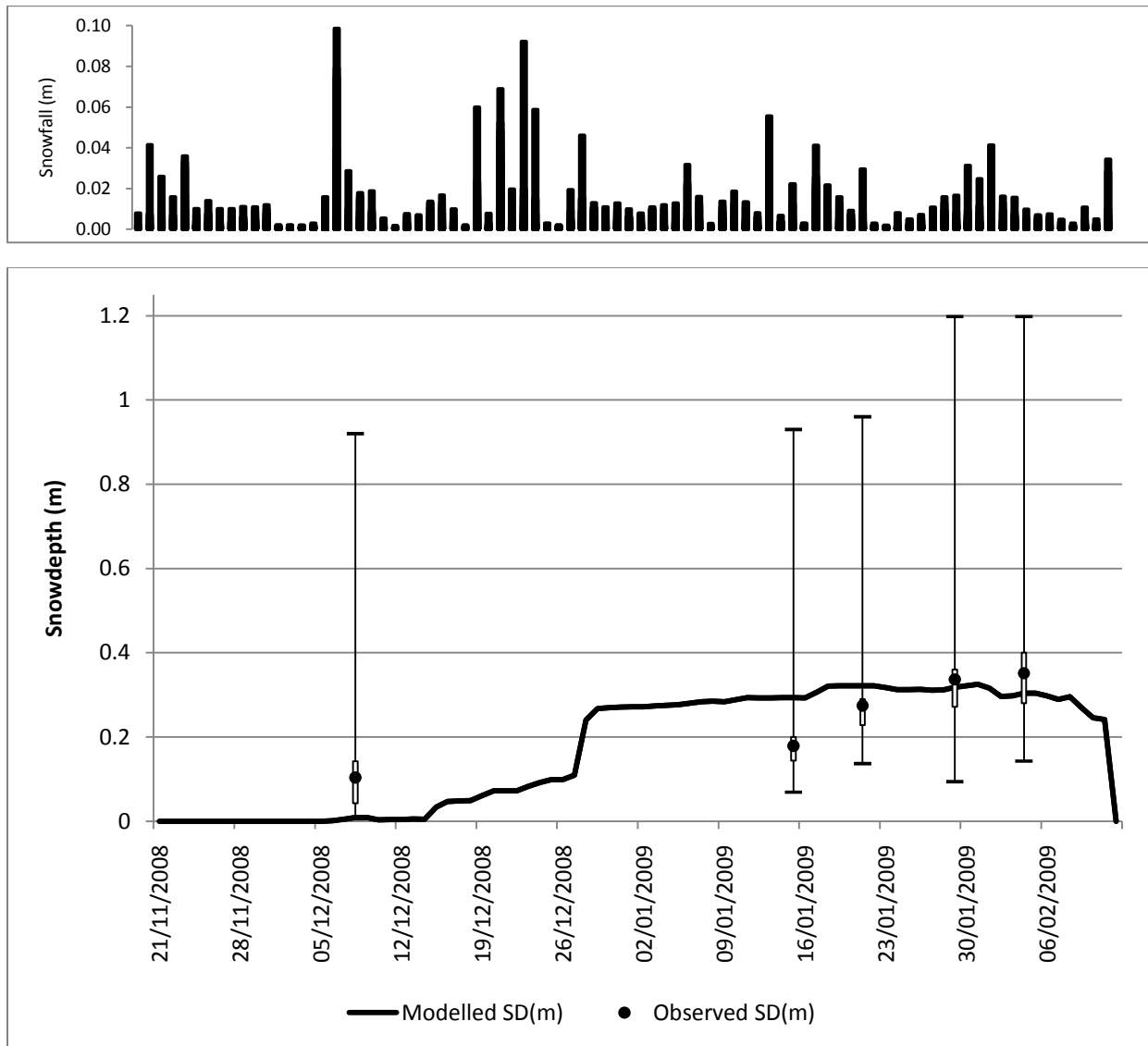


Figure 5-2 Comparison of averaged model (lumped) and observed snow depth during the 2008-2009 winter season. The snowfall graph is added to demonstrate snowfall activity throughout the season.

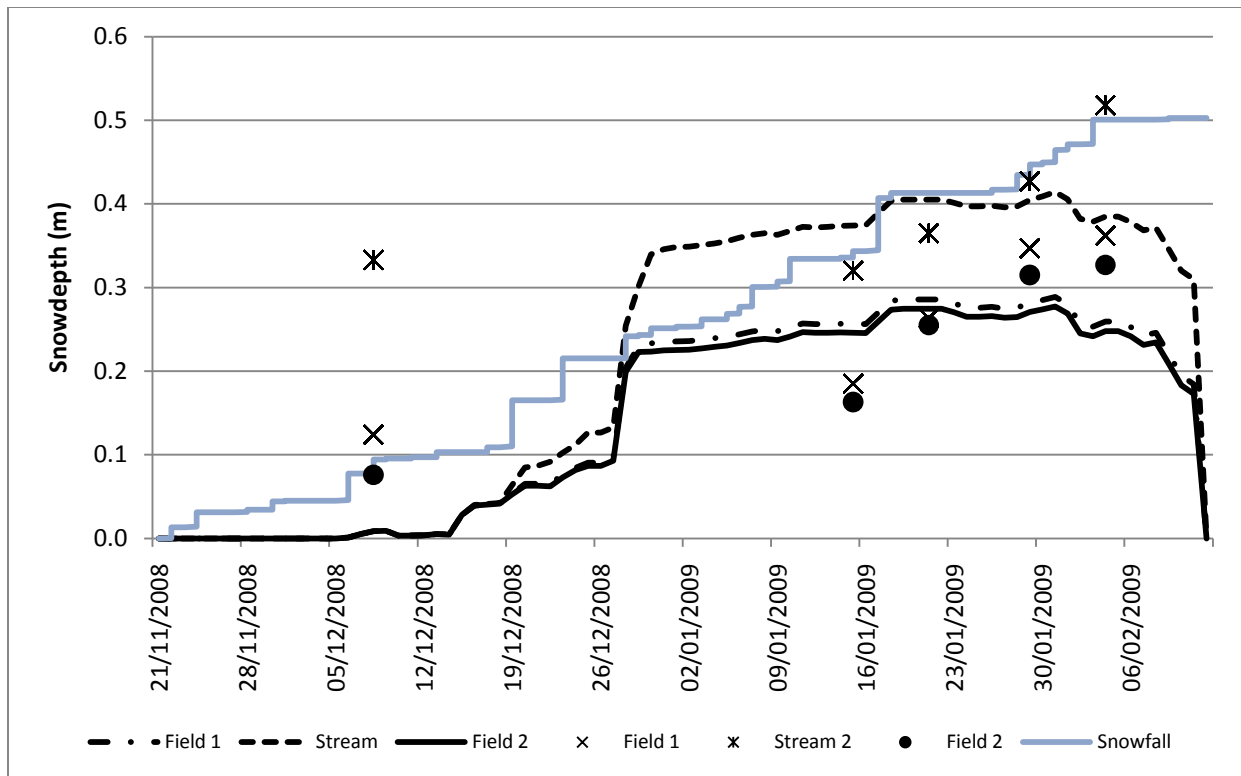


Figure 5-3 Comparison of averaged simulated model snow depth and cumulative snowfall (lines) and observed snow depth (symbols) for each HRU in the distributed approach over the 2008-2009 winter season.

Accumulation of snow depth in all three HRUs fall predominantly below the cumulative snowfall line which suggest that the entire field site is subjected to the effects of erosion from the wind and therefore acts as a source of blowing snow. The only exception to this occurs in the stream HRU between the end of December and the middle of January. In this case, the stream acts as a blowing snow sink.

5.3 Comparison of Simulated Model Results and Observed Snow Survey Results at the Point and Field Scales.

The simulated model results and field observations of snow depth were compared to one another in three different methods. The first two methods make use of model results from the lumped modelling approach and compare them to field observations at the point and field scales respectively. The third method makes use of model results from the distributed modelling

approach and compares them with field observations which have been collected from each of the three HRUs used in the model (Field 1, Stream, and Field 2). Table 5-2, below, displays the sample size (n value) used in the statistical analysis for the observed snow depth for each day of survey.

Date	Sample size (n)				
	Lumped		Distributed		
	Point Scale	Field Scale	Field 1	Stream	Field 2
Dec. 08/08	20	1138	426	44	668
Jan. 15/09	20	856	340	40	476
Jan. 21/09	20	1687	874	112	832
Jan. 29/09	20	1346	614	90	642
Feb. 04/09	20	1280	638	56	638

Table 5-2 Sample sizes of snow depth for each day of snow survey used for statistical analysis

5.3.1 Point Scale Model Results: Lumped

To quantify the performance of the model's ability at predicting snow depth at the point scale, RMSD, NS, and MB we computed for each individual date of snow survey during the 2008-2009

Date	RMSD (m)	NS	MB
Dec.08/08	0.074	-0.097	-0.943
Jan. 15/09	0.051	0.650	0.532
Jan. 21/09	0.022	0.969	0.160
Jan. 29/09	0.004	0.999	-0.027
Feb. 04/09	0.024	0.978	-0.135

Table 5-3 Root Mean Squared Deviation (RMSD), Nash-Sutcliffe coefficient (NS), and Model Bias (MB) for the comparison of point-scale simulated snow depth in a lumped approach and observed snow depth for each date of snow transect surveys during the 2008-2009 winter season.

winter season (Table 5-3). RMSD and NS values range from 0.004 m to 0.074 m and -0.097 to 0.999 respectively. The model performs well on Jan. 21/09 and Feb. 04/09 and performs really well on Jan. 29/09. As was previously mentioned, the model performed poorly in the early half of the season which is evident in the statistical analysis, most notably on Dec. 08/08 where the RMSD value was 0.074 m and the NS value was -0.097. The amount of overestimation and

underestimation for total snow depth is within 16% for the latter three survey days which is well within an acceptable range of 30% (Fang and Pomeroy, 2009), however, the model underestimates by as much as 94% on the first survey day and then overestimates by more than 52% on the following survey day which is unacceptable.

5.3.2 Field Scale Model Results: Lumped

Upscaling from the point scale the field scale is accomplished by including observations from the entire field site instead of only those which are in close proximity to the meteorological station.

Date	RMSD (m)	NS	MB
Dec.08/08	0.047	0.163	-0.913
Jan. 15/09	0.056	0.600	0.631
Jan. 21/09	0.014	0.977	0.150
Jan. 29/09	0.010	0.995	-0.068
Feb. 04/09	0.023	0.978	-0.147

Table 5-4 Root Mean Squared Deviation (RMSD), Nash-Sutcliffe coefficient (NS), and Model Bias (MB) for the comparison of field-scale simulated snow depth in a lumped approach and observed snow depth for each date of snow transect surveys during the 2008-2009 winter season.

By incorporating more field observations, there is an averaging effect on the statistical analysis (Table 5-4). Once again the model performs well on the final three days of snow surveys, most notably on Jan. 29/09, with RMSD values for those three days ranging from 0.010 m to 0.023 m and NS values ranging from 0.977 to 0.995. The model still performs poorly on the first two survey days but performs slightly better at the field scale than at the point scale. The amount of overestimation and underestimation is within 15% at the field scale which is slightly closer to the observations than the point scale modeling results over the last three days of snow surveys. The model underestimates snow depth by 91% on the first survey day which is slightly better than the point scale results but then over estimates by 63% on the second survey day which is worse than the result at the point scale. The faults of the results are likely due to uncertainty in the modelling of blowing snow over both complex terrain and varying vegetation.

5.3.3 Field Scale Model Results: Distributed

The final method compares field observations that were assigned to each of the HRUs with simulated snow depths using a distributed modelling approach at the field scale for each of the five days of snow survey. RMSD, NS, and MB were calculated for each HRU and can be seen below in Table 5-5.

Date	RMSD (m)			NS			MB		
	<i>Field 1</i>	<i>Stream</i>	<i>Field 2</i>	<i>Field 1</i>	<i>Stream</i>	<i>Field 2</i>	<i>Field 1</i>	<i>Stream</i>	<i>Field 2</i>
Dec. 08/08	0.058	0.162	0.033	0.132	-0.039	0.218	-0.928	-0.973	-0.881
Jan. 15/09	0.036	0.027	0.042	0.848	0.968	0.736	0.387	0.170	0.511
Jan. 21/09	0.012	0.020	0.010	0.992	0.987	0.994	0.088	0.111	0.078
Jan. 29/09	0.032	0.011	0.022	0.965	0.997	0.981	-0.186	-0.051	-0.139
Feb. 04/09	0.048	0.067	0.040	0.926	0.929	0.941	-0.271	-0.258	-0.242

Table 5-5 Root Mean Squared Deviation (RMSD), Nash-Sutcliffe coefficient (NS), and Model Bias (MB) for the comparison of field-scale simulated snow depth in a distributed approach and observed snow depth for each HRU on each date of snow transect surveys during the 2008-2009 winter season.

There is a large variation in the values of RMSD and NS which range from 0.010 m to 0.162 m and -0.039 to 0.997 respectively. Although the model still fails to adequately simulate snow depth during the initial snow accumulation period, the distributed approach does a better job than the lumped approach on the second day of snow surveying and continues to perform well throughout the remainder of the season. By examining the model performance for each HRU on each survey date we can see that the model does not perform well at all on Dec. 08/08. On Jan. 15/09 the model still has trouble simulating snow depth in both Field 1 and Field 2 but does well simulating it in the Stream, only overestimating by 17%. By Jan. 21/09 the model is performing very well in all three HRUs and is overestimating by less than 11%. The model begins to lose performance by Jan. 29/09 but is still performing well, especially in the Stream. The model is now underestimating snow depth by less than 19% but is still within the acceptable range as mentioned above. By the final survey date, Feb. 04/09, the model continues to lose performance

and underestimates snow depth in all three HRUs. This underestimation ranges from 24-27% which although is worse than the previous survey date, is still within the acceptable range of model performance. On the whole, the model performs better for the two field HRUs during the latter three days of surveying but performs better during the middle three days for the Stream HRU. Examinations of MB values indicate that the model is able to generate mid to late season snow depth values that are moderately close to the observations, keeping well within the acceptable range of 30%.

5.4 Summary

Field and model results are examined in this chapter. Field results of both meteorological and *in situ* snow surveys demonstrate that the 2008-2009 winter season was above average for temperature, relative humidity, and snow depth but was below average for wind speed, resulting in a shorter than average winter season with larger amounts of snow depth and less than average redistribution of snow. A constant wind direction allows for a definitive and predictable pattern of snow distribution across the entire field site. Examination of cumulative snowfall and snow depth suggest that the field site acts predominantly as a blowing snow source throughout the majority of the winter season with the exception of the stream HRU acting as a blowing snow sink from the end of December to the middle of January.

The model appears to perform fairly well in both the lumped and distributed approaches once a stable base layer of snow is established on the ground. Early seasonal snow accumulation is not modelled well no matter what approach is taken at any scale. The model also begins to lose performance at the tail end of the season, specifically in the distributed approach but is still performing at an acceptable range. When comparing the point scale with the field scale in the

lumped approach, the model performs almost identically with only a few minor differences. When comparing the lumped approach to the distributed approach the performance is similar but is spatially more accurate in the distributed approach due to the spatial discretization of this modelling approach. Reasons for the poor model performance and sources of error will be discussed further on in the discussion section of this thesis.

Chapter 6.

Discussion and Conclusions

6.1 Evaluating Model Performance and Sources of Error

Even though the model represented the average snow depth fairly well for most of the winter season, there are many sources of error that influenced the outcome of the model which prevented a better outcome. The following section discusses the model performance and sources of error that affected the outcome of the model results. Some of the topics include proper terrain representation, poor early-season simulation, model limitations, and adjustments to meteorological forcing data.

Terrain representation was a challenge with this model. The model platform used in this study assumed a flat terrain and did not allow for the incorporation of a digital elevation map or any changes to topography within the basin. The only exception was the ability to adjust the HRU elevation. Upon initial testing however, this proved to be effective only when the change in elevation was significant ($>15\text{m}$) and over a significantly larger area than the HRUs created in this study. Therefore it was assumed that the field site was flat. In actuality however, the total change in elevation was 9 m and the field site had several topographic features including hills, the creek, and a sloping terrain on either side of the creek. In addition to the natural topography of the field site, there were many objects (both man-made and natural) that added to the difficulty in accurately modelling the terrain. These objects included the many farm buildings located at the centre of the field, the elevated driveway, and all of the trees that bordered the property, driveway, and buildings. All of these variations in terrain create changes in the distribution of snow as it accumulates on the ground throughout the winter season. The hills are important areas for erosion and deposition of blowing snow on both the windward and leeward

sides respectively. The sloped terrain helps to channel saltating and suspended snow to areas of lower topography, namely the creekbed which in turn, was the largest sink of blowing snow across the entire field site. The steep banks of the narrow creek allowed for deep drifts to accumulate on either side and in some instances, completely fill the 1.5 m deep creekbed, creating little snow bridges across several sections of the creek. The farm buildings provide a significant amount of sheltering effect and a fair amount of drifting was observed in the lee of these buildings. However, due to the proximity of the buildings to the creek, much of the drifting was contained within the creek bed and did not progress significantly into the downwind field. The elevated driveway produces a small amount of drifting on either side. The tall trees that surround the buildings and run along portions of the elevated driveway are considered to be within the sheltering effects of these man-made objects and therefore did not significantly alter the drifting that occurred. The trees that are located along the perimeter of the property act as wind barriers and allow for the accumulation of deep snow drifts around their bases. Air flow through these trees is complex and difficult to model realistically. Previous studies have been conducted to observe the relationship between trees and snow including the effects of shelterbelt trees and shrubs (Sturges, 1983) and snow fences (Tabler, 1980a). The version of CRHM used in this study does have a module that can incorporate the effect of canopy interception and wind flow through trees but it was not incorporated because it involves a much greater amount of input variables which was far outside the realm of this study. Furthermore, without the coupling of this model to a 3-D windflow and terrain model such as the Mason and Sykes three-dimensional extension of the Jackson and Hunt theory (MS3DJH) terrain wind-flow model (Walmsley et al., 1986), correct terrain model representation is unobtainable, therefore leading to increased error.

Secondary to the topic of proper terrain modelling would be the inclusion of an updated working GIS interface. The version used in this thesis was ArcGIS/ArcView 9.3 but the model was configured to use ArcView version 3.1 and would not allow for more than one HRU shape file to be uploaded at a time. Personal conversation with the model developer, Tom Brown, from the University of Saskatchewan has determined that this is an area that needs to be updated and improved upon.

The model does not simulate the early onset of snow and this can be attributed to a combination of module assumptions from both PBSM and MSM and the inability to accurately model physical processes at a fine scale in the natural environment. As was mentioned above, the early winter season had several small snowfall and melt periods which are very difficult to accurately model. The MSM module negates any effect of energy coming from the ground, from precipitation, and internally from within the snow pack, thus altering the energy and mass balance equations. In the early winter season the heat energy coming from the substrate and from rain can significantly affect the overlying snowpack. Internal changes to the snowpack are minimal due to the presence of such a small amount of snow on the ground unless significant snowfall has occurred in various phases, resulting in a stratified snowpack. Nevertheless, MSM is unable to simulate these small periods of melt during the early part of the winter season. PBSM sequentially distributes any transported snow from areas of low snow holding capacity to areas of higher snow holding capacity regardless of wind direction. Although this method works in theory, it is not always the case in the natural environment. As well, snow transport within PBSM only occurs once the first HRU has reached its snow holding capacity. This becomes an issue in the beginning of the winter season in both the lumped and distributed approaches. In the lumped approach, a snow depth amount of 5 cm is needed before any snow transportation can

occur. In the distributed approach an amount of 5 cm and 10 cm is necessary to accumulate in Field 2 and Field 1 respectively before any snow is distributed to the Stream. In addition to the minimum snow depth requirements, the sequence in which snow transport occurs between HRUs does not represent the natural process very well. Since there is no method of accounting for wind direction within the module, PBSM distributed snow based solely on snow-holding capacity. In the case for Strawberry Creek snow distribution would follow in the format of Field 2 to Field 1 and then into the Stream. This is not the natural format of the field site (as seen in Figure 4-6). As well, the prevailing wind direction actually comes from the west, resulting in a natural sequence of snow distribution from Field 1 to Stream and then to Field 2. In addition to the above mentioned sources of error, another significant factor is the inability to simulate accurate amounts of snow depth in the initial HRU due to the fact that data from outside of the study domain cannot be captured before it enters the study domain.

Once however, all (or the majority) of the snow-holding capacities have been reached, the model performs really well at simulating the average snow depth across the entire field site, as seen in the model results section. The snowpack becomes one homogenous layer and snow transport is allowed to flow naturally between the HRUs. This is evident in the middle of the winter season. The end of season snowmelt underestimation is primarily due to the previously mentioned assumptions found within the MSM module. The HRU that is best represented throughout the entire season is Field 2. This is due to the fact that it has the lowest snow-holding capacity (5cm) and any blowing snow is placed into this HRU before moving onto the next. Although the natural progression would see blowing snow come from Field 1 and the Stream HRUs, or from outside the study domain, the model's ability to represent this HRU well is partially coincidental.

Accounting for precipitation events throughout the winter season can be a challenging endeavour. Initially, precipitation in the form of rain would be collected using a tipping-bucket rain gauge and snowfall would be a product of the difference in changes of accumulated snow depth from the SR50a snow depth sensor. However, after consulting with the model developer, we came to realize that the current version of the CRHM platform did not allow for separate precipitation inputs from rain and snow at the same time. It is assumed that the model user would be using a Geonor precipitation sensor and that the difference between rain and snow would be determined within the model by applying a set temperature to which precipitation would either be rain or snow. These parameters are known as 'tmax_allrain and tmax_allsnow'. Unfortunately this realization did not arise until halfway through the winter season and resulted in all precipitation data in the form of rain being neglected. This was unfortunate because the heat energy from rain can be a significant source of melting, especially in Southern Ontario.

The adjustments made to account for snowfall precipitation were necessary as there was no other accessible method to account for this form of precipitation throughout the winter season. The daily snow depth values from the SR50a sensor overestimate a bit more than the values from the Waterloo-Wellington airport but were chosen because they represent values from the actual field site rather than from a location 10km away. The calculations necessary to acquire the precipitation data (difference in accumulated snowfall) are simple and straight forward but they are heavily reliant on the quality of data acquired by the snow depth sensor. Fortunately though, the sensor had good signal quality (between 152 and 210) 89.9% of the time.

6.2 Future Considerations

If given the task of performing this study over again, a few changes would be made. In terms of modelling, PBSM would be coupled with the Energy Balance Snowmelt Model (EBSM) (Gray and Landine, 1987) as well as with a terrain wind-flow model such as MS3DJH (Walmsley et al., 1986). These models have proven to be very effective in prairie-like conditions.

In terms of instrumentation, a Geonor precipitation gauge and a particle detector would be added to the list of instrumentation and would significantly increase model simulation results because snowfall rates, blowing snow events, and proper designation and inclusion of both forms of precipitation can all be accounted for. As well, CRHM should be updated so that it could accommodate the newest version of a GIS interface. This would allow for an enhanced representation of terrain through a more user-friendly interface by simultaneously incorporating multiple shape files for each HRU as well as digital terrain models. In doing so, the sheltering effects of farm buildings and surrounding trees could be incorporated and a better representation of blowing snow redistribution would be possible.

In terms of methodology, the sampling strategy would be kept the same but the inclusion of several snowpits along each transect where values for SWE and density would be collected. These values would help in the testing of the model.

Temporal analysis of the model performance indicates that the model does very well at simulating the average snow depth across the entire season, regardless of the difficulty of attaining reasonable simulations for the initial onset of snow. This suggests that if given the correct seasonal data, the model may be used as a tool to compare seasonal averages for any number of studies across a number of years.

6.3 Conclusions

This thesis was an attempt at modelling snow depth across an agricultural field in a small subcatchment in Southern Ontario during the 2008-2009 winter season. It incorporated the modules of the Prairie Blowing Snow Model (PBSM) and the Minimal Snowmelt Model (MSM) within the Cold Regions Hydrological Model platform. Two different modelling approaches (Lumped and Distributed) were compared at various scales (point scale and field scale) to a series of *in situ* snow depth measurements, collected from snow surveys, which were completed throughout the winter season using a semi-automated snow depth sensor. The model performs well to simulate mid season snow depth averages in both the lumped and distributed approaches but has a hard time dealing with the onset of snow as well as the smaller scale effects of vegetation and terrain. There was very little change to model performance when upscaled from the point scale to the field scale. From an experimental point of view, this demonstrates that there are no scaling effects to be found at this size of domain.

This model is much better suited for large-scaled applications where these small-scale effects are negligible. When available, it is also best to couple the model with a 3-D terrain model which will increase the model's ability to accurately simulate the conditions across the entire study domain (Fang and Pomeroy, 2009; Essery and Pomeroy, 2004). Modelling the natural environment is extremely challenging and unless you are able to factor in all of the possible variables as they change throughout the entire season at every possible scale there is no way of reproducing 100% of the natural environment. The solution is to focus on the objective and attempt to minimize the amount of error being produced. Design the experiment to suit the study domain. The results posted in this thesis however, demonstrate that it is still possible to simulate seasonal snow depth at a variety of scales with relative accuracy. The Prairie Blowing Snow

Model was designed for much larger study domains but this thesis proves that with a little modification to the model and forcing data and if coupled with a snowmelt module, acceptable results can be generated at a much smaller scale.

References

- Bagnold, R. A. (1941). *The Physics of Blown Sand and Desert Dunes*. Methuen & Co., London. 265 pp.
- Bartelt, P., Lehning, M. (2002) "A physical SNOWPACK model for the Swiss avalanche warning Part 1: numerical model" *Cold Regions Science and Technology*, 35. No. 3: 123-145
- Benson, C.S (1982). "Reassessment of winter precipitation on Alaska's Arctic Slope and measurements on the flux of windblown snow". Geophysical Institute, University of Alaska Report UAG R-288, September 1982.
- Benson, C.S. and Sturm, M. (1993). Structure and wind transport of seasonal snow on the Arctic Slope of Alaska. *Ann. Glaciol.*, 18, 261–267.
- Bintanja, R. (1998a). The contribution of snowdrift sublimation to the surface mass balance of Antarctica. *Ann. Glaciol.*, 26, 167-173
- Brun, E. et al, (1989) "An energy and mass model of snow cover suitable for operational avalanche forecasting", *J. of Glaciol.*, 35, No. 121: 333-342
- Cavazos, T, Hewitson, B.C. (2005) Performance of NCEP-NCAR reanalysis variables in statistical downscaling of daily precipitation. *Climate Research* 28:95–107
- Chapman. L.J., Putnam. D.F. (1984). *The physiography of southern Ontario*. 270p.
- Chow, V.T., Maidment, D.R., Mays, L.W., (1988). *Applied Hydrology*. McGraw-Hill, New York
- Colbeck, S. (1978) *Adv. Hydrosoci* .11. pp 165 – 206.
- Déry, S.J. and Taylor, P.A. (2006). Some aspects of the interaction of blowing snow with the atmospheric boundary layer. *Hydrol. Process.* 10, 1345-1358
- Déry, S.J. and Yau, M.K. (2001). Simulation of blowing snow in the Canadian Arctic using a double-moment model. *Bound.-Layer Meteorol.*, 99, 297–316.
- Déry, S.J. and Yau, M.K. (2002). The large-scale mass balance effects of blowing snow and surface sublimation. *J. Geophys. Res.*, 107(D23), 4679, DOI:10.1029/2001JD001251.
- DeWalle, D. R., Rango, A. (2008) "Principles of Snow Hydrology" Cambridge University Press, Cambridge. pp. 21
- Diamond, M., Lowry, W.P. (1953) "Correlation of density of new snow with 700mb temperature". *Research Paper 1, Snow, Ice and Permafrost Research Establishment*. US Army Corps of Engineers; pp 3.

Dingman, S. L. (2002) "Physical Hydrology" 2nd ed. Prentice-Hall Inc., Upper Saddle River, New Jersey

Diskin, H.M.,(1970) Research Approach to Watershed Modelling, Definition of Terms, *ARS and SCS Watershed Modelling Workshop*, Tuscon, Ariz., March

Elder, K., Dozier, J., and Michaelsen, J., (1991). Snow accumulation and distribution in an alpine watershed. *Water Res Res*, 27: 1541-1552

Environment Canada, (2010) "Canadian Climate Normals or Averages 1971-2000"
http://www.climate.weatheroffice.gc.ca/climate_normals/index_e.html

Environmental Systems Research Institute, Inc., (1998) ArcGIS 9/ArcView version 9.3. Redlands, California, U.S.A.

Essery R, Etchevers P. (2004). "Parameter sensitivity in simulations of snowmelt". *Journal of Geophysical Research* 109 (D20111): Doi:10D1029/2004JD005036.

Essery R, Yang ZL. (2001). An Overview of Models Participating in the Snow Model Intercomparison Project (SNOWMIP). SnowMIP Workshop 11 July 2001. 8th Scientific Assembly of IAMAS. Innsbruck

Essery, R., Bunting, P., Hardy, J., Link, T., Marks, D., Melloh, R., Pomeroy, J., Rowlands, A. and Rutter, N.J. (2008). "Radiative transfer modelling of a coniferous canopy characterized by airborne remote sensing." *Journal of Hydrometeorology*. Vol 9: Issue 2, pp. 228-241

Fassnacht, S.R. (2000) "Distributed Snowpack Simulation Using Weather Radar with an Hydrologic – Land Surface Scheme Model". *PhD Thesis*. University of Waterloo.

Fang, X. And Pomeroy, J.W. (2009) "Modelling blowing snow redistribution to prairie wetlands", *Hydrological Processes*. 23: 2557-2569 DOI: 10.1002/hyp.7348

Fekete, B.M., Vörösmarty, C.J., Roads, J.O., Willmott, C.J. (2004) Uncertainties in precipitation and their impacts on runoff estimates. *Journal of Climatology* 17:294–304

Flato, G.M., Boer, G.J., Lee, W.G., McFarlane, N.A., Ramsden, D., Reader, M.C., and Weaver, A.J., 2000: The Canadian Centre for Climate Modelling and Analysis Global Coupled Model and its Climate. *Climate Dynamics*, 16, pp. 451-467.

Geiger, R. (1965) "The Climate Near the Ground". In *Boundary Layer Climates*. T.R. Oke. 2nd ed. Routledge

Goerre, S. et al. (2007) "Impact of weather and climate on the incidence of acute coronary syndromes" *International Journal of Cardiology*, vol 118, issue 1, pp. 36-40

Goodison, B.E., Ferguson, H.L., McKay, G.A. (1981) "Measurement and data analysis". In *Handbook of Snow –Principles, Processes, Management & Use*. D.M. Gray and D.H. Male (Eds). Pergamon Press: Oxford, England; pp 191 - 274.

Goodison, B. E., B. Wilson, K. Wu, and J. Metcalfe (1984) An inexpensive remote snow-depth gauge: An assessment. *Proc. 52nd Annual Western Snow Conf.*, Sun Valley, ID, 188–191.

Goodison, B.E., Louie, P.Y.T. and Yang, D. (1998). “WMO solid precipitation measurement intercomparison, final report”. WMO/TD 872, World Meteorological Organisation, Geneva.

Gordon, C. et al. (2000) “The simulation of SST, sea ice extents and ocean heat transports in a version of the Hadley Centre coupled model without flux adjustments” *Climate Dynamics*, 16, No. 2-3: 147-168

Grand River Conservation Authority, (2008)

<http://www.grandriver.ca/index/document.cfm?Sec=12&Sub1=55&Sub2=24>

Greeley, R. and Iversen, J.D., (1985). “Wind as a Geological Process on Earth, Mars, Venus and Titan.” Cambridge University, Cambridge, 333 pp.

Grody, N. (1996) “Global identification of snowcover using SSM/I measurements” *Geoscience and Remote Sensing*, 34, No. 1, pp 237-249

Harris, M. (1999). *Nitrate attenuation in a narrow non-forested riparian buffer zone in an agricultural watershed in southern Ontario*. MES Thesis. Department of Geography and Environmental Studies, Wilfrid Laurier University. 339p

Hedstrom, N.R., Pomeroy, J.W. (1998) “Measurements and modelling of snow interception in the boreal forest”. *Hydrological Processes* 12(10-11): pp 1611 – 1625.

Hiemstra, C.A., Liston, G.E. and Reiners, W.A. (2002). Snow redistribution by wind and interactions with vegetation at upper treeline in the Medicine Bow Mountains, Wyoming, USA. *Arctic, Antarctic, Alpine Res.*, 34(3), 262–273.

Hinzman, L.D., Goering, D.J. and Kane, D.L. (1998). A distributed thermal model for calculating soil temperature profiles and depth of thaw in permafrost regions. *J. Geophysical Res.*, 103(D22), 28975–28991.

Jordan, R. (1991) “A one-dimensional temperature model for a snow cover: Technical documentation for SN THERM.89”, *Spec. Rep. 91-16*, U.S. Army Corps of Eng., Cold Reg. Res. and Eng. Lab., Hanover, N.H.

Karrow, P. F. (1968). *Pleistocene geology of the Guelph area*. Geological Report 61. Ontario Department of Mines.

Karrow, P.F. (1974). Till stratigraphy in parts of southwestern Ontario. *Geological Society of America Bulletin* 85. 761-768.

Karrow, P. F. (1993). *Quaternary geology of the Stratford-Conestogo Area*. Report 283. Ontario Geological Survey.

- Kind, R. J. (1990). Mechanics of aeolian transport of snow and sand', *J. Wind Engrg and Ind. Aerodynam.*, 36, 855-866.
- King, J.C., Anderson, P.S. and Mann, G.W. (2001). The seasonal cycle of sublimation at Halley, Antarctica. *J. Glaciol.*, 47, 1-8.
- Kobayashi, D. (1972) Studies of snow transport in low-level drifting snow. *Contrib. Inst. Low Temp. Sci., Ser A* 24, 1-58
- Kuusisto, E. (1986) "The energy balance of a melting snow cover in different environments." In E. M. Morris, ed. *Modeling Snowmelt-Induced Processes*. Wallingford, UK: International Association of Scientific Hydrology Press. (IAHS Publication No. 155)
- La Chapelle, E. (1961) "Snow Layer Densification" Alta Avalanche Study Center, Project F, Progress Report No. 1, US Department of Agriculture Forest Service, Wasatch National Forest.
- Larson, L.W. and Peck, E.L. (1974). Accuracy of precipitation measurements for hydrologic modeling. *Water Res. Res.*, 10, 857-863.
- Lee, L. W. (1975). "Sublimation of snow in a turbulent atmosphere", *PhD Thesi.*7, University of Wyoming, Laramie, Wyoming, 162 pp.
- Liston, G.E. (1999). Interrelationships among snow distribution, snowmelt, and snow cover depletion: implications for atmospheric, hydrologic, and ecologic modeling. *J. Appl. Meteorol.*, 38(10), 1474-1487.
- Liston, G., M. Sturm (1998). "A snow-transport model for complex terrain" *Journal of Glaciology*, 44. No. 148: 498-516.
- Liston, G.E. and Sturm, M. (2002). Winter precipitation patterns in arctic Alaska determined from a blowing-snow model and snow-depth observations. *J. Hydrometeorol.*, 3, 646-659.
- Liston, G.E. and Sturm, M. (2004). The role of winter sublimation in the Arcic moisture budget. *Nordic Hydrol.*, 35 (4-5), 325-334
- Liston, G.E., McFadden, J.P., Sturm, M. and Pielke, R.A., Sr. (2002). Modeled changes in arctic tundra snow, energy, and moisture fluxes due to increased shrubs. *Global Change Biol.*, 8, 17-32.
- Male, D.H. (1980) "The Seasonal Snowcover". In *Dynamics of Snow and Ice Masses*. SC Colbeck (Ed). Academic Press: New York, U.S.A.; pp 305 - 395.
- Mann, G.W., Anderson, P.S. and Mobbs, S.D. (2000). Profile measurements of blowing snow at Halley, Antarctica. *J. Geophys. Res.*, 105(D19), 24491-24508.

Marsh, P. (1990) "Snow Hydrology". In *Northern Hydrology – Canadian Perspectives*. Prowse TD, Ommanney CSL (Eds). NHRI Science Report No. 1: Environment Canada, Saskatoon; pp 37 - 62.

Marshall, H.P., G. Koh, and R. Forster, (2004). CLPX-Ground: Ground-Based Frequency Modulated Continuous Wave (FMCW) radar. *National Snow and Ice Data Center Digital Media*, Boulder, CO, USA. <http://nsidc.org/data/nsidc-0164.html>.

McCuen, R. H., Leahy, R. B., and Johnson, P. A. (1990) Problems with logarithmic transformations in regression. *Journal Hydraulic Engineering*, 116: 3, 414–428.

McMuen, R.H., Knight, Z., Cutter, A.G. (2006) Evaluation of the Nash-Sutcliffe Efficiency Index, *Journal of Hydraulic Engineering*, 11: 6, 597-602, DOI: 10.1061/(ASCE)1084-0699(2006)11:6(597)

McEwan, I. K. (1993). Bagnold's kink: a physical feature of a wind velocity profile modified by blown sand?, *Earth Surf. Process. Landf.* 18, 145-156.

Nash, J.E., Sutcliffe, J.V. (1970) River flow forecasting through conceptual models. Part 1 – A discussion of principles. *Journal of Hydrology*, 10: 282-290

Nelson, F.E., Hinkel, K.M., Shiklomanov, N.I., Mueller, G.R., Miller, L.L. and Walker, D.K. (1998). Active-layer thickness in north central Alaska: Systematic sampling, scale, and spatial autocorrelation. *J. Geophys. Res.*, 103 (D22), 28963–28973.

NWS, cited (1996) Snow measurement guidelines. NOAA/NWS, Silver Springs, MD. <http://www.noaa.gov/os/coop/snowguid.htm>

Oke, T.R. (1987) "Boundary Layer Climates" 2nd ed. Routledge,

Oke, T.R. and Hannell, F.G., (1966) "Variations of temperature within a soil" *Weather* 21. pp 21-8

Pietroniro, A et al. (2006) "Using the MESH modelling system for hydrological ensemble forecasting of the Laurentian Great Lakes at the regional scale" *Hydrology and Earth System Sciences*, No. 0000: 0001-15

Pomeroy, J.W., (1988) Wind Transport of Snow, Ph. D. Dissertation, University of Saskatchewan, Saskatoon, pp 226

Pomeroy, J.W., (1989) "A process-based model of snow drifting" *Ann Glaciol.*, 13, pp. 237-240

Pomeroy, J.W. and Gray, D. M. (1990). Saltation of snow, *Warter. Res. Res.*, 26 (7), 1583-1594.

Pomeroy, J. W., Gray, D.M. and Landine, P.G. (1993). The Prairie Blowing Snow Model: characteristics, validation, operation. *J. Hydrol.*, 144, 165–192.

Pomeroy, J.W. et al, (2007b) “The Cold Regions Hydrological Model, a Platform for Basing Process Representation and Model Structure on Physical Evidence” *Hydrological Processes*, 21. No.19: 2650- 2667.

Pomeroy, J.W. and Gray, D. M. (1994). Sensitivity of snow relocation and sublimation to climate and surface vegetation in Jones, H. G., Davies, T. D., Ohmura, A., and Morris, E. M. (Eds), *Snow and Ice Covers: Interactions with the Atmosphere and Ecosystems*. IAHS Publ. No. 223. Wallingford. pp. 213-225.

Pomeroy, J.W. and Gray, D.M. (1995). “Snowcover Accumulation, Relocation and Management, National Hydrology Research Institute Science Report No. 7”, Hydrological Sciences Division, NHRI Division of Hydrology, University of Saskatchewan, Saskatoon.

Pomeroy, J.W. and Male, D. H. (1986). Physical modelling of blowing snow for agricultural production, in Steppuhn, H. And Nicholaichuk, W. (Eds), *Proceedings Symposium of Snow Management for the Great Central Plains Agriculture Council*. Publ. No. 120, Water Studies Institute, Saskatoon, Saskatchewan. pp. 73- 108

Pomeroy, J.W. and Male, D. H. (1992). Steady-state suspension of snow. *J. Hydrol.*, 136, 275--301.

Pomeroy, J.W., Marsh, P. and Gray, D.M. (1997). Application of a distributed blowing snow model to the Arctic. *Hydrol. Process.*, 11, 1451–1464.

Pullum, G.K. (1991) *The great Eskimo vocab hoax and other irreverent essays on the study of language*, The University of Chicago Press, pp. 160

Purves, R.S., J.S. Barton, W.A. Mackaness and D.E. Sugden. (1998) The development of a rule-based spatial model of wind transport and deposition of snow. *Ann. Glaciol.*, 26, 196-202

Rechard, P.A. and Larson, L.W. (1971). “The use of snow fences for shielding precipitation gauges”. Proc. 39th Western Snow Conference, Billings, Montana, pp. 56–62.

Roeckner, E., et al., (1992) “Simulation of the present day climate with the ECHAM model: Impact of model physics and resolution.” Max Planck Institute for Meteorology Rep. 93: 171

Roeckner, E. et al., (1996) “The atmospheric general circulation model ECHAM-4: Model description and simulation of present day climate.” Max Planck Institute for Meteorology Rep. 218: 90.

Roeckner, E. et al., (2003) “The atmospheric general circulation model ECHAM5: Part I.” Max Planck Institute for Meteorology Rep. 349: 127

Rutter, N. et al. (2009) “Evaluation of forest snow processes models (SnowMIP2)” *J. Geophys. Res.*, 114, D06111, doi:10.1029/2008JD011063

- Ryan, W. Et al. (2008) "Evaluation of Ultrasonic Snow Depth sensors for U.S. Snow Measurements" *Journal of Atmospheric and Oceanic Technology.*, pp. 667-684, DOI: 10.1175/20077JTECHA947.1
- Rykiel, E.J., Jr. (1996) Testing ecological models: the meaning of validation. *Ecological Modelling*, 90, 229-244
- Schmidt, R.A. (1972). "Sublimation of wind-transported snow - a model". Research Paper RM-90, Rocky Mtn. Forestry and Range Expr. Sta., Forestry Service, US Department of Agriculture, Fort Collins, CO.
- Schmidt, R.A. (1982). Vertical profiles of wind speed, snow concentration, and humidity in blowing snow. *Boundary-Layer Meteorol.*, 23, 223-246.
- Schmidt, R.A. (1986). Transport rate of drifting snow and the mean wind speed profile. *Boundary-Layer Meteorol.* 34, (3) 213-241
- Schmidt, R.A. (1991). Sublimation of snow intercepted by an artificial conifer. *Agric. Forest Meteorol.*, 54, 1-27.
- Schmidt, R.A. Jr, Gluns, D.R. (1991) "Snowfall interception on branches of three conifer species". *Canadian Journal of Forest Research.* 21: pp 1262 – 1269.
- Shiklomanov, A.I., Lammers, R.B. and Vorosmarty, C.J. (2002). Widespread decline in hydrological monitoring threatens Pan-Arctic research. *EOS Trans, Am. Geophys. Union*, 83(2), 13, 16, 17.
- Spitalnic, S. et al. (1996) "An association between snowfall and ED presentation of cardiac arrest." *The American Journal of Emergency Medicine*, vol 14, issue 6, pp 572-573
- Singh, V.P., (1995) Computer Models of Watershed Hydrology. Water Resources Publication
- Sturges, D. L., (1983) Establishment and growth of shelterbelt species and grass barriers on windswept Wyoming rangeland. *Transportation Research Record*, 93 pp 4-11
- Sturm M, Holmgren J, Liston GE. (1995) A seasonal snow cover classification system for local to global applications. *Journal of Climate*, 8 1261-1283.
- Sturm, M., Liston, G.E., Benson, C.S. and Holmgren, J. (2001a). Characteristics and growth of a snowdrift in arctic Alaska. *Arctic, Antarctic Alpine Res.*, 33(3), 319-332.
- Sturm, M. and Liston, G.E. (2003). The snow cover on lakes of the Arctic Coastal Plain of Alaska, U.S.A. *J. Glaciol.*, 49(166), 370-380.

- Sundsbo, P.-A. (1997) "Numerical modelling and simulation of snow drift" Ph.D. thesis, Norwegian University of Science and Technology, Trondheim; Narvik Institute of Technology, Department of Building Science, Narvik
- Tabler, R.D. (1975). "Estimating the transport and evaporation of blowing snow." In: Snow Management on Great Plains Symp., Bismarck, N. Dakota, July 1975, Proc. Great Plains Agric. Counc. Publ. vol 73, pp. 85–104.
- Tabler, R. D. (1980a) Geometry and density of drifts formed by snow fences. *Journal of Glaciology*, 26(94), pp 405-419
- Takeuchi, M. (1980) Vertical profiles and horizontal increase of drift snow transport, *J. Glaciol.*, 26, 481-492.
- Tarboton, D. G., T. G. Chowdhury and T. H. Jackson, (1995) "A Spatially Distributed Energy Balance Snowmelt Model". In K. A. Tonnessen, M. W. Williams and M. Tranter (Ed.), *Proceedings of a Boulder Symposium*, July 3-14, IAHS Publ. No. 228: 141-155.
- UNESCO/IHP (2009) "International Classification of Seasonal Snow on the Ground" *IHP-VII Technical Documents in Hydrology N° 83-IACS Contribution N° 1*, UNESCO Working Series SC-2009/WS/15
- Verseghy, D.L. (2000) "Canadian Land Surface Scheme (CLASS): Its History and Future" *Atmosphere-Ocean*, 38. No. 1: 1-13
- Walmsley, J. L., P. A. Taylor, and T. Keith, (1986) A simple model of neutrally stratified boundary-layer flow over complex terrain with surface roughness modulations (MS3DJH/3R). *Boundary-Layer Meteorology*, 36, pp. 157-224
- Willmott, C.J., Matsuura, K, (2005) Advantages of the mean absolute error (MAE) over the root mean square error (RMSE) in assessing average model performance. *Climate Research* 30:79-82
- Yang, D., Goodison, B.E., Metcalfe, J.R., Golubev, V.S., Bates, R., Pangburn, T. and Hanson, C.L. (1998). Accuracy of NWS 800 standard nonrecording precipitation gauge: results and application of WMO intercomparison. *J. Atmospher. Oceanic Tech.*, 15, 54–68.
- Yang, D., Kane, D.L., Hinzman, L.D., Goodison, B.E., Metcalfe, J.R., Louie, P.Y.T., Leavesley, G.H., Emerson, D.G. and Hanson, C.L. (2000). An evaluation of the Wyoming gauge system for snowfall measurement. *Water Res. Res.*, 36, 2665–2677.
- Yang, D. and Ohata, T. (2001). A bias-corrected Siberian regional precipitation climatology. *J. Hydrometeorol.*, 2, 122–139.

Appendix 1

Parameter Definitions:

Basin Module

- basin_area (km²) - basin area.
- hru_area (km²) - HRU area.
- hru_lat (°) - latitude.
- hru_elev (m) - altitude.
- hru_GSL (°) - ground slope.
- hru_AS_L (°) - aspect.
- basin_name – name given to the basin
- hru_names – name given to the HRUs
- run_ID - integer number.

Obs Module

- basin_area (km²) - basin area.
- hru_area (km²) - HRU area.
- hru_elev (m) - altitude.
- obs_elev (m) - altitude.
- lapse_rate (°C/100m) - lapse rate correction.
- tmax_allrain (°C) - precipitation is all rain when the temperature is greater or equal to this value.
- tmax_allsnow (°C) - precipitation is all snow when the temperature is less or equal to this value.
- catchadjust () – 0 = for none 1 = Goodison
- ppt_daily_distrib () – 0 = daily precip all in first interval, 1 = equally divided over the day

MSM Org Module

- a1 (s) - Albedo decay time constant for cold snow.
- a2 (s) - Albedo decay time constant for melting snow.
- amin () - Minimum albedo for aged snow.
- amax () - Maximum albedo for fresh snow.
- smin (mm) - Minimum snowfall to refresh snow albedo.
- Z0snow (m) - snow roughness length.
- Zref (m) - reference height.
- basin_area (km²) - basin area.
- hru_area (km²) - HRU area.
- hru_elev (m) - altitude.

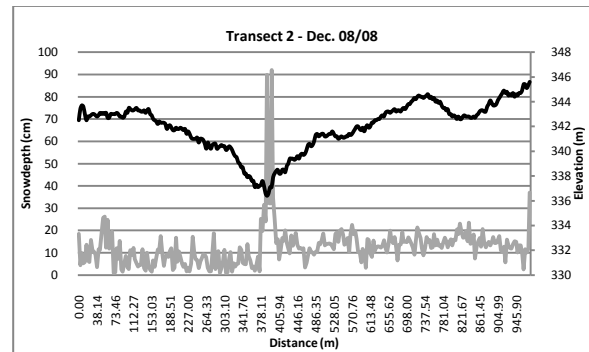
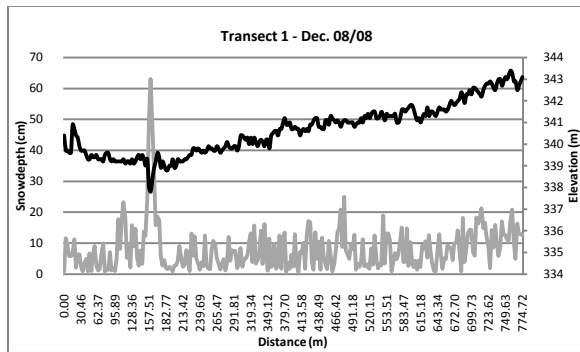
PBSM Module

- fetch (m) - fetch distance. (300-1000m)
- Ht (m) - crop height.

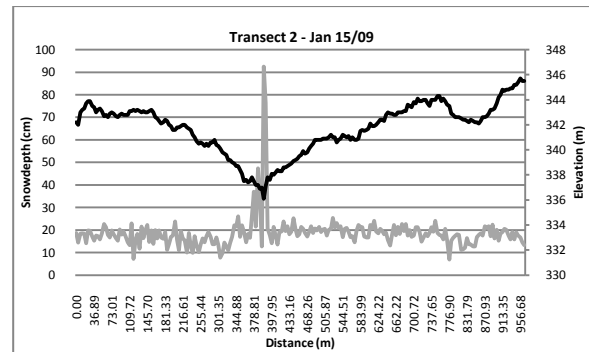
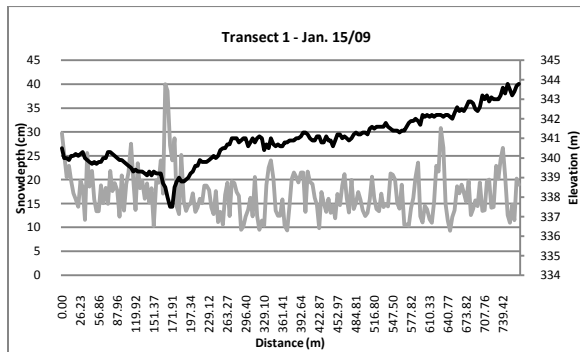
- `distrib ()` - distribution fractions. Value for HRU 1 controls snow transport into the basin.
- `N_S (1/m2)` - vegetation number density.
- `A_S (m)` - stalk diameter or silhouette.
- `basin_area (km2)` - basin area.
- `hru_area (km2)` - hru_area.
- `inhibit_evap (flag)` - an output parameter set true when the SWE is greater than zero. It is used to inhibit evaporation from the evaporation modules.
- `inhibit_bs (flag)` - an input inhibiting blowing snow when set equal to 1. Inhibited HRU is still able to receive drift from other HRUs.

Appendix 2

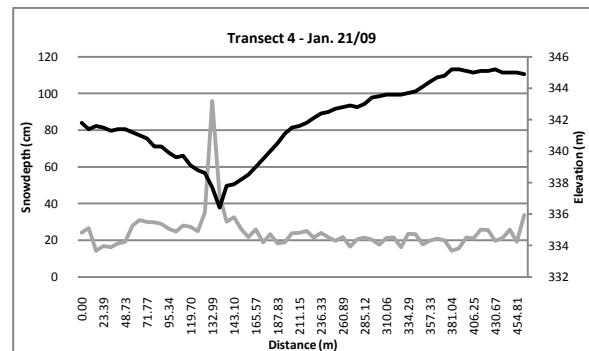
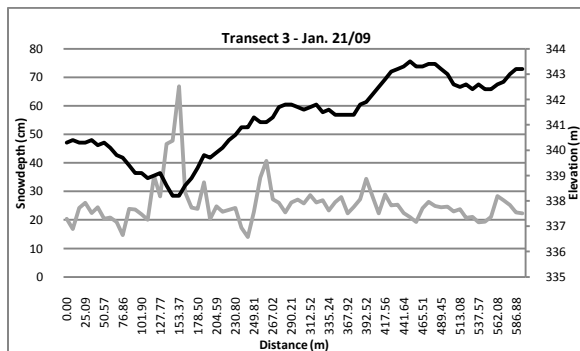
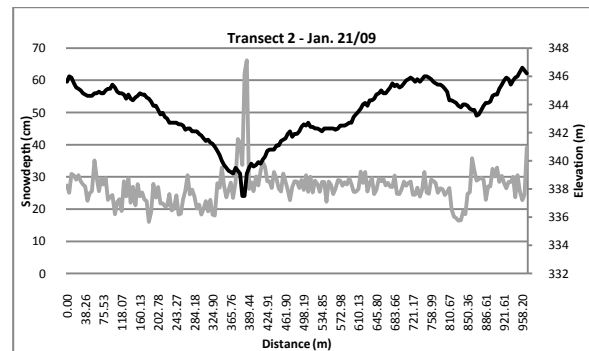
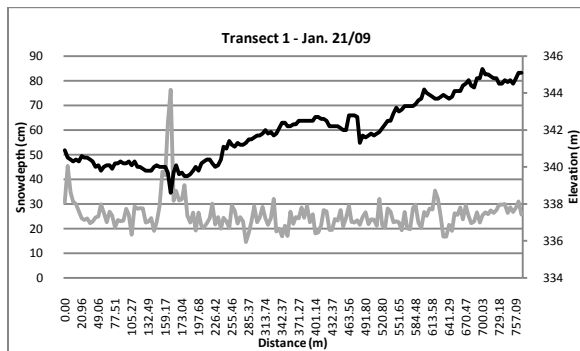
Dec. 08/08

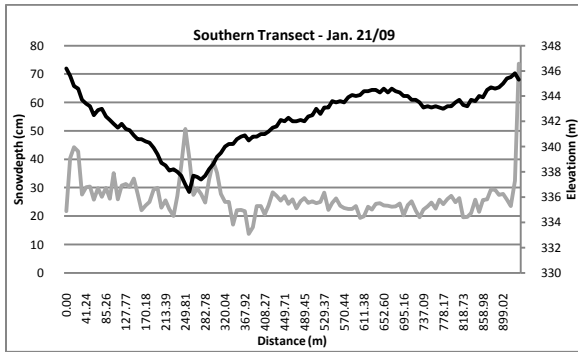
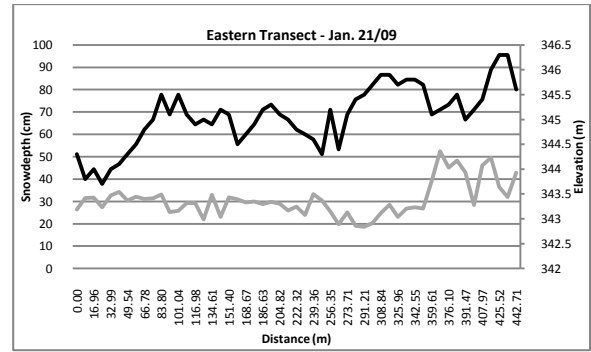
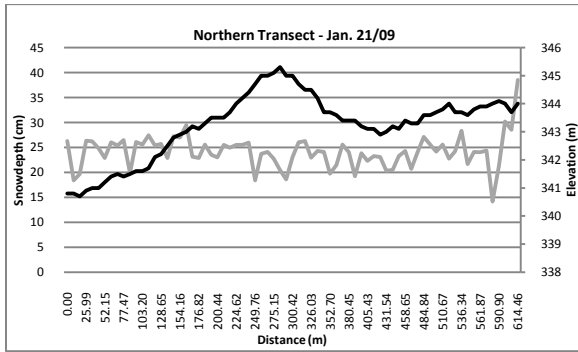
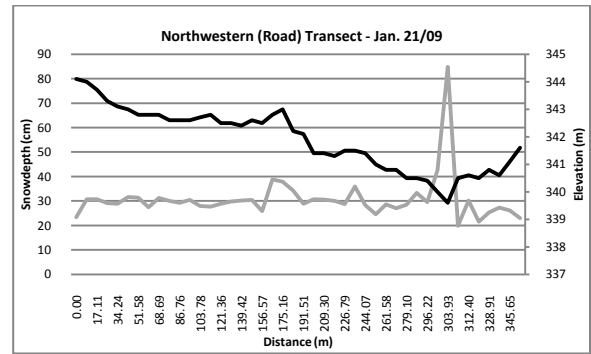
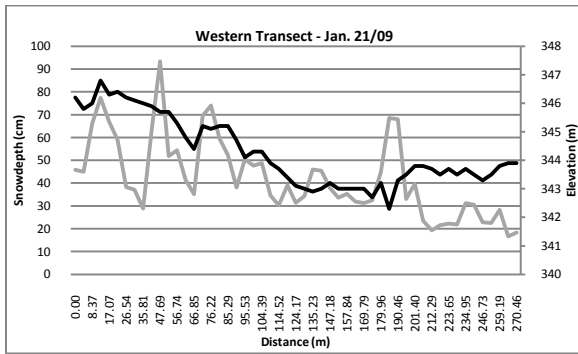


Jan. 15/09

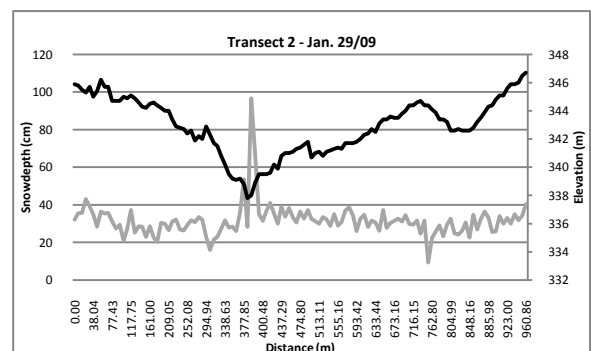
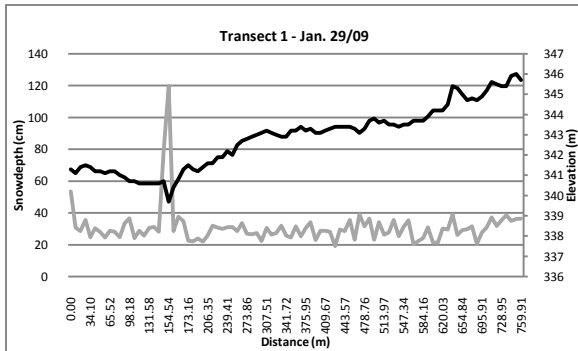


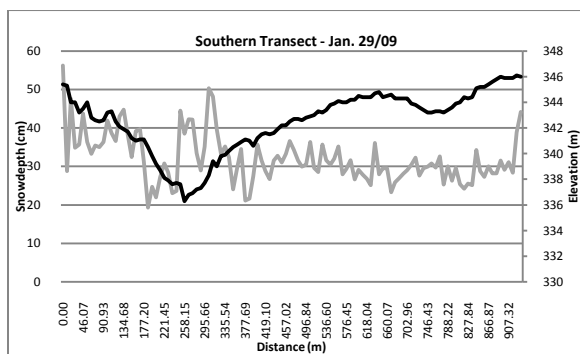
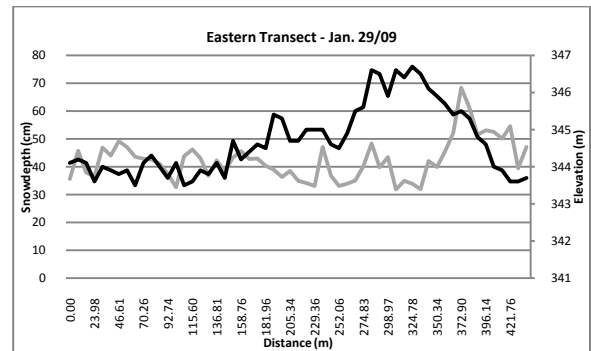
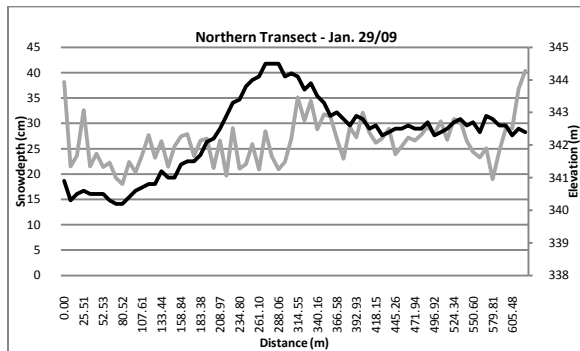
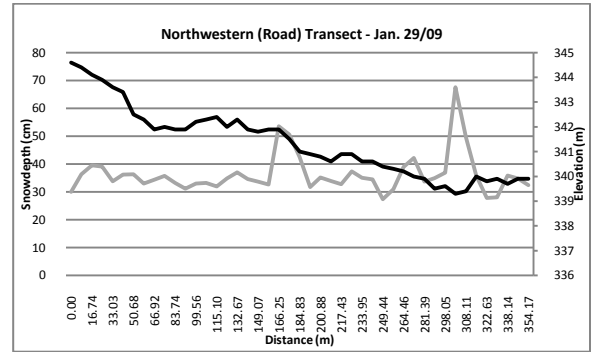
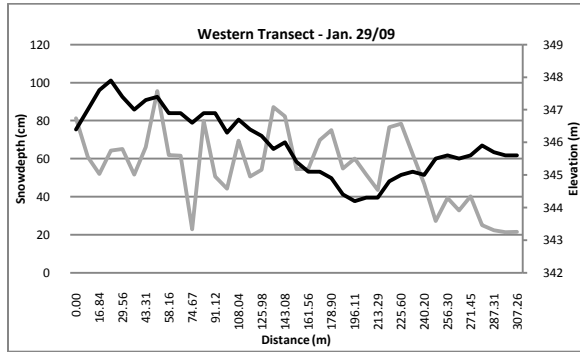
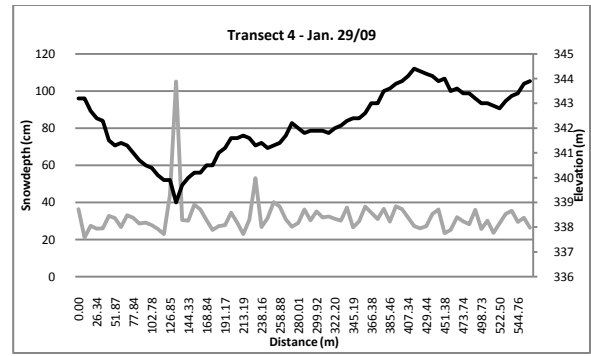
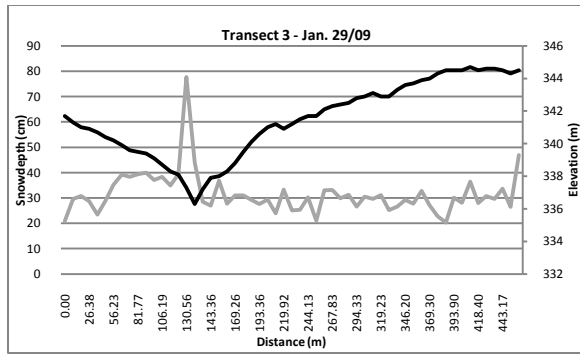
Jan. 21/09





Jan. 29/09





Feb. 04/09

